



Comparing discrete, continuous and hybrid modelling approaches of gene regulatory networks

Shahrad JAMSHIDI

Dissertation
zur Erlangung des Grades
Doktor der Naturwissenschaften (Dr. rer. nat.)
am Fachbereich Mathematik und Informatik
der Freie Universität Berlin

December 2012

Freie Universität Berlin
Berlin, Germany

Datum der Disputation: 15 April, 2013

Gutachter:

Prof. Dr. Alexander Bockmayr, Freie Universität Berlin

Prof. Dr. Jean-Paul Comet, L'Université de Nice Sophia Antipolis

Acknowledgments

My deepest and heartfelt gratitude for my advisor Prof. Dr. Alexander Bockmayr for his proofreading, support and guidance from the start to the end of the PhD. I have developed and learned so much thanks to his patience, thoroughness and objectivity throughout my time here. Also, his suggestion allowed me to come across the BMS and the opportunity to continue my studies in Berlin for which I am always grateful.

Thanks to the BMS for allowing me to achieve this dissertation in Berlin. Big thanks to Prof. Dr. Günter Ziegler who helped me through the German bureaucracy and got me on my feet in Berlin and also to the one stop office for their support throughout my time here, especially to Tanja and Nadja for their advice and energy. To my mentors Prof. Dr. Martin Vingron and Prof. Dr. Martin Skutella for discussing and guiding me through Phase 1 and 2.

A very big thanks to Prof. Dr. Heike Siebert for being a fantastic co-supervisor and for having a hardworking, funny and warm personality to add to the working environment. Her suggestions and advice have always helped to improve my writing and presentation skills.

I would like to thank all the present and former members in the workgroups of Heike and Alexander for creating such a friendly and supportive atmosphere throughout my time here, namely Katja, Amir, Corinna, Laszlo, Ling, Marco, Yaron. Thanks to the group members who proof read various sections of the thesis, Firdevs, Kirsten, Aljoscha and Adam. To Hannes Klärner for being a fantastic office mate throughout the entire PhD. Thankyou for providing a listening ear when brainstorming ideas and joining me for random coffee breaks to discuss anything and everything.

Thanks to all of my friends who supported me every step of the way. To Anna Plumeyer for improving my quality of life in Germany. To Zubin Sethna for his wisdom and humour. To Moritz Minzlaff for his companionship especially whilst writing up. To all those for their emotional support through the tough times, Johannes Buchner, Sarah Alles, Ambros Gleixner, Erik Richardson, Tatjana Prost and Dror Atariah. To Katy Metzler for her optimism and creativity that kept me motivated throughout the writing up phase.

Finally, I dedicate this thesis to my family for their ongoing support and encouragement from the other side of the world.

Abstract

Mathematical modelling of biological networks can help us understand the complex mechanisms that are behind cell proliferation, differentiation and other cellular processes. From these models, we are able to replicate and predict system behaviour that can help in the design of experiments in the systems biology context.

Multiple formalisms capture the evolution or dynamics of a system as implied by the network. Ordinary differential equation (ODE) models provide a precise representation of the system, where the concentrations of network components evolve based on chemical kinetics, e.g. mass action kinetics. The kinetic parameters required to generate the dynamics accurately, however, are often lacking, which has led to the development of more qualitative or discrete modelling methods. Discrete formalisms, like the well known Thomas formalism, provide a very coarse but realistic representation of the systems dynamics, whilst still highlighting fundamental features of the network structure.

When modelling a given system, it could occur that the different approaches yield contrary dynamics. From a modelling perspective, this is highly impractical as we expect the system to behave uniquely irrespective of the modelling approach used. By mathematically relating different formalisms, we can analyse the dynamics of the formalisms and determine conditions for which the dynamics of each formalism are common or contrary between formalisms.

Hybrid modelling approaches, that is formalisms that combine discrete and continuous methods, help in relating the purely discrete Thomas formalism with the purely continuous ODE formalism. Approximating the ODEs, we obtain piecewise affine differential equations (PADEs), which have well defined dynamics that can be discretised to reflect features of the Thomas formalism. Incorporating the hybrid formalism of PADEs into our analysis, we can break up the otherwise rough transformation between ODE and Thomas formalisms. In doing so, we can specify with greater accuracy the conditions for contrary dynamics to occur between formalisms.

Our main result compares the qualitative approach of PADEs with the Thomas formalism. In particular, we show that even though the qualitative parameter information of the PADEs is inherent in the Thomas formalism and vice versa, the dynamics in both models still yield contrary dynamics. However, with the well-defined correspondences of the transition systems implied by the two approaches, we can either provide proofs of paths and terminal strongly connected components that are common between both formalisms or present counterexamples that display contrary dynamics.

From this result, we can also show that specific behaviours of the ODE formalism that normally require the quantitative kinetic parameters can also be deduced from the qualitative parameter information present in the Thomas formalism.

With our analysis, we bridge the gap between discrete and continuous modelling methods so that the formalisms are united in their statements about the system. More specifically, we establish the dynamics that is common regardless of the choice of formalism and the dynamics that can be seen as artefacts of the formalism, which have to be interpreted with greater care. From this analysis, therefore, we achieve a more rigorous modelling framework that allows us to model and predict biological systems with greater accuracy.

Zusammenfassung

Mathematische Modellierung von biologischen Netzwerken hilft uns, die komplexen Mechanismen hinter Zelldifferenzierung, Proliferation und anderen zellulären Prozessen zu verstehen. Abstrakte Modelle erlauben uns, das Verhalten eines Systems bis zu einem gewissen Grad nachzubilden und vorherzusagen. Die dabei gewonnenen Erkenntnisse können zum Beispiel beim Entwurf von Experimenten im systembiologischen Kontext eingesetzt werden.

Die Evolution bzw. Dynamik eines durch ein Netzwerk implizierten Systems kann durch verschiedene Formalismen beschrieben werden. Modelle auf Basis gewöhnlicher Differentialgleichungen (ODE-Modelle) geben eine präzise Beschreibung eines Systems, in dem sich die Konzentrationen der Netzwerkkomponenten gemäß chemischer Kinetik, z.B. Massenwirkungsgesetzes, verhalten. In der Praxis sind die kinetischen Parameter eines ODE-Modells, die für die Beschreibung der Dynamik notwendig sind, oft unbekannt, was verstärkt zur Entwicklung von qualitativen und diskreten Modellierungsmethoden geführt hat. Diskrete Modelle, wie zum Beispiel der bekannte Thomas-Formalismus, liefern oft nur eine sehr grobe Beschreibung der Systemdynamik in der Form eines Transitionssystems, zeigen aber dennoch die fundamentalen Eigenschaften, die durch die Netzwerkstruktur vorgegeben sind.

Obwohl ein System sich eindeutig verhalten sollte, können verschiedene Modellierungsansätze widersprüchliche Ergebnisse liefern. Dies kann die Verlässlichkeit der Modelle grundsätzlich in Frage stellen. Ein mathematischer Vergleich der unterschiedlichen Formalismen kann Bedingungen aufzeigen, unter denen sie sich gleich bzw. verschieden verhalten.

Hierbei können hybride Modellansätze, die diskrete und kontinuierliche Methoden kombinieren, helfen, den rein diskreten Thomas-Formalismus mit dem rein kontinuierlichen ODE-Formalismus in Verbindung zu bringen.

ODE-Modelle können durch stückweise affine Differentialgleichungen (PADEs) approximiert werden, die sowohl eine wohldefinierte Dynamik vorsehen, gleichzeitig aber auch diskretisiert werden können und dabei Eigenschaften des Thomas-Formalismus zeigen. Mit dieser Eigenschaft bilden PADEs eine Brücke zwischen den ODE-Modellen und dem Thomas-Formalismus, die uns erlaubt, die Bedingungen für widersprüchliche Dynamiken zu analysieren.

Unser Hauptergebnis besteht in einem detaillierten Vergleich von qualitativen PADE-Modellen und dem Thomas-Formalismus. Insbesondere zeigen wir, dass die qualitative Parameterinformation der PADEs inhärent im Thomas-Formalismus enthalten ist und umgekehrt, obwohl beide Methoden widersprüchliche Ergebnisse liefern können. Die entsprechenden Tran-

sitionssysteme, welche aus den jeweiligen Methoden hervorgegangen sind, zeigen auf, dass es sowohl Modelle mit gemeinsamen Dynamiken als auch Gegenbeispiele mit widersprüchlichen Ergebnissen gibt. Daraus leiten wir ab, ob die kompliziertere Dynamik, nämlich Pfade und terminal stark zusammenhängende Komponenten, in beiden Formalismen sich entsprechen oder nicht. Wir nutzen diese Ergebnisse um zu zeigen, dass sich gewisse Verhaltenseigenschaften von quantitativen ODE-Modellen, die normalerweise Wissen über spezifische kinetische Parameter erfordern, bereits aus einer qualitativen Analyse des Thomas-Formalismus ableiten lassen.

Unsere Analyse schlägt eine Brücke zwischen diskreten und kontinuierlichen Modellierungsmethoden und macht die Aussagen mehrerer Formalismen einheitlich. Insbesondere trennen wir die Dynamiken, die den Formalismen gemeinsam sind, von denen, die sich als Artefakte des gewählten Modellierungsansatzes ergeben und bei deren Interpretation daher besondere Vorsicht geboten ist. Damit führen unsere Ergebnisse zu einem genaueren Rahmen für die Modellbildung und erlauben akkuratere Modelle und Vorhersagen über biologische Systeme.

Contents

1	Introduction	1
1.1	General Introduction	1
1.2	State of the Art	4
1.3	Thesis Overview	10
2	Formalisms	13
2.1	Continuous Models	13
2.1.1	ODE Model	13
2.1.2	PMA Model	14
2.2	Piecewise Affine Differential Equations	17
2.2.1	Discretised Approach (PADE-D)	20
2.2.2	Qualitative Approach (PADE-Q)	21
2.2.3	Refined Approach (PADE-R)	25
2.3	Discrete Models	28
2.3.1	Thomas Formalism	29
2.3.2	Singular State Formalism	30
3	Qualitative Formalisms	35
3.1	The Thomas and PADE-Q Formalisms	35
3.2	The Discrete Formalisms	48
3.3	Representation of ODE Equilibria in the Qualitative Formalisms	59
4	The PADE Formalisms	65
4.1	Comparing the PADE-Q and PADE-R Formalisms	65
4.2	How do the PADE-Q and PADE-D Formalisms differ?	71
4.3	From Transition Graphs to PADE Solutions	86

5	Relating PADE, PMA and ODE models	91
5.1	The Kinetic Parameters	93
5.2	The Hill Coefficient	100
6	Case Study: Cytokinin Signalling in <i>Arabidopsis thaliana</i>	103
6.1	Biological Background	103
6.2	Model	106
6.3	Reduction	109
6.4	Parameter Estimation	113
7	Conclusion	121
A	Nomenclature	135
B	Curriculum Vitae	137

Introduction

1.1 General Introduction

When modelling a biological system, it is important to understand how molecular components such as genes or proteins interact to give rise to specific behaviour. The interplay of many different components and molecular species takes part in the regulatory mechanism that gives rise to cellular processes such as proliferation, differentiation, circadian rhythms, and the cell cycle. Large interaction networks are constructed so that modelling methods can replicate and predict behaviours of the biological system.

A first step of the modelling procedure is to capture the network of interactions in a directed graph. The so-called interaction graph represents the network structure, where the vertices of the graph correspond to the network components and edges signify dependencies between components. Analysis of the network from a graph theoretical perspective can yield results that inform us about the network structure. Such statements, however, are static in that they do not describe how the system evolves over time as expected by biological processes. Dynamical modelling of the network helps us gain information about the evolution of the system.

A popular dynamical modelling method of biological networks is with a set of coupled ordinary differential equations (ODEs). The continuous variables, that is non-negative finite real variables, represent the concentrations of the components in the network. The temporal evolution of these variables can be described by functions that express the dependence of a component on the concentrations of other components or other substances present in the cell. These functions usually represent the synthesis or degradation of network components and are derived from basic principles of chemical kinetics or simplified expressions, e.g. Michaelis-Menten enzymatic kinetics. One such simplified expression is captured by the Hill function, which monotonically

increases between zero and one taking the value half at a threshold value. The Hill function allows the synthesis or degradation of one component in the network to be described in terms of the concentration of that component's predecessors in the network. In the context of gene regulatory networks, the Hill function simplifies the process of expression, where the highest rate of expression is achieved when an activating protein concentration is above the threshold value.

System-specific information, like reaction rate constants and sensitivities, is encoded as constant kinetic parameters. The system of differential equations with specific kinetic parameters is what we call an ODE model, which is then studied using the mathematics of non-linear dynamics. By solving the ODE model, we obtain a solution trajectory that describes the evolution of the system from any given initial concentration of network components. Because of the non-linearities, the ODE model cannot easily be solved and thus only simulating the ODEs allows us to determine how the system evolves [21, 42, 68]. The long term behaviour of these simulations or attractors of the ODEs, e.g. the stable equilibria and limit cycle oscillations, are thus interpreted as the stable behaviours of the network, where a small perturbation from an attractor would return to the attractor after some time.

In order to model the system accurately, that is have a reasonable representation of the network based on the fundamental principles, we need precise values of the kinetic parameters. These kinetic parameters, however, are not necessarily obtainable from the experimental data. Still, the experimental data share some qualitative information about how the system tends to evolve. As a result, qualitative formalisms, such as discrete modelling methods, have been developed to incorporate the qualitative parameter information. In general, the discrete modelling methods generate dynamics represented as transition systems with states of the system defined as nodes and transitions between nodes describing the evolution of the system. Although the discrete models provide a coarse representation of the biological system, a question that arises is whether this alternative dynamical modelling method is consistent with the network behaviour generated by the ODE formalism.

In the 1960s, S. Kauffman [31] introduced the very abstract representation of a gene regulatory system in terms of Boolean networks. In particular, the network components are interpreted as Boolean variables, where the value 1 represents gene activity. The state of the network is then described by a Boolean vector of values for all network components. The behaviour of each component is described by a Boolean function on the state space, often called the update function, which depends only on the values of the predecessors of that component in the interaction graph.

While the network structure provides information about the interdependencies of the different variables in the Boolean function, the values of the Boolean function still need to be specified. In other words, the evolution of each network component needs to be specified in terms of the presence or absence of the component's predecessors. In that sense, each Boolean variable can be defined by a truth table of all variables, where the specific values are determined through logic NOT, AND and OR gates of the predecessors. We refer to the specification of the truth table as the logical parameters. Hence, the update function captures the dynamics of the system based on the network structure and the logical parameters.

The update function then maps a state to an image state. In other words, the update function represents the dynamics of the system via transitions from a given state to its image state. This method to derive state transitions is called synchronous update. The dynamics of the system is represented by a directed graph, the state transition graph, where the vertices correspond to the states and edges connect each state to its image. Hence, the interpretation of the synchronous update is that all processes involved in a state transition are executed in the same amount of time. The state transition graph can be used to interpret the dynamics of the system, where trajectories are represented by paths and attractors by terminal strongly connected components.

In order to generalise the Boolean modelling approach, R. Thomas and colleagues [62, 63, 64] suggested the extension to multi-valued discrete variables, which accounts for multiple activity levels of network components. They also introduced the asynchronous update method that only allows one component to be updated per discrete time step, i.e., a state and its successor only differ in one component value. Consequently, the resulting Thomas formalism provides a non-deterministic representation of the dynamics. In other words, in the corresponding state transition graph, the out-degree of a vertex will generally be greater than one, reflecting the different choices of components that could be updated. In that sense, the asynchronous update method provides a more realistic representation of the systems behaviour, where no two components can switch simultaneously. Moreover, the activity of a component increases and decreases without bypassing intermediate levels of activity in a single transition.

Although the asynchronous state transition graph is more difficult to analyse than its synchronous counterpart, the more realistic behaviour implied by asynchronous update suggests a more accurate representation, which also reflects the dynamics in the ODE formalism [22, 63]. In particular, the threshold values of the Hill function partition the real values of the continuous variable, which naturally discretises into a multi-valued discrete variable.

By relating the Thomas and ODE formalisms, we can mathematically compare the dynamics implied by both formalisms. From this relation of ODE and Thomas formalisms, we can then observe consistent and inconsistent behaviours, that is paths and attractors in the Thomas model that are either consistent or inconsistent with the solutions and long term behaviour of the ODE model respectively.

The major focus of this dissertation is to identify the consistent and inconsistent behaviours between the ODE and Thomas formalisms, from which we can better understand how each formalism handles the parameter information in order to generate the dynamics. This is advantageous from a modelling perspective because the consistent dynamics imply the same behaviours regardless of the formalism chosen, whereas the inconsistent dynamics imply that the behaviours should be interpreted with caution. From a mathematical perspective, relating the Thomas and ODE formalisms bridges the gap between discrete and continuous modelling. On the one hand, we determine how sensitive the precise dynamics of the ODE formalism are when interpolating the abstract dynamics of the Thomas formalism. On the other hand, we discover how well the Thomas formalism can be used to analyse the ODE formalism.

1.2 State of the Art

Throughout the literature, the Thomas formalism is related to the ODE formalism either by discretising the ODE model [8, 12, 22, 58] or by interpolating the discrete states of the Thomas model to construct an ODE model [69, 34].

There are results in the literature that have already stated some consistent dynamics between the Thomas and ODE formalisms. In particular, a steady state in the Thomas model corresponds to an asymptotically stable equilibrium in the related ODE model [56, 8, 22, 69, 34]. Here, an asymptotically stable equilibrium means that all trajectories that start in a small neighbourhood of the equilibrium point will approach the equilibrium point with increasing time. Also, a steady state is referring to a discrete state in a directed graph, in this case of the state transition graph, that is its own successor or has no outgoing edges.

Three major inconsistencies between the Thomas (or Kauffman) and ODE models have already been observed by Glass and Kauffman in [22]. More specifically,

- there are some cyclic attractors of the Thomas model, that is attractors

of the state transition graph that are not steady states, that correspond to solutions that approach equilibria in the ODE model.

- there are equilibria of the ODE model that do not appear in the Thomas model, and
- there are discrete paths in the Thomas model that have no corresponding trajectory in the ODE model.

For now, we can only claim that these inconsistent dynamics arise due to the transformation between the ODE and Thomas formalisms. In particular, when discretising an ODE model to obtain a Thomas model, the exact values of the kinetic parameters are traded for the more qualitative logical parameters and the deterministic properties of the solution trajectories are not conserved in the discrete paths. Also, when interpolating a Thomas model to construct an ODE model, the choice of the kinetic parameters could have large effects on the ODE solutions. Because the transformation between the Thomas and ODE formalisms is very rough in the sense that the former is discrete and the latter is continuous, we are unable to specify at what stage of the discretisation resp. interpolation the inconsistent dynamics arises. For this reason, in order to identify the conditions for consistent and inconsistent dynamics between the ODE and Thomas formalisms, we break up the transformation between the formalisms.

Hybrid formalisms, that is modelling approaches that combine discrete and continuous methods, provide a compromise between the purely discrete Thomas and purely continuous ODE approaches. Examples of hybrid formalisms include approximating the ODE formalism [12, 21, 41, 10] or introducing continuous dynamics to the Thomas formalism [1, 2, 20, 55, 9]. Hence, hybrid methods help break up the otherwise rough transformation between Thomas and ODE models and help in identifying consistent and inconsistent dynamics between the Thomas and ODE formalisms.

One popular hybrid modelling method is that of piecewise affine differential equations (PADEs) [21], which are also known as piecewise linear differential equations. The PADE formalism simplifies the ODE formalism by approximating the Hill functions with step functions, which take the values zero below and one above the threshold value. Because the step function can be interpreted as a Hill function with infinite slope at the threshold, it is considered to be a reasonable approximation of the Hill function. Thus, the PADE formalism is also a reasonable approximation of the ODE formalism.

The step functions, which are piecewise constant, make the differential equations piecewise affine, hence PADEs. Therefore, all points of the phase space that are located in a so-called regular domain satisfy the same system

of affine differential equations, where regular domains are defined such that the differential equations have no discontinuities on them. Hence, the PADE system is solvable within the regular domains. More specifically, all solutions starting in a regular domain converge towards a point in the phase space, the so-called focal point, which is uniquely defined for every regular domain by the kinetic parameters. A solution starting in a regular domain, whose focal point is not contained within itself, eventually leaves the regular domain. The piecewise nature of the PADEs, however, means that after a solution crosses a threshold hyperplane into a new regular domain, the solution converges towards the focal point of that regular domain. This switching behaviour caused by the step functions is the discrete feature that makes the PADEs a hybrid formalism.

Although the PADEs are a clear approximation of the ODE formalism, the relation between trajectories of the ODE and PADE formalisms is less clear. Polynikis et al. [42] and Widder et al. [68] used simulations to show that the PADE and ODE solutions have some corresponding stable equilibria, but their results come from small and simple networks. Unfortunately, the non-linear nature of the ODE formalism makes it difficult to compare solutions [21].

In 1989, Snoussi [56] uses the regular domains to discretise the PADEs, where the threshold values partition each continuous variable into discrete multi-valued variables. By exploiting the association of regular domains and their corresponding focal points, Snoussi captures the dynamics of the PADE system in a discrete function, where the regular domains and their focal points correspond to a discrete state and its image respectively. The asynchronous state transition graph of the discrete function then has a form similar to that of the Thomas formalism. For this reason, we consider the PADE formalism to be an excellent intermediate formalism that helps break up the transformation between the Thomas and ODE formalisms.

By discretising the PADEs to obtain a Thomas model, Snoussi [56] observed two important results. The first immediate result is that every steady state in the asynchronous state transition graph corresponds to an asymptotically stable equilibrium in the corresponding regular domain. The second result sheds some light on one of the three inconsistent dynamics observed by Glass and Kauffman (see above and [22]): Snoussi showed that a cyclic attractor that oscillates in one or two variables always corresponds to a stable equilibrium in either the threshold hyperplanes or in the intersection of threshold hyperplanes, which are also referred to as singular domains, in the PADEs. He showed that the remaining cyclic attractors, namely attractors that oscillate in three or more variables, correspond to limit cycle oscillations in the related PADEs. Because the PADEs approximate the ODE model, the

PADEs capture some qualitative dynamics of the ODE model. In that sense, Snoussi determined conditions for the existence of inconsistent dynamics between the Thomas and ODE formalisms with the help of the intermediate PADE modelling method.

Even though Snoussi found some stable equilibria on the singular domains, he does not clearly define the specific dynamics on singular domains. That is, the step functions of the PADEs give rise to the discontinuities that cannot be solved by standard ODE theory. In 1993, Thomas and Snoussi [57] suggested a discrete extension or refinement of the Thomas formalism, known as the singular state formalism, with the introduction of singular states, that is states that lie between adjacent (regular) states of the Thomas formalism. The intention of these singular states is to have a logical representation of the singular domains of the PADE formalism. Richard et al. [48] formally defined the singular state formalism, where all states, i.e., including the singular states, have an update, which are determined by the well-defined interaction graph and logical parameters. Furthermore, the asynchronous update scheme of the singular state formalism is inherited from the Thomas formalism. In their work, Richard et al. [48] prove the statement claimed in [57] that the singular steady states, that is the singular states that are their own successors in the respective transition graph, are characteristic of feedback loops in the interaction graph. Our focus, however, is purely on the relation of dynamics between different modelling approaches and not the relation of dynamics and structure of a network, which is otherwise very well studied in the literature [49, 46, 47, 61, 59, 45]. In any case, the authors in [57, 48] claim that the singular steady states are representative of equilibria in the corresponding ODE formalism.

To avoid the complications of defining the dynamics on singular domains, Plahte et al. [41] introduced a differential equation formalism, which is not as rough an approximation of the ODE formalism as the PADEs. In particular, they introduced the approximation of the Hill function known as the logoid function [41], which rises monotonically from zero to one in a narrow threshold interval and takes the value zero below and the value one above this interval. The logoid function is not only a continuous approximation of the Hill function but also has constant values, which would then imply solvable regions of the phase space similar to the step function. One particular logoid function that has a linear increase or decrease in the threshold interval is referred to as the ramp function. Replacing the Hill functions in the ODE model with ramp functions makes the resulting differential equations piecewise multi-affine. Hence, we refer to the resulting differential equations as the PMA model. Here, multi-affine means that the right hand side of the differential equation is composed of polynomials such that each variable has

degree of at most one. In other words, the PMA model is a compromise between the discontinuities of the PADE as well as the non-linearities of the ODE model.

In [40, 36], E. Plahte and colleagues showed that the PMA model can help provide insight into what occurs on the singular domains in PADEs. In particular, they show that a PMA model, whose ramp functions have a very steep slope, has solutions that approach the limit solutions uniformly in a finite time interval, where the limit solutions refer to the solutions when ramp functions of the PMA model approach step functions. An interpretation of this is that the solutions of the PMA model interpolate the solutions on singular domains of the PADEs. In other words, the PMA model bridges the gap between PADEs and the ODE model.

There is still the issue of defining the dynamics on the singular domains of the PADEs. In [23, 16, 14, 15], H. de Jong and colleagues dealt with the discontinuities of the PADEs by converting the PADEs to differential inclusions (following the methods of A. Filippov [18]). Consequently, the differential inclusions imply a generalised concept of solution such that the PADEs can be solved on the regular and singular domains giving rise to what we call PADE solutions. In [51, 50], Ropers et al. compare the numerical simulations of the ODE and PADE models. In their comparison, they define distance and correlation measures to show that the solutions of both models are very closely related. For this reason, we interpret the PADE approximation as legitimate in conserving the solution trajectories of the ODE formalism.

Solving the differential inclusion on singular domains could often imply non-unique dynamics. For this reason, there was a need to define the so-called singular equilibria, that is points in singular regions that have equilibrium properties, but due to non-unique dynamics cannot be defined identically to ODE equilibria. In 2006, Casey et al. [7] defined and observed the properties of singular equilibria in greater detail. In particular, they adapted the concept of stability from ODE equilibria to singular equilibria, from which they conjectured the stability of these singular equilibria in terms of the transitions that are present in the qualitative transition graph. Our focus in the thesis is not on the stability but rather on the existence of the singular equilibria and the claim that they represent equilibria in the ODE model.

With the defined solutions on the singular domains, de Jong et al. [15] could discretise all dynamics implied by the PADEs into a so-called qualitative transition graph. In particular, the node set consists of regular and singular domains and the transitions between these nodes occurs whenever a solution exists that traverses two adjacent domains. This discrete representation of the PADE system is more representative of the ODE formalism compared to Snoussi's discretisation because the singular domains have a

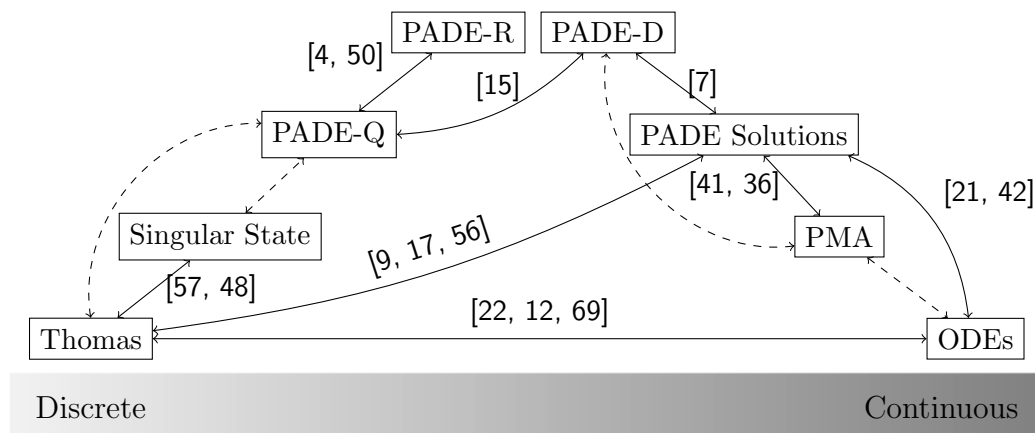


Figure 1.1: Our formalisms of interest, which make up a spectrum that ranges from discrete on the very left to continuous on the very right. The PADE, PMA and singular state formalisms bridge the gap between the purely continuous ODE formalism and the purely discrete Thomas formalism. The different analysis approaches of the PADEs also range between discrete and continuous in terms of either their parameters or dynamics. The arrows depict transformations between the respective formalisms and are labelled with the references that deal with the transformation. The dashed arrows represent the formalisms that have not yet been compared in the literature and will be addressed in the thesis.

discrete representation similar to the singular state formalism. Still, because of the discrete representation of the dynamics, we consider the qualitative transition graph to be a formalism on its own and refer to it as the discretised PADE (PADE-D) formalism.

One major advantage of the discrete representation of the PADEs in a qualitative transition graph is that it can incorporate qualitative information about the kinetic parameters, where the kinetic parameters satisfy a set of strict inequalities rather than taking specific values. In 2004, de Jong et al. [15] introduced an overapproximation of the PADEs to account for all the dynamics in the PADEs implied by the range of kinetic parameters. We refer to this overapproximation as the qualitative PADE (PADE-Q) formalism. Their main result was that the qualitative transition graph that arises from specific kinetic parameters is a subgraph of the overapproximated qualitative transition graph, which is constructed from the qualitative information of the kinetic parameters. One interpretation of this result is that the dynamics implied by multiple parameter sets are combined into one discrete transition

system.

To incorporate more qualitative parameter information as well as a finer representation of the dynamics, Batt et al. [4] developed the refined approach of the PADEs, where sign of derivative information is included in the nodes of the respective transition graph. Different biological descriptions of different component concentrations, e.g. increasing or decreasing, are often difficult to interpret in the standard PADE formalism. Such descriptions, however, can be directly translated to discrete paths in the refined PADE (PADE-R) analysis and thus allow us to confirm the model more easily with experimental data or observations [51].

It has been claimed in [22] that some paths of the Thomas model do not have a corresponding trajectory in the ODE model. This problem has been shown to crop up when discretising more general ODE systems [6]. Introducing continuous dynamics to the discrete model can reobtain the distinct trajectories [1, 55, 9] but in all cases the existence of these corresponding trajectories is dependent on the specific kinetic parameters. As a result, no general statement can be made about which discrete paths in the Thomas model have no corresponding trajectory in the ODE model.

Although the different formalisms have been developed to either approximate the ODE model, i.e., the PADE and PMA models, or to add detail to the Thomas formalism, i.e., the singular state formalism, they are in their own right valid modelling methods. Hence, by incorporating all formalisms mentioned above into our analysis, we not only break up the transformation between the Thomas and ODE formalisms but also identify the consistent and inconsistent dynamics with other valid modelling approaches. This thesis, therefore, investigates the consistent and inconsistent dynamics between multiple formalisms but with the overall aim of relating and comparing the purely discrete Thomas and the purely continuous ODE formalisms (see Fig. 1.1).

1.3 Thesis Overview

After this introductory chapter on modelling methods of biological networks, six chapters will follow. One chapter to introduce the notation, three to present the main results, one to apply the results to a biological system and a final chapter to conclude the thesis. Chapter 2 introduces the different formalisms of interest that have been described above. Going from continuous to discrete, the ODE and PMA model are introduced, followed by the PADE formalism and its different analysis methods, and finally the Thomas and singular state formalisms. In addition to describing how the dynamics of each

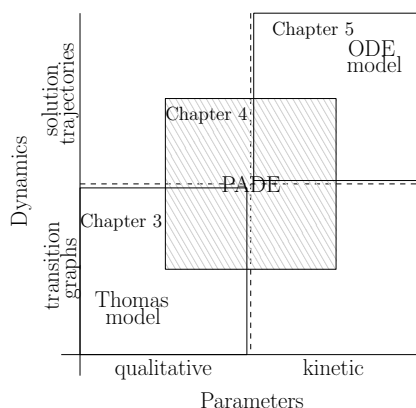


Figure 1.2: The thesis structure depicted by the comparisons that are addressed in each chapter. The major formalisms of interest are classed in terms of whether they need qualitative parameter information or explicit kinetic parameters and whether their dynamical representation is by transition graphs or solution trajectories.

formalism is generated by the logical or kinetic parameters, we also analyse how much parameter information can be determined from the dynamics.

Because the Thomas formalism is a coarse and abstract representation of the fundamental characteristics of the network, it has structural and dynamical features that are expected to be present in all other formalisms. In that sense, by relating the above formalisms with the Thomas formalism, we see how the dynamics of other formalisms contribute to the dynamics of the Thomas formalism. For this reason, we begin the thesis by relating the very abstract Thomas formalism to the other qualitative formalisms before incrementally increasing the detail of the formalisms towards the ODE formalism (Fig. 1.2).

Chapter 3 looks at the different qualitative formalisms, namely the Thomas and singular state formalisms, and their relation with the qualitative analysis of the PADEs. One important result that we present is the equivalent parameter information of all three approaches, that is no information is gained or lost when transforming between the methods. Consequently, the dynamics of all three approaches are directly relatable, meaning we can determine the correspondences of edges between the different transition graphs. From this information, we can then compare the more complex dynamical behaviour of paths and attractors in each of the formalisms and present proofs of consistent dynamics as well as construct examples of inconsistent dynamics.

The PADEs and their multiple analysis approaches are compared in Chapter 4. Here, we are especially interested in the consequences of qualitative and kinetic parameters. Other than establishing the consistent and inconsistent dynamics of the different PADE formalisms, we also present how the qualitative information encoded in the logical parameters suffices in determining the existence of some singular equilibria in the PADEs.

Chapter 5 concentrates on relating the differential equation formalisms, for which we assume the kinetic parameters. We deduce conditions on the kinetic parameters that will ensure that the dynamics are conserved given the relation between the formalisms.

Chapter 6 shows how the analysis over all the formalisms can be applied to model the cytokinin signal transduction network of *Arabidopsis thaliana*. More specifically, after constructing an ODE model from mass action kinetics, we discretise the ODEs into a Thomas model. Then, we simulate the ODEs using kinetic parameters that have been estimated based on the findings in the previous chapters.

The final chapter summarises all our results and gives an outlook of the thesis.

Formalisms

In this chapter, we introduce our formalisms of interest starting with the ODE and the PMA modelling approaches. Then, the hybrid method of PADEs is presented and its multiple analysis approaches. Finally, the Thomas formalism and its extension known as the singular state formalism. Our focus is in presenting the dynamics of each formalism and not how the formalism is constructed from a specific network.

2.1 Continuous Models

2.1.1 ODE Model

Here, we present the ODE modelling approach, which refers to a specific ODE system that involves Hill functions. Consider an n -dimensional *phase space* $\Omega = \Omega_1 \times \dots \times \Omega_n \subset \mathbb{R}_{\geq 0}^n$, where $\Omega_i = \{x_i \in \mathbb{R} \mid 0 \leq x_i \leq \max_i\}$, and $\max_i \in \mathbb{R}_{>0}$. For every continuous variable $x_i \in \Omega_i$ we assume $p_i \in \mathbb{N}$ thresholds $\theta_i^1, \dots, \theta_i^{p_i}$ satisfying the ordering

$$0 < \theta_i^1 < \dots < \theta_i^{p_i} < \max_i, \quad \text{for all } i \in \{1, \dots, n\}. \quad (2.1)$$

We consider a set of ODEs in Ω of the form

$$\dot{x}_i = F_i^H(x) - G_i^H(x)x_i, \quad i \in \{1, \dots, n\}, \quad (2.2)$$

where the functions $G_i^H : \Omega \rightarrow \mathbb{R}_{>0}$ and $F_i^H : \Omega \rightarrow \mathbb{R}_{\geq 0}$ are linear combinations of products of *Hill functions*,

$$H^+(x_i, \theta_i^j, \epsilon_{ij}) = \frac{x_i^{\epsilon_{ij}}}{x_i^{\epsilon_{ij}} + (\theta_i^j)^{\epsilon_{ij}}},$$

and $H^-(x_i, \theta_i^j, \epsilon_{ij}) = 1 - H^+(x_i, \theta_i^j, \epsilon_{ij})$, where the *Hill coefficient* $\epsilon_{ij} \geq 1$ determines the steepness of the function at the threshold θ_i^j for $i \in$

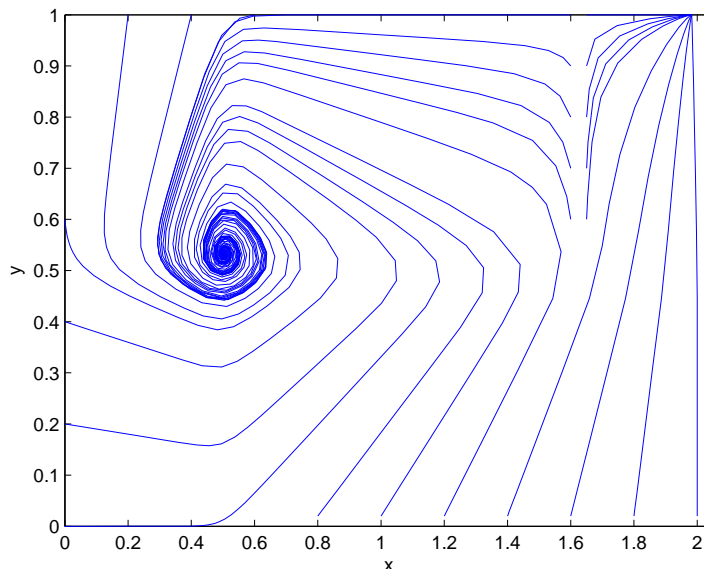


Figure 2.1: The solution trajectories of the ODE model in Ex. 2.1. The initial values of these trajectories are along the borders of the phase space $\Omega = [0, 2] \times [0, 1]$. All trajectories approach either the focus close to the point $(0.5, 0.5)$ or the equilibrium point close to $(2, 1)$.

$\{1, \dots, n\}, j \in \{1, \dots, p_i\}$. The *kinetic parameters* are then the constant coefficients of the terms in G_i^H and F_i^H . We refer to (2.2) as the *ODE model*.

Example 2.1 Consider an ODE model consisting of the two variables x_1 and x_2 , where variable x_1 has the two thresholds, θ_1^1 and θ_1^2 , and variable x_2 has the single threshold θ_2 .

$$\begin{aligned} \dot{x}_1 &= \kappa_1 H^-(x_2, \theta_2, \epsilon_{21}) + \kappa_2 H^+(x_1, \theta_1^2, \epsilon_{12}) - \\ &\quad - \kappa_4 H^-(x_2, \theta_2, \epsilon_{21}) H^+(x_1, \theta_1^2, \epsilon_{12}) - \lambda_1 x_1, \\ \dot{x}_2 &= \kappa_3 H^+(x_1, \theta_1^1, \epsilon_{11}) - \lambda_2 x_2. \end{aligned}$$

The parameter values $\kappa_1, \kappa_2, \kappa_4 = 2, \kappa_3, \lambda_1, \lambda_2 = 1, \theta_1^1 = \theta_2 = \frac{1}{2}, \theta_1^2 = \frac{3}{2}, \max_1 = 2, \max_2 = 1, \epsilon_{11}, \epsilon_{12}, \epsilon_{21} = 17$ yield the trajectories in Fig. 2.1.

2.1.2 PMA Model

Here we introduce the piecewise multi-affine model for which we retain some notation of the ODE model, namely the n -dimensional phase space Ω and the p_i thresholds for every $i \in \{1, \dots, n\}$ with the threshold ordering (2.1).

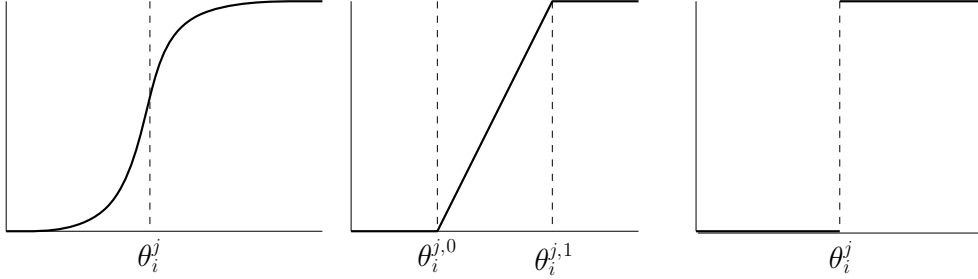


Figure 2.2: Starting from left to right, the Hill, ramp and step function, which give rise to the ODE, PMA and PADE models respectively. In particular, going from left to right are the functions $H^+(x_i, \theta_i^j, \epsilon_{ij})$, $L^+(x_i, \theta_i^{j,0}, \theta_i^{j,1})$ and $S^+(x_i, \theta_i^j)$ with the y -axes ranging from zero to one.

Consider the *threshold interval* $[\theta_i^{j,0}, \theta_i^{j,1}]$ for every threshold θ_i^j of the ODE model, where the bounds of each threshold interval satisfy the ordering $0 < \theta_i^{j,0} < \theta_i^{j,1} < \max_i$.

We consider the threshold intervals do not *overlap*, that is $\theta_i^{j,1} < \theta_i^{(j+1),0}$, for all $i \in \{1, \dots, n\}$ and $j \in \{1, \dots, p_i - 1\}$. Non-overlapping threshold intervals will later make relating the PMA and PADE models simpler. So, we disregard the PMA models with overlapping threshold intervals.

Consider a set of ODEs in Ω , which we refer to as the *piecewise multi-affine (PMA) model*, of the form

$$\dot{x}_i = F_i^L(x) - G_i^L(x)x_i, \quad i \in \{1, \dots, n\}, \quad (2.3)$$

where the functions $G_i^L : \Omega \rightarrow \mathbb{R}_{>0}$ and $F_i^L : \Omega \rightarrow \mathbb{R}_{\geq 0}$ are linear combinations of products of *ramp functions*

$$L^+(x_i, \theta_i^{j,0}, \theta_i^{j,1}) = \begin{cases} 0 & \text{if } x_i < \theta_i^{j,0} \\ 1 & \text{if } x_i > \theta_i^{j,1} \\ m_{ij}x_i + b_{ij} & \text{if } \theta_i^{j,0} \leq x_i \leq \theta_i^{j,1} \end{cases}$$

and $L^-(x_i, \theta_i^{j,0}, \theta_i^{j,1}) = 1 - L^+(x_i, \theta_i^{j,0}, \theta_i^{j,1})$, where $m_{ij}, b_{ij} \in \mathbb{R}$ are chosen such that the ramp function is continuous (see Fig. 2.2). Note that a function $\bar{F} : \mathbb{R}^n \rightarrow \mathbb{R}$ is called *multi-affine* if for all $x \in \mathbb{R}^n$ we have

$$\bar{F}(x) = \sum_{i_j \in \{0,1\}, j \in \{1, \dots, n\}} c_{i_1, \dots, i_n} x_1^{i_1} \dots x_n^{i_n},$$

where $c_{i_1, \dots, i_n} \in \mathbb{R}$. In other words, a multi-affine function is a polynomial of n variables such that the degree of each variable is either zero or one. Therefore,

to ensure that the right hand side of (2.3) is piecewise multi-affine, we have the additional constraint that the function $G_i^L(x)$ is not dependent on x_i for all $i \in \{1, \dots, n\}$.

With the ordering of the threshold intervals, we can partition the phase space into hyperrectangular regions, which we refer to as *rectangles*.

Definition 2.1 (Rectangles) Consider a PMA model of the form (2.3) with phase space Ω and non-overlapping threshold intervals $[\theta_i^{j,0}, \theta_i^{j,1}]$, $i \in \{1, \dots, n\}$, $j \in \{1, \dots, p_i\}$. A *rectangle* $R \subset \Omega$ is defined by $R = R_1 \times \dots \times R_n$, where every R_i is given by one of the following equations.

$$\begin{aligned} R_i &= \{x_i \mid 0 \leq x_i < \theta_i^{1,0}\}, \\ R_i &= \{x_i \mid \theta_i^{k,1} < x_i < \theta_i^{(k+1),0}\} \text{ for } k \in \{1, \dots, p_i - 1\}, \\ R_i &= \{x_i \mid \theta_i^{p_i,1} < x_i \leq \max x_i\}, \\ R_i &= \{x_i \mid \theta_i^{k,0} \leq x_i \leq \theta_i^{k,1}\} \text{ for } k \in \{1, \dots, p_i\}. \end{aligned}$$

By \mathcal{R} , we denote the set of all rectangles in Ω .

We can define a rectangle $R \in \mathcal{R}$ by two vectors $(a_1, \dots, a_n), (b_1, \dots, b_n) \in \Omega$, where $a_i := \inf_{x \in R_i} x$ and $b_i := \sup_{x \in R_i} x$, from which we define the set of *corners*

$$\mathcal{V}(R) := \{v = (v_1, \dots, v_n) \in \Omega \mid \forall i \in \{1, \dots, n\} \text{ either } v_i = a_i \text{ or } v_i = b_i\}.$$

Within each rectangle R , we have that the right hand side of the ODE is multi-affine. The findings of Belta et al. [6, 33, 5] state that the vector field within R is a subset of the convex hull of the vector fields at the corners of R , which implies that for all $x \in R$

$$\dot{x} \in \overline{\text{co}}(\{F(v) - G(v)v \mid v \in \mathcal{V}(R)\}),$$

where $F(v) = (F_1^L(v), \dots, F_n^L(v))$, $G(v) = \text{diag}(G_1^L(v), \dots, G_n^L(v))$ and $\overline{\text{co}}(P)$ is the closed convex hull of all points in P .

When analysing any ODE system, i.e., ODE and PMA models, it is important to identify the *equilibria*, where an equilibrium point is a point $x^0 \in \Omega$ such that $x^0 \in \bigcap_{i \in \{1, \dots, n\}} \text{Null}_i$, where

$$\text{Null}_i := \{x \in \Omega \mid F_i^*(x) - G_i^*(x)x_i = 0\}$$

denotes the *nullcline* of variable x_i for $* \in \{H, L\}$. In other words, an equilibrium point $x^0 \in \Omega$ implies $\dot{x}^0 = \mathbf{0}$.

Because the ODE and PMA models have a continuous and finite right hand side, we are able to solve the system (2.2) and (2.3) given an initial

value $x_0 \in \Omega$. Solving the ODEs gives a *trajectory* $\bar{\xi}(t) \in \Omega$, which is defined for all $t \geq 0$ with $\bar{\xi}(0) = x_0$. The non-linearity of the Hill function makes the ODE model difficult to solve, whereas the piecewise linearity of the ramp function makes the PMA model easier to solve. We can numerically simulate both the ODE systems using ODE solvers in computer programs such as Matlab.

2.2 Piecewise Affine Differential Equations

In the following, we discuss piecewise affine differential equations (*PADEs*) and the different modelling approaches following Filippov's method [23], the discretised (PADE-D) and qualitative (PADE-Q) approaches introduced by de Jong et al. [15], and the refined approach (PADE-R) introduced by Batt et al. [4].

Since the PADEs are an approximation of the ODE model, we also retain a lot of the notation, namely the n -dimensional phase space Ω , the p_i thresholds θ_i^j for $i \in \{1, \dots, n\}$, and their ordering (2.1). We denote the union of the threshold hyperplanes by $\Theta := \bigcup_{i \in \{1, \dots, n\}, j \in \{1, \dots, p_i\}} \{x \in \Omega \mid x_i = \theta_i^j\}$. Consider a set of PADEs in $\Omega \setminus \Theta$ of the form

$$\dot{x}_i = F_i^S(x) - G_i^S(x)x_i, \quad i \in \{1, \dots, n\}, \quad (2.4)$$

where the functions $G_i^S : \Omega \setminus \Theta \rightarrow \mathbb{R}_{>0}$ and $F_i^S : \Omega \setminus \Theta \rightarrow \mathbb{R}_{\geq 0}$ are linear combinations of products of *step functions* $S^+(x_l, \theta_l^k) = \begin{cases} 0 & \text{if } x_l < \theta_l^k, \\ 1 & \text{if } x_l > \theta_l^k, \end{cases}$ and $S^-(x_l, \theta_l^k) = 1 - S^+(x_l, \theta_l^k)$.

The threshold hyperplanes Θ partition the phase space Ω into a set of so-called domains.

Definition 2.2 Consider a set of PADEs of the form (2.4) with phase space Ω and thresholds θ_i^j . The $(n - 1)$ -dimensional hyperplanes corresponding to the equations $x_i = \theta_i^j$, $j \in \{1, \dots, p_i\}$, divide Ω into hyper-rectangular regions called domains. A *domain* $D \subset \Omega$ is defined by $D = D_1 \times \dots \times D_n$, where every D_i is given by one of the following equations

$$\begin{aligned} D_i &= \{x_i \mid 0 \leq x_i < \theta_i^1\}, \\ D_i &= \{x_i \mid \theta_i^k < x_i < \theta_i^{k+1}\} \text{ for } k \in \{1, \dots, p_i - 1\}, \\ D_i &= \{x_i \mid \theta_i^{p_i} < x_i \leq \max_i\}, \\ D_i &= \{x_i \mid x_i = \theta_i^k\} \text{ for } k \in \{1, \dots, p_i\}. \end{aligned}$$

By \mathcal{D} , we denote the set of all domains in Ω . A domain $D \in \mathcal{D}$ is called a *singular domain*, if there exists $i \in \{1, \dots, n\}$ such that $D_i = \{x_i \mid x_i = \theta_i^k\}$ for some $k \in \{1, \dots, p_i\}$. The variable x_i is then called *singular variable*. The *order* of a singular domain is the number of its singular variables. A domain $D \in \mathcal{D}$ is called a *regular domain*, if it is not a singular domain. The set of regular and singular domains are denoted by \mathcal{D}_r and \mathcal{D}_s respectively.

It follows immediately that for any regular domain $D \in \mathcal{D}_r$, the functions $F_i^D := F_i^S(x)$ and $G_i^D := G_i^S(x)$ are constant for all $x \in D$. Thus, (2.4) can be written as a linear system $\dot{x} = F^D - G^D x$ for all $x \in D$, where $G^D = \text{diag}(G_1^D, \dots, G_n^D)$ is a diagonal matrix with strictly positive entries and $F^D = (F_1^D, \dots, F_n^D)$ a positive vector.

Solving the differential equation (2.4) within a regular domain D gives trajectories that converge to the *focal point*, $\phi(D) := (G^D)^{-1}F^D$. Mathematically speaking, the solution $\xi : \mathbb{R}_{\geq 0} \rightarrow D$ of the PADEs in domain $D \in \mathcal{D}_r$ starting at $x^0 \in D$ is

$$\xi_i(t) = \phi_i(D) - (\phi_i(D) - x_i^0)e^{-G_i^D t}, \quad i = 1, 2, \dots, n. \quad (2.5)$$

Therefore, if $\phi(D) \in D$ for some $D \in \mathcal{D}_r$, then $\lim_{t \rightarrow \infty} \xi(t) = \phi(D)$ for all $x^0 \in D$, that is $\phi(D)$ is an asymptotically stable equilibrium point, which is a common result throughout the literature [56, 17, 7].

It has been argued in [15, 14, 56] that due to the zero Lebesgue measure of the threshold hyperplanes, the probability (with respect to the Lebesgue measure) that a focal point is situated on a singular domain is zero. In agreement with these arguments, we assume that each focal point lies in a regular domain.

Although we are able to solve (2.4) inside regular domains, the step function approximation implies that the dynamics on the singular domains remains undefined. The complication of defining the dynamics on singular domains is best demonstrated with an example.

Example 2.2 Consider the one-dimensional PADE for $x \in \Omega = \{x \in \mathbb{R} \mid 0 \leq x \leq 2\}$,

$$\dot{x} = 2S^-(x, 1) - x, \quad x(0) = x^0$$

Solving this PADE, we have that the solution is $\xi(t) = 2 - (2 - x^0)e^{-t}$ when $x^0 < 1$ and $\xi(t) = x^0 e^{-t}$ when $x^0 > 1$. In both cases, there exists $\tau > 0$ such that $\xi(\tau) = 1$. Because $\dot{x} > 0$ for $x < 1$ and $\dot{x} < 0$ for $x > 1$, a continuous solution that has a well defined derivative is only possible if $\xi(t) = 0$ for $x^0 = 1$. This solution however implies $\dot{x} = 0$ when $x = 1$, which is neither the dynamics of $x < 1$ nor $x > 1$.

Therefore, the dynamics on the discontinuities requires a generalised concept of solution so that all solutions on Ω have a well-defined derivative. Filippov [18] defines this general concept with the introduction of *differential inclusions*. For Ex. 2.2, the differential inclusion takes the form:

$$\dot{x} \in \begin{cases} \{2 - x\} & \text{if } x < 1, \\ \{\lambda - x \mid 0 \leq \lambda \leq 2\} & \text{if } x = 1, \\ \{-x\} & \text{if } x > 1. \end{cases}$$

That is, with this definition, we are able to obtain an *absolutely continuous* solution of the system, which implies that the derivative exists almost everywhere for every point along a solution trajectory. The definition of the differential inclusion is described in detail for general differential equations with discontinuous right hand side in [18]. In the following, we present the differential inclusion for general PADEs as presented in [23, 16, 14, 15].

In order to define the differential inclusion on the singular domains formally, we require the following topological concepts.

Definition 2.3 Consider a set of PADEs of the form (2.4) with domain set \mathcal{D} . For every $D \in \mathcal{D}_s$ of order k , let $\text{supp}(D)$ be the $(n - k)$ -dimensional hyperplane in Ω containing D . If $D \in \mathcal{D}_r$, let $\text{supp}(D) = \Omega$. The *boundary* of D in $\text{supp}(D)$ is the set ∂D of all points $x \in \text{supp}(D)$ such that each ball $B_D(x, \epsilon)$ of center x and radius $\epsilon > 0$ in $\text{supp}(D)$ intersects with both D and $\text{supp}(D) \setminus D$. For all $D \in \mathcal{D}_s$, we define the set

$$\rho(D) = \{D' \in \mathcal{D}_r \mid D \subset \partial D'\}.$$

So, $\rho(D)$ is the set of all regular domains that have D in their boundary.

The differential inclusion on Ω is then:

$$\dot{x} \in \mathcal{H}(x) := \begin{cases} \{F^D - G^D x\} & \text{if } x \in D \in \mathcal{D}_r, \\ \overline{\text{co}}(\{F^{D'} - G^{D'} x \mid D' \in \rho(D)\}) & \text{if } x \in D \in \mathcal{D}_s, \end{cases} \quad (2.6)$$

where $\overline{\text{co}}(P)$ is the closed convex hull of the set P . In other words, the dynamics of a singular domain D is a convex combination of the dynamics of the neighbouring regular domains in $\rho(D)$.

Since the regular domain dynamics implies that the solution tends towards the focal point, the differential inclusion implies that in the singular domain D the solutions would converge to the convex hull of the focal points of domains in $\rho(D)$. However, because D is of Lebesgue measure zero, only solutions that continue along the supporting hyperplane $\text{supp}(D)$ remain in D . If the solution does not continue along the supporting hyperplane, then the solution would immediately exit D . These observations suggest the following concept.

Definition 2.4 Consider a set of PADEs with domain set \mathcal{D} . We define the *focal set* $\Phi(D)$ for every domain D as follows:

$$\Phi(D) := \begin{cases} \{\phi(D)\} & \text{if } D \in \mathcal{D}_r \\ \text{supp}(D) \cap \overline{\text{co}}(\{\phi(D') \mid D' \in \rho(D)\}) & \text{if } D \in \mathcal{D}_s \end{cases} .$$

Note that when the focal set is empty then solutions that start in the domain would immediately exit the domain. From [15], we know that in a singular domain D with (non-empty) focal set $\Phi(D)$ for every point $x^0 \in D$ and $\psi \in \Phi(D)$, solution trajectories of (2.4) starting at x^0 converge monotonically in D towards ψ . In other words, the focal set allows us to define solutions on singular as well as regular domains.

An absolutely continuous function $\xi : [0, \infty) \rightarrow \Omega$ is called a *PADE solution* of (2.6) on $[0, \tau]$ if $\xi(0) = x^0 \in \Omega$ and for almost all $t \in [0, \tau]$ it holds that $\xi(t) \in \mathcal{H}(\xi(t))$, where 'for almost all t ' means that the set of time points, for which the condition does not hold, is of Lebesgue measure zero. By the findings in [18, 23], for all initial values $x^0 \in \Omega$, there exists a PADE solution of (2.6). In other words, from the differential inclusion (2.6), we can define the dynamics of (2.4) on the entire phase space Ω .

In the case that $|\Phi(D)| > 1$ for a singular domain D , the dynamics in D is non-unique. Because of the non-unique dynamics on singular domains, we need to redefine equilibria with respect to the differential inclusion (2.6). More specifically, we have a singular equilibrium point $x^0 \in \Omega$ if

$$0 \in \mathcal{H}(x^0).$$

Consequently, if for some $D \in \mathcal{D}_s$ it holds that $\Phi(D) \cap D \neq \emptyset$, then D is said to have a *singular equilibrium set*, where all points in $\Phi(D) \cap D$ are singular equilibria. Examples of singular equilibria are presented in Ex. 2.3.

2.2.1 Discretised Approach (PADE-D)

The non-uniqueness of the PADE solutions in (2.6) suggests the need for a more qualitative representation of the dynamics. In other words, by discretising the PADE solutions, we are able to summarise all possible dynamics implied by the differential inclusion. The following discretisation approach, which we refer to as the *discretised PADE* (PADE-D) formalism, aims to represent all the dynamics of (2.6) in a directed graph.

The domains \mathcal{D} conveniently discretise the phase space Ω to define the node set of the transition graph. We are then able to represent the dynamics between domains via transitions, where a transition exists if a PADE solution traverses two adjacent domains in finite time.

Definition 2.5 Consider a set of PADEs with domain set \mathcal{D} . Let $D, D' \in \mathcal{D}$, where $D' \subset \partial D$, and PADE solution $\xi(t)$, which is defined on a finite time interval $[0, \tau]$.

1. The *transition* (D, D') exists if

$$\begin{aligned} \xi(t) &\in D \text{ for } 0 \leq t < \tau, \text{ and} \\ \xi(\tau) &\in D'. \end{aligned}$$

2. The *transition* (D', D) exists if

$$\begin{aligned} \xi(0) &\in D', \text{ and} \\ \xi(t) &\in D \text{ for } 0 < t \leq \tau. \end{aligned}$$

This definition describes when a solution trajectory exists that reaches D' from D or vice versa in finite time without passing through a third domain.

All transitions of a PADE system are summarised in the following directed graph.

Definition 2.6 Let \mathcal{A} be a set of PADEs of the form (2.4). The *qualitative transition graph*, $QTG^\Phi(\mathcal{A}) = (\mathcal{D}, \mathcal{T}^\Phi)$, is a directed graph with \mathcal{D} being the set of domains and \mathcal{T}^Φ the set of transitions as in Def. 2.5.

The qualitative transition graph, therefore, represents all qualitative behaviours in the PADE model incorporating the non-unique PADE solutions.

2.2.2 Qualitative Approach (PADE-Q)

The PADE solutions and the discretised PADE formalism both require kinetic parameters, which are often lacking. For this reason, de Jong et al. [15] developed the following qualitative approach, referred to as the *qualitative PADE* (PADE-Q) formalism, which assumes that the kinetic parameters satisfy inequalities rather than taking explicit values.

Definition 2.7 (Ordering Constraints) Let \mathcal{A} be a PADE with domain set \mathcal{D} . The *ordering constraints* are the set of constraints on the kinetic parameters such that for every regular domain $D \in \mathcal{D}_r$ and variable $i \in \{1, \dots, n\}$ one of the following inequality pairs is satisfied

$$\begin{aligned} 0 &\leq \phi_i(D) < \theta_i^1, \\ \theta_i^1 &< \phi_i(D) < \theta_i^2, \\ &\dots \\ \theta_i^{p_i} &< \phi_i(D) \leq \max_i. \end{aligned}$$

In other words, each focal point component satisfies strict inequalities with respect to the thresholds, where the ordering of the focal point components with respect to each other is not fixed. The qualitative PADE formalism then aims to express the dynamics of (2.6) in a transition graph assuming the ordering constraints.

In order to incorporate all dynamics implied by the multiple kinetic parameter sets of the ordering constraints into the analysis, de Jong et al. [15] overapproximate the differential inclusion (2.6). One interpretation of the overapproximated differential inclusion is the superposition of all the differential inclusions with specific kinetic parameters that all satisfy the same set of ordering constraints. For this reason, the overapproximated differential inclusion takes the form

$$\dot{x} \in \begin{cases} \{F^D - G^D x\} & \text{if } x \in D \in \mathcal{D}_r, \\ \overline{\text{rect}}(\{F^{D'} - G^{D'} x \mid D' \in \rho(D)\}) & \text{if } x \in D \in \mathcal{D}_s, \end{cases}$$

where $\overline{\text{rect}}(P)$ is the smallest closed hyperrectangular set that contains P . Consequently, the corresponding focal set is also overapproximated.

Definition 2.8 Consider a set of PADEs with domain set \mathcal{D} . We define the *overapproximated focal set* $\Psi(D)$ for every domain D as follows:

$$\Psi(D) := \begin{cases} \{\phi(D)\} & \text{if } D \in \mathcal{D}_r \\ \text{supp}(D) \cap \overline{\text{rect}}(\{\phi(D') \mid D' \in \rho(D)\}) & \text{if } D \in \mathcal{D}_s, \end{cases}.$$

Similar to the differential inclusion, we interpret the overapproximated focal set Ψ as the union of all focal sets Φ that have been generated from all kinetic parameters that satisfy the same ordering constraints. For this reason, solutions starting in $D \setminus \Psi(D)$ for some domain D converge monotonically to the (non-empty) focal set $\Psi(D)$ [22, 23, 15]. However, the behaviour of solutions starting in $D \cap \Psi(D)$ cannot be generalised for each set of kinetic parameters that satisfies the ordering constraints.

Remark 2.1 In order to discern between the two focal sets Φ and Ψ , we say that if $\Phi(D) \neq \emptyset$, then D has a non-empty focal set (also known as sliding mode [15, 23] or black/white wall [41]), while if $\Psi(D) \neq \emptyset$, then D is a *non-transparent* domain. On the other hand, if $\Phi(D) = \emptyset$, then D has an empty focal set (also known as a spontaneous domain [15, 23]), while if $\Psi(D) = \emptyset$ then D is a *transparent* domain. Therefore, by definition, $\Phi(D) \subset \Psi(D)$ for all $D \in \mathcal{D}$ and thus a domain with a non-empty focal set is always a non-transparent domain and a transparent domain always has an empty focal set.

The hyperrectangular form of the domains and the overapproximated focal set means that we can express them as product sets. In consequence, the dynamics of each domain for each dimension can be calculated separately. Hence, we can define the transitions between domains using the relative position.

Definition 2.9 (Relative Position) Consider a set of PADEs of the form (2.4). Let $D \in \mathcal{D}$ and $e \in \Omega$. We call the mapping $v : \mathcal{D} \times \Omega \rightarrow \{-1, 0, 1\}^n$ the *relative position vector* and define it as follows

$$v_i(D, e) = \begin{cases} -1 & \text{if } e_i < x_i, \text{ for all } x \in D \\ 0 & \text{if } e_i = x_i, \text{ for some } x \in D \\ +1 & \text{if } e_i > x_i, \text{ for all } x \in D \end{cases} .$$

Let $E \subset \Omega$ be a non-empty set of points. The set $V(D, E)$ is defined as

$$V(D, E) := \{v(D, e) | e \in E\}.$$

Taking into account the above considerations about the behaviour of the system with respect to the focal points, we can interpret the i -th component of $\nu \in V(D, \Psi(D))$ as an instruction for the variable x_i to increase ($\nu_i = 1$), decrease ($\nu_i = -1$) or remain steady ($\nu_i = 0$) in domain D . Note that the definition of the domains in \mathcal{D} ensures that $V(D, D')$ is a singleton for all $D, D' \in \mathcal{D}$.

The dynamics in a domain D can be determined by the relative position of the focal set $\Psi(D)$ with respect to the domain D .

Definition 2.10 Consider a set of PADEs of the form (2.4). Let $D, D' \in \mathcal{D}$ such that $D' \subset \partial D$.

1. There is a *transition* (D, D') from D to D' if
 - (a) $\Psi(D) \neq \emptyset$, and
 - (b) for $V(D, D') = \{w\}$ there exists $\nu \in V(D, \Psi(D))$ such that $\nu_i w_i = 1$ for every $x_i, i \in \{1, \dots, n\}$ that is a singular variable in D' but not in D .
2. There is a *transition* (D', D) from D' to D if
 - (a) $\Psi(D) \neq \emptyset$, and
 - (b) for $V(D', D) = \{w'\}$ there exists $\nu \in V(D, \Psi(D))$ such that $\nu_i w'_i \neq -1$ for every $x_i, i \in \{1, \dots, n\}$ that is a singular variable in D' but not in D .

Def. 2.10 is extracted from Propositions 6.4 and 6.5 in [15], whose proofs describe the relation between Def. 2.10 and Def. 2.5.

With this definition, we construct the corresponding overapproximated qualitative transition graph, which summarises all the dynamics in (2.4) assuming the ordering constraints.

Definition 2.11 Let A be a set of PADEs of the form (2.4). The *overapproximated qualitative transition graph*, $QTG^\Psi(A) = (\mathcal{D}, \mathcal{T}^\Psi)$, is a directed graph with \mathcal{D} being the set of domains and \mathcal{T}^Ψ the set of transitions as defined in Def. 2.10.

As shown in [15], all systems in the class of PADEs satisfying the same ordering constraints have the same QTG^Ψ . Given that QTG^Ψ is superimposing all dynamics implied by the ordering constraints, it is intuitively clear that every QTG^Φ is a subgraph of a QTG^Ψ [15].

From Def. 2.10, we can easily see that we do not need the full information inherent in the ordering constraints to determine the outgoing transitions for a given domain D . In particular, we can utilize just the set $V(D, \Psi(D))$ for all $D \in \mathcal{D}$ to determine the QTG^Ψ . For a regular domain D , we have

$$V(D, \Psi(D)) = \{v(D, \phi(D))\},$$

by Def. 2.8. For a singular domain D , the situation is not as clear-cut. However, Propositions 6.2 and 6.3 in [15] characterize the set $V(D, \Psi(D))$ also for singular domains. The characterization is rooted in the overapproximation of the set of focal points of adjacent regular domains by a hyperrectangle. The results in [15] are not formulated in terms of relative position vectors, but they can easily be rephrased. Thus, we derive the following proposition.

Proposition 2.1 Consider a set of PADEs of the form (2.4) and let $D \in \mathcal{D}_s$. We have $\Psi(D) \neq \emptyset$ if and only if for all singular variables x_i in D , we have

$$\min_{D' \in \rho(D)} v_i(D, \phi(D')) = -1 \text{ and } \max_{D' \in \rho(D)} v_i(D, \phi(D')) = 1. \quad (2.7)$$

Let $D \in \mathcal{D}_s$ and $\Psi(D) \neq \emptyset$. Define $V_i(D, \Psi(D)) := \{v_i \mid v \in V(D, \Psi(D))\}$. Then, for all $i \in \{1, \dots, n\}$, if x_i is a singular variable, $V_i(D, \Psi(D)) = \{0\}$, and if x_i is a non-singular variable

$$V_i(D, \Psi(D)) = \left[\min_{D' \in \rho(D)} v_i(D', \phi(D')), \max_{D' \in \rho(D)} v_i(D', \phi(D')) \right], \quad (2.8)$$

where $[a, b] = \{a, a+1, \dots, b-1, b\}$ denotes the discrete interval for $a \leq b \in \mathbb{N}$.

To determine the transitions of the QTG^Ψ , we only need to know the set $V(D, \Psi(D))$ for all domains D . Obviously, we can derive this set immediately from $v(D, \phi(D))$ for regular domains D . For a singular domain D' , easy calculation using Prop. 2.1 and the definition of $\Psi(D')$ show that the information inherent in the set $\{v(D, \phi(D)) \mid D \in \mathcal{D}_r\}$ is sufficient to derive $V(D', \Psi(D'))$. We summarize these observations in the following lemma.

Lemma 2.1 *Let \mathcal{A} be a set of PADEs. The positions of the focal points in relation to their corresponding regular domains, i.e., $\{v(D, \phi(D)) \mid D \in \mathcal{D}_r\}$, is sufficient to calculate $QTG^\Psi(\mathcal{A}) = (\mathcal{D}, \mathcal{T})$.*

Conversely, it is easy to see from the definitions that we can derive the relative position vectors $v(D, \phi(D))$ for regular domains from both QTG^Ψ and QTG^Φ .

Example 2.3 Consider the following PADEs, which approximate Ex. 2.1 using step functions,

$$\begin{aligned}\dot{x}_1 &= \kappa_1 S^-(x_2, \theta_2) + \kappa_2 S^+(x_1, \theta_1^2) - \lambda_1 x_1, \\ \dot{x}_2 &= \kappa_3 S^+(x_1, \theta_1^1) - \lambda_2 x_2,\end{aligned}$$

with the ordering constraints

$$0 < \theta_1^1 < \theta_1^2 < \frac{\kappa_1}{\lambda_1}, \frac{\kappa_2}{\lambda_1}, \frac{\kappa_1 + \kappa_2}{\lambda_1} < \max_1 \quad \text{and} \quad (2.9)$$

$$0 < \theta_2 < \frac{\kappa_3}{\lambda_2} < \max_2. \quad (2.10)$$

The system has six regular domains with corresponding focal points, e.g. the focal point of $D = [0, \theta_1^1] \times [0, \theta_2]$ is $(\frac{\kappa_1}{\lambda_1}, \frac{\kappa_3}{\lambda_2})$. Consider the regular domain $D = [0, \theta_1^1] \times [0, \theta_2]$ and singular domain of order one $D' = [\theta_1^1] \times [0, \theta_2]$. We have the corresponding focal sets $\Psi(D) = \{(\frac{\kappa_1}{\lambda_1}, \frac{\kappa_3}{\lambda_2})\}$ and $\Psi(D') = \emptyset$. The relative positions yield $V(D, \Psi(D)) = \{(1, 1)\}$ and $V(D', \Psi(D')) = \emptyset$. Because $D' \subset \partial D$ and $V(D, D') = \{(1, 0)\}$, we have $(D, D') \in \mathcal{T}$. The phase space of the above PADEs and the corresponding QTG^Ψ are displayed in Fig. 2.3. We recognise the point $[\theta_1^1] \times [\theta_2]$ to be a singular equilibrium point and the domain $[\theta_1^2] \times (\theta_2, \max_2]$ to have a singular equilibrium set.

2.2.3 Refined Approach (PADE-R)

A compromise between the lack of kinetic parameters and demand for continuous dynamics is the finer partitioning of the phase space Ω . In particular,

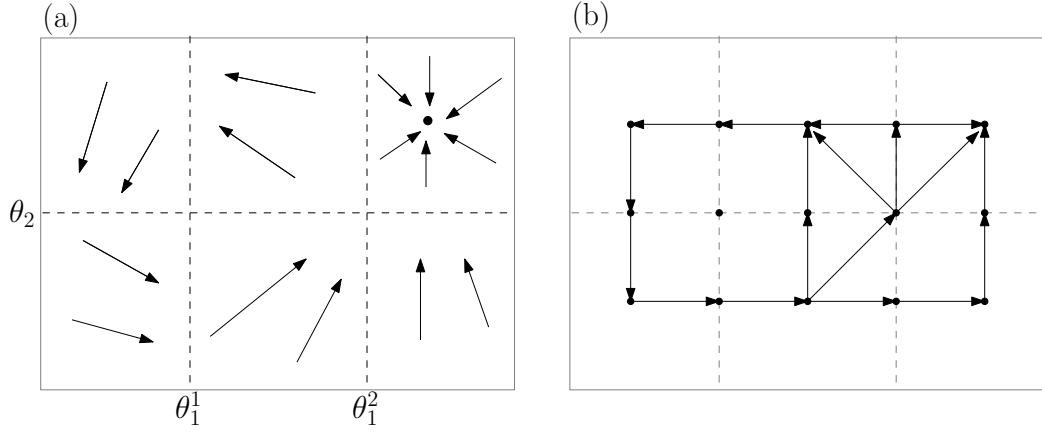


Figure 2.3: In (a), the partitioned phase space of the PADEs in Ex. 2.3, where the dashed grey lines represent the threshold hyperplanes. In (b), the corresponding QTG^Ψ , which overlays the partitioned phase space to allow identification of nodes representing singular and regular domains. The arrows within each regular domain in (a) are directed towards their focal point.

the regular and singular domains described above are further partitioned by means of the $(n - 1)$ -dimensional hyperplanes corresponding to the components of the focal point vectors. The formalism that comes from this refined partition of the phase space is referred to as the *refined PADE* (PADE-R) formalism. To maintain the terminology used by Batt et al. [4], where the refined PADE formalism is introduced, the remainder of this section refers to the domains in \mathcal{D} as *mode domains*.

In order to determine the finer partitioning of Ω , we assume a total ordering, that is strict inequalities, of the threshold concentrations $\{\theta_i^1, \dots, \theta_i^{p_i}\}$ and the components of the focal point vectors $\{\phi_i(D) | D \in \mathcal{D}_r\}$. This ordering is referred to as the *parameter inequality constraints*. Note that the parameter inequality constraints have the additional ordering of the focal point components with respect to each other, which is otherwise lacking in the ordering constraints of the qualitative PADE formalism. From the parameter inequality constraints, we can obtain the finer partitioning of Ω .

Definition 2.12 Consider a set of PADEs with mode domain set \mathcal{D} . We define $\mathcal{M}^D = \mathcal{M}_1^D \times \dots \times \mathcal{M}_n^D$, where \mathcal{M}_i^D is the partition of minimal cardinality of D_i such that for every $M_i \in \mathcal{M}_i^D$,

- if D is regular, either $M_i = \{x_i \in D_i | x_i = \phi_i(D)\}$ or $M_i \subset D_i$ such that $\phi_i(D) \notin M_i$, and
- if D is singular, either $M_i = \{x_i \in D_i | x_i = \phi_i(D') \text{ for some } D' \in \rho(D)\}$

or $M_i \subset D_i$ such that $\phi_i(D') \notin M_i$ for any $D' \in \rho(D)$.

$\mathcal{M} := \bigcup_{D \in \mathcal{D}} \mathcal{M}^D$ is a partition of Ω and a set $M \in \mathcal{M}$ is called a *flow domain*.

The term 'flow domain' is used because the flow of the system is qualitatively identical, meaning that in a flow domain each variable has the same sign of derivative. In mathematical terms, we can define a function $S : \mathcal{M} \rightarrow 2^{\{-1,0,1\}^n}$ that represents the *sign of derivative* of a flow domain $M \in \mathcal{M}$, where

$$S_i(M) = \{sgn(\dot{x}_i) \mid x \in M\}.$$

The non-uniqueness of the differential inclusion means that the cardinality of $S_i(M)$ need not be equal to one.

Every flow domain is included in a single mode domain, a relation captured by the surjective function $mode : \mathcal{M} \rightarrow \mathcal{D}$ defined as $mode(M) = D$ if and only if $M \subset D$. The flow domains \mathcal{M} and the overapproximated focal sets $\Psi(D)$ are hyperrectangular meaning that we can express them as product sets. In consequence, we can compute the qualitative dynamics of each flow domain for each dimension separately. As a result, all the qualitative dynamics of the refined PADE is given by the following graph.

Definition 2.13 Let \mathcal{A} be a PADE whose parameter values satisfy a set of parameter inequality constraints. The qualitative transition system $QTS(\mathcal{A}) = (\mathcal{M}, \rightarrow)$ is a directed graph with the node set \mathcal{M} . The transitions $\rightarrow \subset \mathcal{M} \times \mathcal{M}$ are defined as follows. Let $M, M' \in \mathcal{M}$ such that $M' \subset \partial M$,

1. $M \rightarrow M'$ if and only if $\Psi(mode(M)) \neq \emptyset$ and there exists $x \in M, x' \in M'$ and $\psi \in \Psi(mode(M))$ such that either

- (a) for all $i \in \{1, \dots, n\}$ for which $M'_i \subset \partial M_i$, it holds that

$$(\psi_i - x'_i)(x'_i - x_i) > 0,$$

or

- (b) it holds that $\psi = x'$.

2. $M' \rightarrow M$ if and only if $\Psi(mode(M)) \neq \emptyset$ and there exists $x \in M, x' \in M'$ and $\psi' \in \Psi(mode(M))$ such that for all $i \in \{1, \dots, n\}$ for which $M'_i \subset \partial M_i$, it holds that

$$(\psi'_i - x'_i)(x_i - x'_i) > 0.$$

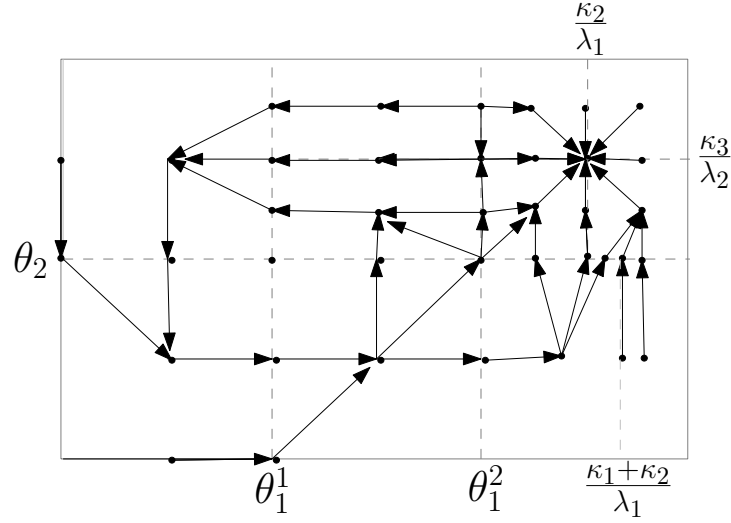


Figure 2.4: The transition system (QTS) of Ex. 2.3 corresponding to the parameter inequality constraints in Ex. 2.4. The phase space is bounded by the unbroken grey line and the dashed grey lines represent either the threshold hyperplanes or the focal point components that partition the phase space into flow domains (depicted by the black dots).

The transition definitions above are extracted from Prop. 7 and 8 in [4].

Example 2.4 Consider the running example in Ex. 2.3 with the parameter inequality constraints:

$$0 < \theta_1^1 < \theta_1^2 < \frac{\kappa_1}{\lambda_1} < \frac{\kappa_2}{\lambda_1} < \frac{\kappa_1 + \kappa_2}{\lambda_1} < \max_1 \quad \text{and} \\ 0 < \theta_2^1 < \frac{\kappa_3}{\lambda_2} < \max_2.$$

Note that the inequalities above contain the ordering of the focal point components with respect to each other unlike the ordering constraints in (2.9). In the QTS in Fig. 2.4, we see that the focal point $\phi(D) = (\kappa_1/\lambda_1, 0)$ partitions the regular mode domain $D = [0, \theta_1^1] \times [0, \theta_2]$ into the two flow domains $(0, \theta_1^1) \times [0, \theta_2]$ and $[0] \times [0, \theta_2]$, that is $\mathcal{M}_1^D = \{[0], (0, \theta_1^1)\}$.

2.3 Discrete Models

Here, we present our two discrete formalisms of interest, the *Thomas* formalism [64, 63] and its extension referred to as the *singular state* formalism [57].

In the following, we use the dimension n and the number of thresholds p_i of the ODE model for related objects in the discrete models.

2.3.1 Thomas Formalism

Consider a gene regulatory network of n components. The activity level of component $i \in \{1, \dots, n\}$ is modeled by a discrete variable q_i , which takes its values in a finite set of natural numbers $Q_i = \{0, \dots, p_i\}$. The *state space* of the Thomas model is $Q = Q_1 \times \dots \times Q_n$ and the regulatory interactions are captured by a discrete *update function* $f = (f_1, \dots, f_n) : Q \rightarrow Q$. The *logical parameters* are interpreted as the images $f(q)$ of each state $q \in Q$.

From f , we obtain the *state transition graph* $STG(f) = (Q, E)$, which is a directed graph with node set Q and edge set $E \subset Q \times Q$. For any $i \in \{1, \dots, n\}$ with $f_i(q) \neq q_i$, $q \in Q$, there is an edge $(q, q') \in E$, where

$$q'_i = q_i + \text{sgn}(f_i(q) - q_i) \text{ and } q'_j = q_j, \text{ for all } j \in \{1, \dots, n\} \setminus \{i\}.$$

Here, $\text{sgn} : \mathbb{R} \rightarrow \{-1, 0, 1\}$ denotes the sign function. If $f(q) = q$, then $(q, q) \in E$ and q is called a *fixed point*.

The update function uniquely determines the state transition graph. Unless f is Boolean, it is not possible to recover f from $G = STG(f)$. However, we may obtain a *unitary update function* $f^G : Q \rightarrow Q$ from G by setting

$$f_i^G(q) = q_i + \sum_{q' \in AS(q)} (q'_i - q_i), \text{ for } i \in \{1, \dots, n\}.$$

Here, $AS(q) := \{q' \in Q \mid (q, q') \in E\}$ denotes the set of *asynchronous successors* of q in G . Note that the superscript notation is used throughout the thesis, where f^X represents the update function derived or constructed from the object X .

Lemma 2.2 *Let $f : Q \rightarrow Q$ be an update function and $G = STG(f)$. Then*

$$STG(f) = STG(f^G).$$

PROOF Let $j \in \{1, \dots, n\}$ and $q \in Q$. By definition of $AS(q)$, there exists at most one $q' \in AS(q)$ such that $|q'_j - q_j| = 1$. This implies $\text{sgn}(f_j(q) - q_j) = q'_j - q_j$. Therefore, $\text{sgn}(f_j(q) - q_j) = \sum_{q' \in AS(q)} (q'_j - q_j)$, and the result follows. \square

The unitary update function f^G captures the information from the original update function f contained in $G = STG(f)$. If f is Boolean, f and f^G are the same. An example of a Thomas model is displayed in Fig. 2.5.

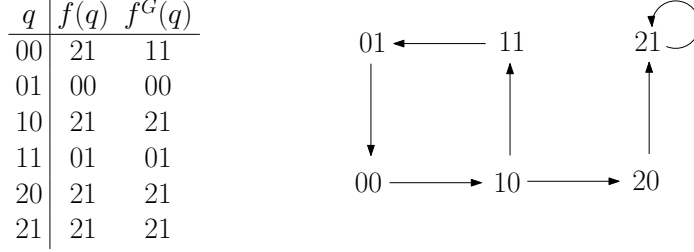


Figure 2.5: For $Q = \{0, 1, 2\} \times \{0, 1\}$, the update function $f : Q \rightarrow Q$ and corresponding unitary update function f^G on the left and state transition graph $G = STG(f)$ on the right.

2.3.2 Singular State Formalism

Because the *singular state formalism* is built on an interaction graph and logical parameters, we introduce them here as in [48]. However, recall that our focus is on relating the dynamics of different formalisms and not the relation of dynamics and structure of a network.

The *interaction graph*, $G = (\{1, \dots, n\}, \bar{E})$, is a directed graph where $\bar{E} \subset \{1, \dots, n\} \times \{1, \dots, n\}$ is the set of interactions. Each interaction $i \rightarrow j \in \bar{E}$ is labeled by a pair $(\alpha_{ij}, t_{ij}) \in \{+, -\} \times \{1, \dots, p_i\}$, such that for all $j' \neq j$ it holds that $t_{ij} \neq t_{ij'}$, where $i \in \text{Pred}(j)$ and $i \in \text{Pred}(j')$, $p_i = |\{j \in \{1, \dots, n\} \mid i \rightarrow j \in \bar{E}\}|$ and

$$\text{Pred}(j) = \{i \in \{1, \dots, n\} \mid i \rightarrow j \in \bar{E}\}.$$

Although p_i is specifically defined here it will later be related to the thresholds of the ODE model. Note that there are more general definitions of the interaction graph in the literature that allow multiple interactions per component (e.g. [37]). However, in order to define the dynamics in the singular state formalism, we require the definition above.

The *logical parameters*, $\{K_{i,\omega}\}$, are a family of integers that describe the evolution of component $i \in \{1, \dots, n\}$ depending on the nodes $\omega \subset \text{Pred}(i)$ and satisfy the properties:

- $K_{i,\emptyset} = 0$ and $K_{i,\omega} \in \{0, \dots, p_i\}$ otherwise, and
- $\omega \subset \omega' \implies K_{i,\omega} \leq K_{i,\omega'}$. (Monotonicity property)

The logical parameter $K_{i,\omega}$ represents the activity level that variable i tends towards given the activating influences of the components in ω . Therefore,

we interpret the monotony property as a component's activity level increasing with increasing activating influences. This assumption, therefore, rules out the case where two activating components have a neutral effect on the target component rather than an activating effect. In other words, the logical parameters and the interaction graph restrict the dynamics generated by the singular state formalism.

The component $i \in \{1, \dots, n\}$ is modelled with the discrete variable s_i , which takes *qualitative values* between 0 and p_i .

Definition 2.14 • A *qualitative value*, denoted $|a, b|$ is a pair of integers ($|a, b| \in \mathbb{N}^2$) where $a \leq b$.

- The relations $=, <, >, \subset$ are defined for 2 qualitative values $|a, b|$ and $|c, d|$:
 - $|a, b| = |c, d|$ if $(a = c)$ and $(b = d)$.
 - $|a, b| < |c, d|$ if $(b < c)$ or $(b = c$ and $(a < b$ or $c < d))$
 - $|a, b| > |c, d|$ if $|c, d| < |a, b|$
 - $|a, b| \subset |c, d|$ if $\begin{cases} |a, b| = |c, d| \text{ or} \\ (a = b) \text{ and } (c < a) \text{ and } (b < d) \text{ or} \\ (a < b) \text{ and } (c \leq a) \text{ and } (b \leq d) \end{cases}$

Therefore, a state $s = (s_1, \dots, s_n)$ in the *extended state space* $\Sigma = \Sigma_1 \times \dots \times \Sigma_N$ is composed of the discrete variables $s_i \in \Sigma_i := \{|0|, |0, 1|, |1|, \dots, |r - 1|, |r - 1, r|, |r|, \dots, |p_i|\}$, where $|a| := |a, a|$. A state s is *singular* if it has at least one singular value, that is $s_i = |r - 1, r|$ for some $i \in \{1, \dots, n\}$, otherwise it is *regular*. The function $ord : \Sigma \rightarrow \{0, 1, \dots, n\}$ denotes the number of singular values of a state $s \in \Sigma$. Note that the function ord is acting on singular states in the singular state formalism, whereas the term *order* is referring to singular domains in the PADEs.

The dynamics inferred by the interaction graph \bar{G} coupled with the logical parameters $\{K_{i,\omega}\}$ are encoded into the function $g : \Sigma \rightarrow 2^\Sigma$ called the *extended update function*, such that for all $s \in \Sigma$ and $i \in \{1, \dots, n\}$,

$$g_i(s) = |K_{i,Reg_i(s)}, K_{i,Reg_i(s) \cup Sing_i(s)}|, \quad (2.11)$$

where 2^Σ is the power set of Σ , the set of *regular resources* $Reg_i(s)$ is

$$Reg_i(s) = \{j \in Pred(i) \mid (s_j > |t_{ji}-1, t_{ji}| \wedge \alpha_{ji} = +) \vee (s_j < |t_{ji}-1, t_{ji}| \wedge \alpha_{ji} = -)\} \quad (2.12)$$

and the set of *singular resources* $Sing_i(s)$ is

$$Sing_i(s) = \{j \in Pred(i) \mid s_j = |t_{ji} - 1, t_{ji}|\}.$$

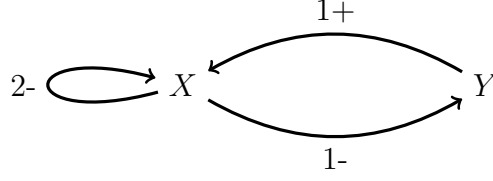


Figure 2.6: Interaction graph of Ex. 2.5. The component X has two outgoing edges, which implies three activity levels, namely 0,1 and $p_X := 2$, while the component Y has one outgoing edge corresponding to two activity levels, namely 0 and $p_Y := 1$.

The extended update function is extracted from Theorem 3.3 in [48]. With the definition (2.11), we see why the logical parameters are defined as they are. In particular, we need the monotony property to hold so that $K_{i,Reg_i(s)} \leq K_{i,Reg_i(s) \cup Sing_i(s)}$, which gives a valid qualitative value (2.11).

From the extended update function g , we present the dynamics of the interaction graph in an *extended state graph* $ESG(g) = (\Sigma, T)$, which is a directed graph with node set Σ and transition set $T \subset \Sigma \times \Sigma$, where

- $(s, s) \in T$ if s is steady, that is $s_i \subset g_i(s)$ for all $i \in \{1, \dots, n\}$.
- $(s, s') \in T$ if there exists $j \in \{1, \dots, n\}$ such that either

$$\begin{cases} s'_j = \Delta_j^+(s) \text{ and } s_j < g_j(s) \\ \text{or} \\ s'_j = \Delta_j^-(s) \text{ and } s_j > g_j(s) \end{cases} \text{ and } s'_i = s_i \text{ for all } i \in \{1, \dots, n\} \setminus \{j\},$$
 where Δ_j^+ and Δ_j^- are the *evolution operators* defined as follows:

$$\begin{aligned} \Delta_j^+(s) &= \begin{cases} |r, r+1| & \text{if } s_j = |r| \\ |r| & \text{if } s_j = |r, r-1| \end{cases}, \text{ and} \\ \Delta_j^-(s) &= \begin{cases} |r, r-1| & \text{if } s_j = |r| \\ |r| & \text{if } s_j = |r, r+1| \end{cases}. \end{aligned}$$

Similar to the Thomas formalism, the extended update function uniquely determines the extended state graph and unless $p_i = 1$ for all $i \in \{1, \dots, n\}$, it is not possible to recover g from $ESG(g)$.

Example 2.5 Consider the interaction graph $\bar{G} = (\{X, Y\}, E)$ in Fig. 2.6 with logical parameters, $K_{X,\emptyset} = K_{Y,\emptyset} = 0$, $K_{Y,X} = 1$ and $K_{X,X} = K_{X,Y} = K_{X,XY} = 2$. The two states $s := (|1\rangle, |0\rangle)$ and $s' := (|1\rangle, |0, 1\rangle)$ have updates $g(s) = (|2\rangle, |0\rangle)$ and $g(s') = (|0, 2\rangle, |1\rangle)$. That is, $g_1(s') = |K_{X,\emptyset}, K_{X,X}| = |0, 2|$ and $g_2(s') = |K_{Y,X}, K_{Y,X}| = |K_{Y,X}| = |1|$. The resulting extended state graph is displayed in Fig. 2.7

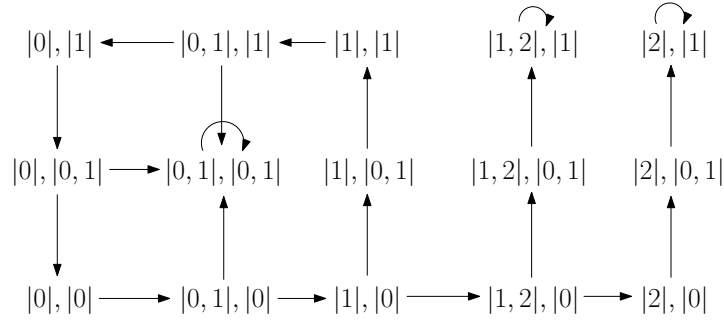


Figure 2.7: The extended state graph of Ex. 2.5 displayed on the extended state space, $\Sigma := \{|0|, |0, 1|, |1|\} \times \{|0|, |0, 1|, |1|, |1, 2|, |2|\}$.

A summary of all the formalisms presented in this chapter is given in Table 2.1.

Formalism	Parameter Information	Dynamical information
ODE	kinetic parameters + $\theta_i^j + \epsilon_{ij}$	$\bar{\xi}(t)$
PMA	kinetic parameters + $[\theta_i^{j,0}, \theta_i^{j,1}]$	$\bar{\xi}(t)$
PADE solutions	kinetic parameters + θ_i^j	$\xi(t)$
PADE-D	kinetic parameters + θ_i^j	QTG^Φ
PADE-Q	ordering constraints	QTG^Ψ
PADE-R	parameter inequality constraints	QTS
Thomas	update function	STG
Singular state	logical parameters	ESG

Table 2.1: A summary table of all the formalisms of interest in terms of their parameter and dynamical information.

Qualitative Formalisms

We start our investigation by relating the Thomas, singular state and qualitative PADE formalisms. All three modelling approaches have the common feature of using qualitative parameter information in the form of logical parameters for the Thomas [63] and singular state formalisms [48], and ordering constraints for the qualitative PADE (PADE-Q) formalism [15]. In this chapter, we show that the logical parameters and ordering constraints share the same information in the sense that we can convert the logical parameters to ordering constraints and vice versa without losing information. This common underlying parameter information then allows us to directly compare the transition graphs of each formalism. We will see that in spite of the existence of a direct relationship between the edges in the transition graphs, we still are able to find inconsistent complex dynamics, that is paths and attractors do not generally coincide. In other words, we aim to show that the singular state and qualitative PADE formalisms are not refinements of the Thomas formalism. Then, we discuss how the singular state and qualitative PADE formalisms attempt to represent the equilibria in the ODEs. We start this chapter with the already published result [29] that relates the qualitative PADE and Thomas formalisms.

3.1 The Thomas and PADE-Q Formalisms

In the following, we show that the qualitative PADE and the Thomas formalism contain the same information in the sense that we can transform a PADE system with given ordering constraints into a discrete update function and vice versa.

To obtain a discrete update function from a PADE system, we can use a straightforward method originally proposed by Snoussi in [56]. First, we discretise the continuous phase space of the PADE system according to its

threshold values.

Definition 3.1 Let \mathcal{A} be a set of PADEs as in (2.4), where each variable x_i has p_i threshold values that satisfy the ordering (2.1). Let $Q := Q_1 \times \cdots \times Q_n$, where $Q_i := \{0, 1, \dots, p_i\}$, $i \in \{1, \dots, n\}$. Define the bijective mapping $d^{\mathcal{A}} : \mathcal{D}_r \rightarrow Q$, where

$$d_i^{\mathcal{A}}(D) := \begin{cases} 0 & \text{if } D_i = \{x \in \mathbb{R} \mid 0 \leq x < \theta_i^1\}, \\ q & \text{if } D_i = \{x \in \mathbb{R} \mid \theta_i^q < x < \theta_i^{q+1}\}, \\ p_i & \text{if } D_i = \{x \in \mathbb{R} \mid \theta_i^{p_i} < x \leq \max_i\}. \end{cases}$$

Second, we exploit the localisation of the focal points in the regular domains in order to construct an update function on the discretised state space Q that shares the dynamical properties of the PADE system \mathcal{A} . Note that, in general, such a focal point may lie on a threshold plane, which by definition has no corresponding value in Q . As in the previous chapter, we exclude the comparatively small set of PADE systems with focal points on a threshold plane.

Definition 3.2 Let \mathcal{A} be a set of PADEs as in (2.4) such that all focal points lie in regular domains and let $d = d^{\mathcal{A}}$ be the mapping in Def. 3.1. Define an update function $f^{\mathcal{A}} : Q \rightarrow Q$ by

$$q \mapsto d(D_{\phi((d^{-1}(q)))}),$$

where $D_{\phi(D')}$ denotes the regular domain containing the focal point $\phi(D')$ of the regular domain D' .

The function $f^{\mathcal{A}}$ is uniquely determined by the ordering constraints for \mathcal{A} . Consequently, the set of PADE systems \mathcal{A} satisfying given ordering constraints can be associated with a single discrete update function $f^{\mathcal{A}}$. Conversely, a discrete update function can easily be transformed into a PADE system that shares the same qualitative dynamics.

Definition 3.3 Let $f : Q \rightarrow Q$ be an update function. We denote by $PADE(f)$ the system of PADEs on $\Omega := \prod_{i=1}^n [0, \max_i]$, $\max_i \in \mathbb{R}_{>0}$ for all $i \in \{1, \dots, n\}$, of the form $\dot{x}_i = F_i(x) - x_i$, $i \in \{1, \dots, n\}$, where

$$F_i(x) = \sum_{q \in Q} f_i(q) \prod_{j=1}^n S(x_j, q_j), \text{ with}$$

$$S(x_j, q_j) = \begin{cases} S^+(x_j, \theta_j^{q_j}) S^-(x_j, \theta_j^{q_j+1}) & \text{if } q_j \in \{1, \dots, p_j - 1\}, \\ S^-(x_j, \theta_j^1) & \text{if } q_j = 0, \\ S^+(x_j, \theta_j^{p_j}) & \text{if } q_j = p_j, \end{cases}$$

and $\theta_j^k = k - 1/2$ for $j \in \{1, \dots, n\}$, $k \in \{1, \dots, p_j\}$.

The choice of threshold values is generic, ensuring an obvious correspondence between the values $0, 1, \dots, p_i$ in Q_i , $i \in \{1, \dots, n\}$, and the intervals $[0, \theta_i^1)$, $(\theta_i^k, \theta_i^{k+1})$ for $k \in \{1, \dots, p_i - 1\}$, and $(\theta_i^{p_i}, \max_i]$. If we calculate the regular domains according to the threshold values and their focal points, we have $\phi(D) = F(x) = f(d(D))$ for all $x \in D$, where $d := d^{PADE(f)}$ and $D \in \mathcal{D}_r$. Equivalently, it holds that $\phi(d^{-1}(q)) \in d^{-1}(f(q))$ for $q \in Q$, which immediately implies that the focal points of $PADE(f)$ satisfy the set of corresponding ordering constraints. Therefore, we can apply Def. 3.2 to $PADE(f)$ and by construction, we then have $f^{PADE(f)} = f$.

In contrast, we generally do not have equality of the PADE systems \mathcal{A} and $PADE(f^{\mathcal{A}})$ due to the normalised form of $PADE(f^{\mathcal{A}})$. However, threshold order and relative focal point positions obviously coincide, i.e., \mathcal{A} and $PADE(f^{\mathcal{A}})$ satisfy the same ordering constraints. In consequence, the two corresponding overapproximated qualitative transition graphs are isomorphic, and only differ in the specific set of real vectors contained in corresponding domains, i.e., the designation of the vertices of the QTG^Ψ s. We summarise the preceding observations in the following proposition.

Proposition 3.1 *Let $f : Q \rightarrow Q$ be an update function and \mathcal{A} be a PADE system such that all focal points lie in regular domains. We then have*

$$f^{PADE(f)} = f \text{ and therefore } STG(f^{PADE(f)}) = STG(f).$$

Furthermore,

$$QTG^\Psi(\mathcal{A}) \cong QTG^\Psi(PADE(f^{\mathcal{A}})),$$

where ' \cong ' denotes graph isomorphism.

Using these two transformations, we can associate a class of PADE systems characterised by their ordering constraints with a unique discrete update function, and vice versa. In other words, the information necessary for constructing the STG resp. QTG^Ψ is inherent in both representations. In that sense, we can identify every STG with a QTG^Ψ and vice versa. However, this does not imply that the resulting qualitative dynamics are the same. In the following, we analyse differences and similarities between the STG and QTG^Ψ of a discrete function resp. the corresponding set of PADE systems.

Example 3.1 Our update function f in Fig. 2.5 generates $PADE(f)$ whose parameter values satisfy the ordering constraints of the PADE system \mathcal{A} introduced in Ex. 2.3. Therefore, $PADE(f)$ belongs to the class of PADEs represented by \mathcal{A} in Fig. 2.3. Similarly, if we discretise \mathcal{A} using Snoussi's method, we obtain the update function f in Fig. 2.5.

Correspondence of Edges

Throughout this section we consider an update function $f : Q \rightarrow Q$ and the PADE system $\mathcal{A} := PADE(f)$ representing the class of PADE systems corresponding to f according to the preceding section. In particular, discretisation of \mathcal{A} via the function $d := d^{\mathcal{A}}$ yields f . The aim of this section is the comparison of $STG(f) = (Q, E)$ and $QTG^{\Psi}(\mathcal{A}) = (\mathcal{D}, \mathcal{T})$.

Although we can obtain $STG(f)$ from $QTG^{\Psi}(\mathcal{A})$ and vice versa, it is not clear whether the two graphs can be constructed from each other without knowing the underlying formalisms. In the multi-valued other than in the Boolean setting, the state transition graph $STG(f)$ generally does not carry enough information to reconstruct f . However, by definition it is possible to derive the unitary update function $\tilde{f} := f^{STG(f)}$. We have already seen that $\tilde{f}(q) - q_j = \text{sgn}(f_j(q) - q_j)$ for all $q \in Q$, $j \in \{1, \dots, n\}$. Furthermore, we know from the preceding section that $\phi(d^{-1}(q)) \in d^{-1}(f(q))$. Applying the definition for the relative position vector $v_j(d^{-1}(q), \phi(d^{-1}(q)))$ (see Def. 2.9), we immediately obtain the following lemma.

Lemma 3.1 *For all $q \in Q$ and $j \in \{1, \dots, n\}$, we have*

$$v_j(d^{-1}(q), \phi(d^{-1}(q))) = \tilde{f}_j(q) - q_j, \quad (3.1)$$

and similarly,

$$v_j(D, \phi(D)) = \tilde{f}_j(d(D)) - d_j(D)$$

for all $D \in \mathcal{D}_r$.

Given the right hand side of (3.1), we are able to reconstruct $STG(f)$ by definition of the state transition graph, while Lemma 2.1 ensures that we can build $QTG^{\Psi}(\mathcal{A})$ knowing the relative position vectors given by the left hand side of (3.1). In addition, given $STG(f)$ and $QTG^{\Psi}(\mathcal{A})$, we can extract the unitary update function and the relative position vectors for regular domains. Consequently, we can construct $STG(f)$ given $QTG^{\Psi}(\mathcal{A})$ and vice versa. In the following, we will see that despite this correspondence of $STG(f)$ and $QTG^{\Psi}(\mathcal{A})$, it is difficult to relate the dynamical behaviours that the different graphs represent.

The discretisation in Def. 3.1 implies that the vertices of $STG(f)$ correspond to the regular domain vertices of $QTG^{\Psi}(\mathcal{A})$. However, there is no representation of the singular domains in the purely discrete setting. To overcome this problem, we associate with every singular domain D the set $H(D) \subset Q$ corresponding to the discretisation of those regular domains that have D in their boundary. We thus introduce the mapping $H : \mathcal{D} \rightarrow 2^Q$, where

$$H(D) := \begin{cases} \{d(D)\}, & \text{if } D \in \mathcal{D}_r, \\ \{d(D') \in Q \mid D' \in \rho(D)\} & \text{if } D \in \mathcal{D}_s. \end{cases}$$

For example, for a singular domain D' of order one, $H(D')$ constitutes the set $\{d(D), d(\tilde{D})\}$ for the two regular domains D, \tilde{D} adjacent to D' . With this definition, we are able to state the correspondences between edges in $QTG^\Psi(\mathcal{A}) = (\mathcal{D}, \mathcal{T})$ and $STG(f) = (Q, E)$.

Theorem 3.1 *Let $D \in \mathcal{D}$ and $D' \subset \partial D$. Denote by I (resp. I') the index set of singular variables in D (resp. D'). Then we have: (cf. Fig. 3.1)*

- (1) $\Psi(D) \neq 0$ if and only if for all $i \in I$ one of the following conditions holds (where $e^i = (0, \dots, 1, \dots, 0)$ denotes the i -th unit vector in \mathbb{R}^n):
 - (a) there exist $q, q' \in H(D)$ with $q' = q + e^i$ such that $(q, q') \in E$ and $(q', q) \in E$.
 - (b) there exist $q, q' \in H(D)$ with $q' = q + e^i$ such that $(q, q') \notin E$ and $(q', q) \notin E$.
 - (c) there exist $q, q' \in H(D)$ and $\tilde{q}, \tilde{q}' \in H(D)$ with $q' = q + e^i, \tilde{q}' = \tilde{q} + e^i$ such that both $(q, q') \in E, (q', q) \notin E$, and $(\tilde{q}', \tilde{q}) \in E, (\tilde{q}, \tilde{q}') \notin E$.
- (2) $(D, D') \in \mathcal{T}$ if and only if $\Psi(D) \neq 0$ and for all $i \in I' \setminus I$ there exist $q \in H(D)$ and $q' \in H(D') \setminus H(D)$ with $q_i \neq q'_i$ and $(q, q') \in E$.
- (3) $(D', D) \in \mathcal{T}$ if and only if $\Psi(D) \neq 0$ and for all $i \in I' \setminus I$ there exist $q \in H(D)$ and $q' \in H(D') \setminus H(D)$ such that $q_i \neq q'_i, q'_j = q_j$ for all $j \neq i$ and $(q, q') \notin E$.

PROOF The conditions for the existence of transitions in $QTG^\Psi(\mathcal{A})$ are basically the two conditions given in Def. 2.10 reformulated in the context of edges of $STG(f)$.

We start by showing that the condition $\Psi(D) \neq \emptyset$ is equivalent to condition (1) in the theorem. If D is a regular domain, then $\Psi(D) \neq \emptyset$ by definition and condition (1) is true by default since I is empty. Therefore, we now assume $D \in \mathcal{D}_s$. We observe $|q_i - q'_i| \leq 1$ for all $q, q' \in H(D)$ and $i \in \{1, \dots, n\}$ by definition of $H(D)$. In particular, $1 + \min_{\tilde{q} \in H(D)} \tilde{q}_i = \max_{\tilde{q} \in H(D)} \tilde{q}_i$ for all $i \in I$.

First, we want to transform the condition $\Psi(D) \neq \emptyset$ into a condition expressed in terms of the unitary update function \tilde{f} . Suppose $D_i = \{x_i \mid x_i = \theta_i^k\}$ for some $i \in I$. By Prop. 2.1, a domain $D \in \mathcal{D}_s$ is non-transparent (cf. Rem. 2.1), i.e., $\Psi(D) \neq \emptyset$, if for all $i \in I$ there exist $D', D'' \in \rho(D)$ such $v_i(D, \phi(D')) = -1$ and $v_i(D, \phi(D'')) = 1$.

We now look at the condition $v_i(D, \phi(\tilde{D})) = 1$ and what it is equivalent to in terms of the update function. For fixed $i \in I$ and due to the adjacency

of each $\tilde{D} \in \rho(D)$ to D , we have for all $\tilde{D} \in \rho(D)$ that $v_i(D, \phi(\tilde{D})) = 1$ is equivalent to

$$v_i(\tilde{D}, \phi(\tilde{D})) \in \begin{cases} \{1\} & \text{if } w_i = -1 \\ \{0, 1\} & \text{if } w_i = 1 \end{cases}, \quad (3.2)$$

where $V(D, \tilde{D}) = \{w\}$. That is, if $\tilde{D} \in \rho(D)$ is below the threshold θ_i^k and $v_i(D, \phi(\tilde{D})) = 1$, then its focal point is definitely above θ_i^k and hence $v_i(\tilde{D}, \phi(\tilde{D})) = 1$. If, however, \tilde{D} is above θ_i^k and $v_i(D, \phi(\tilde{D})) = 1$, then its focal point is either within or above \tilde{D}_i , that is $v_i(\tilde{D}, \phi(\tilde{D})) \in \{0, 1\}$. Applying Lemma 3.1 and the definition of $H(D)$, (3.2) can be reformulated such that for all $\tilde{D} \in \rho(D)$, the condition $v_i(D, \phi(\tilde{D})) = 1$ is equivalent to

$$\tilde{f}_i(d(\tilde{D})) - d_i(\tilde{D}) \in \begin{cases} \{1\} & \text{if } d_i(\tilde{D}) = \min_{\tilde{q} \in H(D)} \tilde{q}_i \\ \{0, 1\} & \text{if } d_i(\tilde{D}) = \max_{\tilde{q} \in H(D)} \tilde{q}_i \end{cases}. \quad (3.3)$$

Analogously, we can derive for all $\tilde{D} \in \rho(D)$ that the condition $v_i(D, \phi(\tilde{D})) = -1$ is equivalent to

$$\tilde{f}_i(d(\tilde{D})) - d_i(\tilde{D}) \in \begin{cases} \{-1, 0\} & \text{if } d_i(\tilde{D}) = \min_{\tilde{q} \in H(D)} \tilde{q}_i \\ \{-1\} & \text{if } d_i(\tilde{D}) = \max_{\tilde{q} \in H(D)} \tilde{q}_i \end{cases}. \quad (3.4)$$

We next show that there exists $\tilde{D} \in \rho(D)$ with $v_i(D, \phi(\tilde{D})) = 1$ iff there exist $q, q' \in H(D)$ with $q' = q + e^i$ such that $(q, q') \in E$ or $(q', q) \notin E$. Suppose $\tilde{D} \in \rho(D)$ with $v_i(D, \phi(\tilde{D})) = 1$. If $d_i(\tilde{D}) = \min_{\tilde{q} \in H(D)} \tilde{q}_i$, let $q = d(\tilde{D})$. Then, $\tilde{f}_i(q) - q_i = 1$, i.e., for $q' = q + e^i$, we get $(q, q') \in E$. If $d_i(\tilde{D}) = \max_{\tilde{q} \in H(D)} \tilde{q}_i$, let $q' = d(\tilde{D})$. Then $\tilde{f}_i(q') - q'_i \neq -1$, i.e., for $q = q' - e^i$, we have $(q', q) \notin E$. The reverse direction uses the same arguments. Analogous arguments imply that there exists $\tilde{D} \in \rho(D)$ with $v_i(D, \phi(\tilde{D})) = -1$ iff there exist $q, q' \in H(D)$ with $q' = q + e^i$ such that $(q, q') \notin E$ or $(q', q) \in E$.

As stated before, we have $\Psi(D) \neq \emptyset$ iff there exist $D', D'' \in \rho(D)$ such $v_i(D, \phi(D')) = -1$ and $v_i(D, \phi(D'')) = 1$. Logical reformulation leads to the three cases (a), (b), (c) in condition (1) of the theorem, cf. Fig. 3.1 for illustration.

Next, we consider conditions (2) and (3) of the theorem, provided that condition (1), and thus $\Psi(D) \neq \emptyset$, holds. Condition 1(b) of Def. 2.10 states that there exists $\nu \in V(D, \Psi(D))$ such that $\nu_i w_i = 1$ for every $i \in I' \setminus I$, where $V(D, D') = \{w\}$. Let us first remark that $w_i \neq 0$ iff $i \in I' \setminus I$. Moreover, $w_i = q'_i - q_i$ for all $q \in H(D)$, $q' \in H(D') \setminus H(D)$ for $i \in I' \setminus I$. Now, let $i \in I' \setminus I$, i.e., $w_i \neq 0$, and choose $q \in H(D)$, $q' \in H(D') \setminus H(D)$ with $(q, q') \in E$ and $q_i \neq q'_i$ according to condition (2) of the theorem. Let us assume that $w_i = 1$, the case $w_i = -1$ can be treated analogously. Then, $1 = w_i = q'_i - q_i$, i.e., $q'_i > q_i$. It follows that $\tilde{f}_i(q) > q_i$, and thus $\max_{\tilde{q} \in H(D)} \tilde{f}_i(\tilde{q}) - \tilde{q}_i = 1$. If D is a regular

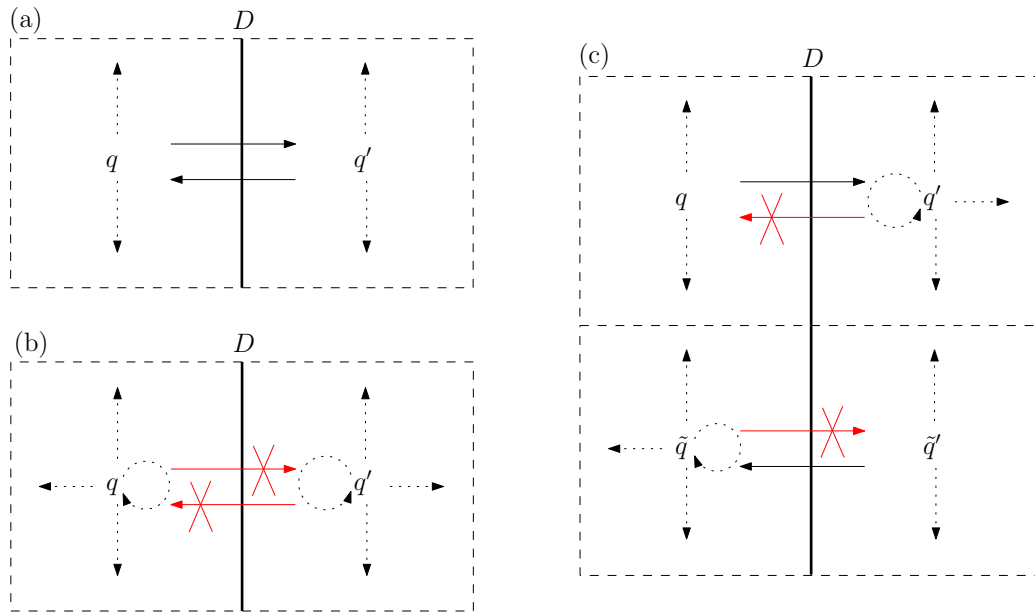


Figure 3.1: Illustration of the condition (1) of Theorem 3.1 for a singular domain D . The property $\Psi(D) \neq \emptyset$ translates to edge constraints for outgoing edges of discrete states in $H(D)$. Here are the three cases in (1) of Theorem 3.1, where the vertical line denotes the threshold of a singular variable of D separating either two (in (a) and (b)) or four (in (c)) regular domains. Edges that do not conflict with the conditions in the theorem are depicted as dotted lines, mandatory edges are depicted as solid lines and the edges that are not allowed are crossed out.

domain, then $v_i(D, \phi(D)) = 1$ by Lemma 3.1. If D is a singular domain, then $1 \in [\min_{\tilde{q} \in H(D)} \tilde{f}_i(\tilde{q}) - \tilde{q}_i, \max_{\tilde{q} \in H(D)} \tilde{f}_i(\tilde{q}) - \tilde{q}_i] = V_i(D, \Psi(D))$ according to Prop. 2.1 and Lemma 3.1. In both cases, there exists $\nu_i \in V(D, \Psi(D))$ with $\nu_i w_i = 1$. Since the definition of $V(D, \Psi(D))$ for regular domains and Prop. 2.1 allow for a componentwise argument, the existence of a vector $\nu \in V(D, \Psi(D))$ with $\nu_i w_i = 1$ for all $i \in I' \setminus I$ follows.

To show the reverse statement, assume that there exists $\nu \in V(D, \Psi(D))$ with $\nu_i w_i = 1$ for all $i \in I' \setminus I$, and choose $i \in I' \setminus I$. Again, we restrict ourselves to the exemplary case $w_i = 1$. Then, $\nu_i = 1$, and therefore, there exists $q \in H(D)$ with $\tilde{f}_i(q) - q_i = 1$ according to Lemma 3.1 and Prop. 2.1. In particular, $(q, q') \in E$ for $q' \in Q$ with $q'_i = q_i + 1$ and $q'_j = q_j$ for all $j \neq i$. Then $q' \notin H(D)$, since $q'_i \neq q_i$ and $i \notin I$, but $q' \in H(D')$, since $q'_i = q_i + w_i$. Thus, condition (2) of the theorem holds.

Lastly, we show equivalence of the condition (3) of the theorem and condition 2(b) in Def. 2.10. Suppose there exists $\nu \in V(D, \Psi(D))$ with $\nu_i w_i \neq -1$ for all $i \in I' \setminus I$. Let $i \in I' \setminus I$, then $w_i \neq 0$. Again, we only show the exemplary proof for the case $w_i = 1$. Then, $\nu_i \neq -1$, and thus, $\max_{\tilde{q} \in H(D)} \tilde{f}_i(\tilde{q}) - \tilde{q}_i \geq 0$ according to Prop. 2.1 and Lemma 3.1. Then, there exists $q \in H(D)$ with $q_i \leq \tilde{f}_i(q)$, which yields $q_i \leq p_i$ for all asynchronous successors $p \in AS(q)$. Now, let $q' \in H(D') \setminus H(D)$ with $q'_i \neq q_i$ and $q'_j = q_j$ for all $j \neq i$. Since $w_i = 1$, we have $q'_i < q_i$. In particular, q' cannot be an asynchronous successor of q , i.e., $(q, q') \notin E$.

Conversely, given $i \in I' \setminus I$ and q, q' according to condition (3) of the theorem, i.e., $q \in H(D)$, $q' \in H(D') \setminus H(D)$ with $q_i \neq q'_i$, $q_j = q'_j$ for all $j \neq i$, and $(q, q') \notin E$, then $w_i = q_i - q'_i$. Again, let us just focus on the case $w_i = 1$, i.e., $q_i > q'_i$. Since $(q, q') \notin E$, we have $p_i \geq q_i$ for all $p \in AS(q)$, i.e., $\tilde{f}_i(q) - q_i \in \{0, 1\}$. It follows from Prop. 2.1 and Lemma 3.1 that $\max_{\tilde{D} \in \rho(D)} v_i(\tilde{D}, \phi(\tilde{D})) \geq 0$. Thus, we can find $\nu \in V(D, \Psi(D))$ with $\nu_i \neq -1$, and in particular $\nu_i w_i \neq -1$. Again, the definition of $V(D, \Psi(D))$ for regular domains and Prop. 2.1 allow for a componentwise argument, and we can fulfill condition 2(b) of Def. 2.10. \square

Example 3.2 Using Thm. 3.1, we can determine whether the singular domain $D' := [\theta_1^1] \times [\theta_2^1]$ of order two in the QTG^Ψ on the right of Fig. 3.2a) is transparent or non-transparent, by looking at the edges within $H(D') := \{00, 01, 10, 11\}$ in the STG on the left of Fig. 3.2a). For the second variable, the edges (00, 01) and (11, 10) satisfy 1(c) of Thm. 3.1, while for the first variable the edges (00, 10) and (10, 00) satisfy 1(a), which means that D' is non-transparent. The edges (00, 10) and (10, 00) also mean that the singular domain $D := [\theta_1^1] \times [0, \theta_2^1)$ of order one is non-transparent. Thus, transitions between D and D' can be determined from the edges between the states

$H(D) = \{00, 10\}$ and $H(D') \setminus H(D) = \{01, 11\}$. From the conditions (2) and (3) of Thm. 3.1, we have that $(00, 01) \in E$ corresponds to $(D, D') \in \mathcal{T}$ and $(10, 11) \notin E$ corresponds to $(D', D) \in \mathcal{T}$ respectively.

In the same example in Fig. 3.2a), the singular domain $\tilde{D} := [0, \theta_1^1] \times [\theta_2^2]$ of order one is non-transparent as reflected by the edges $(01, 02)$ and $(02, 01)$, which also imply that 1(a) is satisfied for the second variable of $\tilde{D}' := [\theta_1^1] \times [\theta_2^2]$. For the first variable, however, we have that the edges $(01, 11)$ and $(02, 12)$ do not satisfy any subcase in (1) of Thm. 3.1, which means that \tilde{D}' is transparent. We see that either $(01, 11) \in E$ or $(02, 12) \in E$ corresponds to $(\tilde{D}, \tilde{D}') \in \mathcal{T}$ by (2) of Thm. 3.1. However, both edges $(01, 11)$ and $(02, 12)$ correspond to $(\tilde{D}', \tilde{D}) \notin \mathcal{T}$ because (3) of Thm. 3.1 is not satisfied.

Looking at the simplest case of the theorem, we can see how edges (or missing edges) between two nodes $q, q' \in Q$, $q \neq q'$, in $STG(f) = (Q, E)$ always correspond to edges in $QTG^\Psi(\mathcal{A}) = (\mathcal{D}, \mathcal{T})$ for the singular domain D' of order one with $H(D') = \{q, q'\}$.

Corollary 3.1 *Let $D \in \mathcal{D}_r$, and let $D' \subset \partial D$ be a singular domain of order one. Set $q := d(D)$ and denote by q' the unique element in the set $H(D') \setminus H(D)$. Then, $(D, D') \in \mathcal{T}$ if and only if $(q, q') \in E$, and $(D', D) \in \mathcal{T}$ if and only if $(q, q') \notin E$.*

This statement agrees with the observations of [8] for boolean discrete models and with [23]. Thus, the basic correspondences of edges known from the literature is also incorporated in the result. Moreover, Thm. 3.1 provides the basis for elucidating the correspondences between more complex structures, such as paths or attractors. On the one hand, it can be used for proof building on local considerations concerning the edges involved. On the other hand, it provides ideas for the construction of counterexamples. In the following, we illustrate both uses of the theorem.

Comparing Paths and Attractors

We start by considering reachability properties. In simple cases, we can find conditions ensuring the existence of corresponding paths. The following proposition applies Cor. 3.1 repeatedly and states the paths that correspond in the two graphs.

Proposition 3.2 *There exists a path (D^1, \dots, D^{2k+1}) in $QTG^\Psi(\mathcal{A})$ with $D^i \in \mathcal{D}_r$ for $i \in \{1, \dots, 2k+1\}$ odd and D^i a singular domain of order one for $i \in \{1, \dots, 2k+1\}$ even, if and only if (q^1, \dots, q^k) is a path in $STG(f)$ such that $(q^j, q^{j-1}) \notin E$ for all $j \in \{2, \dots, k\}$ and $q^i = d(D^{2i+1})$ for all $i \in \{0, \dots, k\}$.*

In spite of Prop. 3.2, we are able to construct examples of paths that do not correspond in the two graphs.

Example 3.3 We see in Fig. 3.2 (a) that state (0,2) is reachable from (1,0) in the STG via the path indicated in grey. In contrast, all paths starting in the regular domain corresponding to (1,0) and all adjacent singular domains do not cross the first threshold plane of the second component. In Fig. 3.2 (b), we see by considering the reachability of state (1,1) from (0,0) that reachability properties of the QTG^Ψ are also not conserved in the corresponding STG.

These two examples thus illustrate that in general reachability properties are not conserved between the two graphs. A further important characteristic of $QTG^\Psi(\mathcal{A})$ and $STG(f)$ are their respective attractors. The next definition introduces our terminology.

Definition 3.4 Let G be a directed graph and S a subset of the nodes of G . The set S is *strongly connected* if any two nodes in S are connected by a path in S . The set S is a *trap set* if there is no path leaving S . An *attractor* of a graph is a strongly connected trap set. A *steady state* is an attractor consisting of a single node. A *cyclic attractor* is an attractor of cardinality greater than one. A *complex attractor* is a cyclic attractor that has at least one node that has two or more outgoing edges.

Note that we consider each node set of cardinality one to be strongly connected by default, i.e., not depending on the existence of a loop on the respective node. The steady states in a discrete state transition graph correspond to the fixed points of the update function f , and by definition there exists an edge (q, q) for each fixed point q . In contrast, the steady states of the QTG^Ψ are, by definition of the transitions, nodes without outgoing edges. Note that here a steady state is simply a singleton terminal strongly connected component in a graph.

We often denote a cyclic attractor $\{s^1, \dots, s^k\}$, which is not a complex cyclic attractor, by the path (s^1, \dots, s^k, s^1) traversing the cycle and refer to it as a *non-complex* cyclic attractor. Similar to the reachability properties, we are able to find correspondences between attractors of $STG(f)$ and $QTG^\Psi(\mathcal{A})$.

Proposition 3.3 *The following relations hold for attractors in $QTG^\Psi(\mathcal{A})$ and $STG(f)$.*

1. *A regular domain D is a steady state in $QTG^\Psi(\mathcal{A})$ if and only if $d(D)$ is a steady state in $STG(f)$. A singular domain D of order one is a steady state in $QTG^\Psi(\mathcal{A})$ if and only if $H(D)$ is a non-complex cyclic attractor in $STG(f)$.*

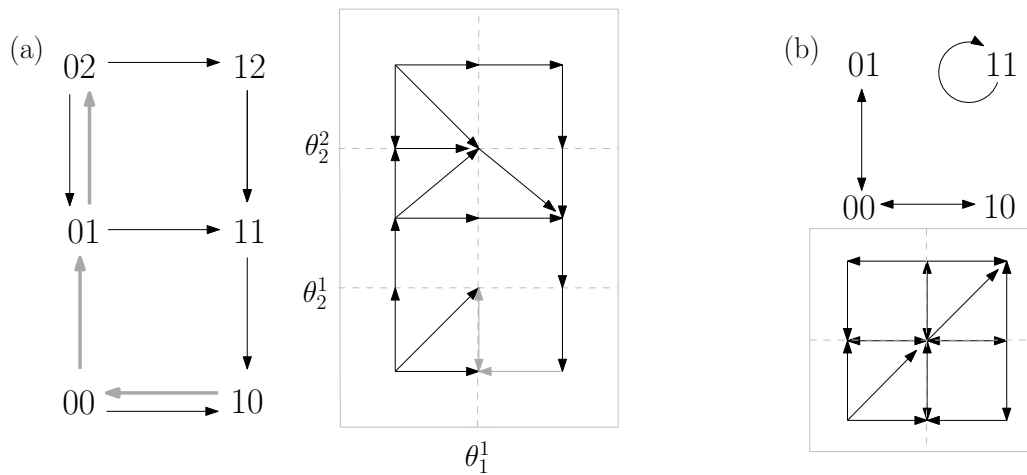


Figure 3.2: Corresponding STGs and QTG^Ψ s. The partitioned phase space of a corresponding PADE underlying a QTG^Ψ is shown in fine grey lines (dashed for threshold planes) underneath the QTG^Ψ and allows identification of nodes representing singular resp. regular domains. In (a), the STG of a two-component network on the left with the corresponding QTG^Ψ on the right. In (b), the STG of a two-component Boolean network with the corresponding QTG^Ψ below it. Heavier grey edges illustrate reachability properties discussed in the text.

2. *There is a non-complex cyclic attractor $(D^1, D^2, \dots, D^{2m}, D^1)$ with $D^{2j} \in \mathcal{D}_r$ for $j \in \{1, \dots, m\}$ in $QTG^\Psi(\mathcal{A})$, if and only if $(d(D^2), d(D^4), \dots, d(D^{2m}), d(D^2))$ is a non-complex cyclic attractor in $STG(f)$.*

PROOF 1. The first statement immediately follows from Lemma 3.1, where a regular domain D is a steady state if and only if $v(D, \phi(D)) = 0$, which is equivalent to $f(d(D)) = d(D)$. Now, let $\{\tilde{q}, \tilde{q}'\}$ be a non-complex cyclic attractor in $STG(f)$ and D be the singular domain of order one with $H(D) = \{\tilde{q}, \tilde{q}'\}$. According to Thm. 3.1, if there exists an edge from D to a singular domain D' of higher order, then we could find $q \in H(D)$, $q' \in H(D') \setminus H(D)$, i.e., $q \in \{\tilde{q}, \tilde{q}'\}$ and $q' \notin \{\tilde{q}, \tilde{q}'\}$, with $(q, q') \in E$, which would be contradictory to $H(D)$ being a non-complex cyclic attractor. If there exists an edge from D to a regular domain \tilde{D} , then, since $H(D) \setminus H(\tilde{D}) = \{q\}$ and $H(\tilde{D}) = \{q'\}$ for some $q, q' \in H(D)$ with $q \neq q'$, we would have $(q', q) \notin E$ according to Thm. 3.1, which contradicts $\{\tilde{q}, \tilde{q}'\}$ being a non-complex cyclic attractor. In summary, D has no outgoing edges and is a steady state.

If $H(D) = \{q, q'\}$ is not a non-complex cyclic attractor, then either one of the edges (q, q') , (q', q) is missing in $STG(f)$ or there exists an edge leaving $H(D)$. In the first case, there exists a transition from D to a regular domain, as we can see immediately from Thm. 3.1. If $(q, q'), (q', q) \in E$, then condition 1(a) of Thm. 3.1 holds for D , i.e. $\Psi(D) \neq \emptyset$. If we find an additional edge leaving $H(D)$, then condition (2) of Thm. 3.1 holds as well, and we find an edge from D to some singular domain. In any case, D is not a steady state.

2. If there is a non-complex cyclic attractor $(D^1, D^2, \dots, D^{2m}, D^1)$ in $QTG^\Psi(\mathcal{A})$, then $(d(D^2), d(D^4), \dots, d(D^{2m}), d(D^2))$ is a non-complex cyclic attractor in $STG(f)$ according to Cor. 3.1. If, on the other hand, $(d(D^2), d(D^4), \dots, d(D^{2m}), d(D^2))$ is a non-complex cyclic attractor in $STG(f)$, then, again according to Cor. 3.1, each regular domain D^{2j} has only one outgoing edge, namely (D^{2j}, D^{2j+1}) , where $2m+1$ is identified with index 1. For the singular domains D^{2j+1} in the cycle, we can derive the existence of only one outgoing edge, namely (D^{2j+1}, D^{2j+2}) , from condition (3) of Thm. 3.1. □

In spite of the findings in Prop. 3.3, the number of attractors is not necessarily preserved in general.

Example 3.4 While in Fig. 3.2(a) both systems have one attractor, the STG in Fig. 3.2(b) exhibits two attractors, a fixed point and a cyclic attractor. However, the corresponding QTG^Ψ has only one attractor, namely a steady

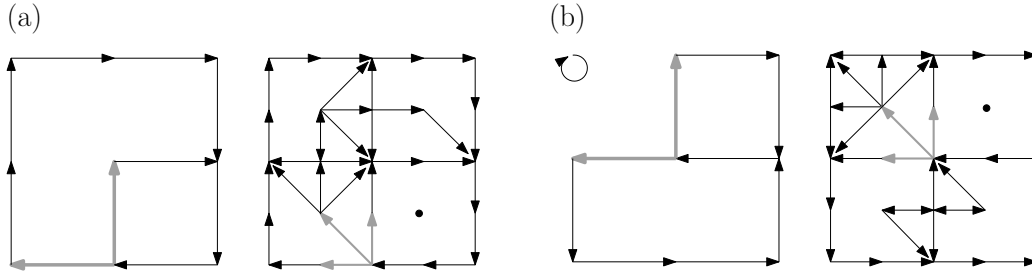


Figure 3.3: Two examples for networks with two components and three activity levels for each component. In each case, the STG is depicted on the left, the corresponding QTG^Ψ on the right. Depiction of the graphs corresponds to that in Fig. 3.2, only the explicit labeling of the STG nodes is omitted. In (a), the STG consists of a single cyclic attractor, while the QTG^Ψ has an additional steady state at the lower right singular node depicted by a fat dot. In (b), both STG and QTG^Ψ have a steady state in the upper left node, but the STG has an additional cyclic attractor. The QTG^Ψ has no cyclic attractor, but an additional singular steady state at the upper right singular node depicted by a fat dot.

state in the upper right node. In Fig. 3.3(a), the STG has fewer attractors than the corresponding QTG^Ψ .

In addition, the relation between the attractor structure is not clear-cut. While the cyclic attractor of the STG in Fig. 3.2(a) comprises all nodes of the STG and contains nodes with multiple outgoing edges, the cyclic attractor in the QTG^Ψ is a non-complex cyclic attractor consisting only of two nodes joined by the heavier grey double edge in the lower part of the graph. In Fig. 3.2(b), the cyclic attractor in the STG vanishes in the corresponding QTG^Ψ . The same happens in Fig. 3.3(b), but here an additional steady state can be observed in a singular node.

Let us also consider a singular domain D of order greater than 1 which is a steady state in the QTG^Ψ . Translating the condition of D having no outgoing edges obviously imposes constraints on a corresponding STG via Thm. 3.1. However, these constraints are generally not strong enough to link D to some unique structure in the STG.

Example 3.5 In Fig. 3.4, we see two examples, where both QTG^Ψ s contain a singular domain of order two, which is a steady state. However, the corresponding STGs differ, the one in (a) consisting of a complex attractor and the one in (b) consisting of a non-complex cyclic attractor.

So, in general the number, structure and uniqueness of the corresponding attractors cannot be assured. Nevertheless, we are able to narrow down the locations of attractors by observing the trap sets. In particular we can show that hyper-rectangular trap sets correspond in the two graphs.

Proposition 3.4 *Let $\mathcal{Y} := \mathcal{Y}_1 \times \cdots \times \mathcal{Y}_n \subset Q$ be a discrete hyperrectangle, i.e., \mathcal{Y}_i is an integer interval $[a_i, b_i] \subset Q_i$ for all $i \in \{1, \dots, n\}$. Then \mathcal{Y} is a trap set in $STG(f)$ if and only if $U := \{D \mid H(D) \subset \mathcal{Y}\}$ is a trap set in $QTG^\Psi(\mathcal{A})$.*

PROOF Let U be a trap set in $QTG^\Psi(\mathcal{A})$. Let $q \in \mathcal{Y}$ and $q' \in Q$ with $(q, q') \in E$. Then Thm. 3.1 ensures that there exists $D' \subset \partial D$, $D := d^{-1}(q)$, with $(D, D') \in \mathcal{T}$ and $H(D') = \{q, q'\}$. Since U is a trap set, we have $D' \in U$. Then, by definition, $H(D') \in \mathcal{Y}$, i.e., $q' \in \mathcal{Y}$.

Now, let \mathcal{Y} be a trap set in $STG(f)$. Let $D \in U$ and $D' \in \mathcal{D}$ with $(D, D') \in \mathcal{T}$. If $D \subset \partial D'$, then $H(D') \subset H(D) \subset \mathcal{Y}$, and therefore, by definition, $D' \in U$. If $D' \subset \partial D$, then condition (2) of Thm. 3.1 yields the existence of an edge $(q, q') \in E$ such that $q \in H(D)$, i.e., $q \in \mathcal{Y}$, and $q' \in H(D') \setminus H(D)$ with $q_i \neq q'_i$ for all indices i indicating singular variables of D' but not of D . Since \mathcal{Y} is a hyperrectangle, we then have $H(D') \subset \mathcal{Y}$, that is, $D' \in U$. \square

The above proposition may be helpful in elucidating the correspondences of attractors in the STG and the QTG^Ψ further. Since a trap set always contains at least one attractor, we can relate attractors that we can separate using hyperrectangles.

Overall, we see that the relations between attractors in corresponding STGs and QTG^Ψ s are not clear-cut. The examples illustrate that, in general, neither number nor properties of attractors are preserved.

3.2 The Discrete Formalisms

In the following, we show that the singular state and the Thomas formalisms (see Sect. 2.3) contain the same information in the sense that we can transform an extended update function (2.11) into an update function of the Thomas formalism and vice versa. For the sake of the singular state formalism, we consider for the remainder of this section an interaction graph $\bar{G} = (\{1, \dots, n\}, \bar{E})$ with logical parameters $\{K_{i,\omega}\}$, from which we can define the extended state space $\Sigma = \Sigma_1 \times \cdots \times \Sigma_n$ (see Sect. 2.3.2).

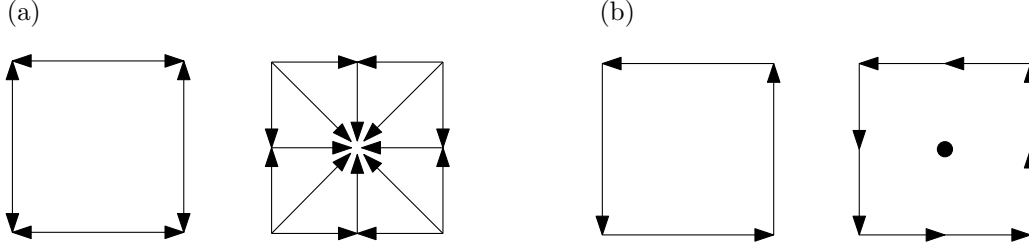


Figure 3.4: STGs and QTG^Ψ s for networks with two components and two activity levels for each component, the STG shown on the left, the corresponding QTG^Ψ on the right of each figure. Both the QTG^Ψ s in (a) and (b) have a steady state in the singular domain of order two.

First, we relate the state spaces of both formalisms. Using the maximum qualitative value p_i of Σ_i , we can define $Q_i := \{0, 1, \dots, p_i\}$ and thus the state space $Q = Q_1 \times \dots \times Q_n$ of the Thomas formalism can be defined. We observe that Σ is constructed in order to refine the state space Q . More specifically, we have an intuitive correspondence of every qualitative value $|q_i| \in \Sigma_i$ with the integer value $q_i \in Q_i$ for each variable i , and thus every state $q \in Q$ conveniently maps to a regular state $|q| := (|q_1|, \dots, |q_n|) \in \Sigma$. Since the extended update of the regular states is also a regular state, we are able to transform an extended update function into an update function such that the extended update of a regular state $|q| \in \Sigma$ is related to the update of the state $q \in Q$.

Definition 3.5 Let \bar{G} be an interaction graph, $\{K_{i,\omega}\}$ logical parameters and g the extended update function in (2.11). Define the mapping $f^g : Q \rightarrow Q$, where for all $i \in \{1, \dots, n\}$

$$f_i^g(q) = K_{i, \text{Reg}_i(|q|)},$$

where $|q| := (|q_1|, \dots, |q_n|) \in \Sigma$ and $\text{Reg}_i(s)$ is as in (2.12).

In other words, we are able to capture the regular state dynamics of the extended update function in an update function.

Since the singular states in Σ have no direct representation in Q , the reverse transformation of an update function into an extended update function is not as straightforward. In particular, the singular states have no representation in Q . Nonetheless, the singular states are shown in [57] to have an association with their adjacent regular states, which suggests the mapping $\delta = \delta_1 \times \dots \times \delta_n$, where $\delta_i : \Sigma \rightarrow 2^{Q_i}$ is defined as

$$\delta_i(s) = \begin{cases} \{r\} & \text{if } s_i = |r| \\ \{r, r+1\} & \text{if } s_i = |r, r+1| \end{cases}, \quad (3.5)$$

and 2^{Q_i} is the power set of Q_i . That is, δ maps every singular state $s \in \Sigma$ to the states in Q that correspond to the $2^{ord(s)}$ regular states neighbouring s .

By exploiting the transformation in Def. 3.5, we see how the singular state dynamics can be determined from the regular state dynamics. Given an extended update function g , the monotonicity property of the logical parameters implies that for any $s \in \Sigma$,

$$\min_{q \in \delta(s)} f_i^g(q) = K_{i, Reg_i(s)} \text{ and } \max_{q \in \delta(s)} f_i^g(q) = K_{i, Reg_i(s) \cup Sing_i(s)}. \quad (3.6)$$

Therefore, the dynamics of a singular state $s \in \Sigma$ can be determined from the dynamics of the states $\delta(s) \subset Q$. This observation suggests the following transformation of an update function into an extended update function.

Definition 3.6 Let $f : Q \rightarrow Q$ be an update function. Define $g^f : \Sigma \rightarrow \Sigma$ such that for all $s \in \Sigma$ and $i \in \{1, \dots, n\}$,

$$g_i^f(s) = |\min_{q \in \delta(s)} f_i(q), \max_{q \in \delta(s)} f_i(q)|. \quad (3.7)$$

Remark 3.1 The transformation above assumes that g^f has not been constructed from an interaction graph and strictly defined logical parameters. Therefore, with the transformation in Def. 3.6, we are suggesting a *general* form of the singular state formalism.

From our previous observations, we see that the dynamics on singular states can be deduced from the dynamics on regular states. That is, the dynamics of the Thomas and singular state formalisms is captured by the dynamics on the states $q \in Q$ and the regular states in Σ respectively. Using the transformations in Def. 3.5 and Def. 3.6, we get that every update function has a unique corresponding extended update function and vice versa, which yields the following result.

Proposition 3.5 Let $f : Q \rightarrow Q$ be an update function. From Def. 3.5 and Def. 3.6, we have

$$f = f^{g^f} \text{ and thus } STG(f) = STG(f^{g^f}).$$

Let $\bar{G} = (\{1, \dots, n\}, \bar{E})$ be an interaction graph, $\{K_{i,\omega}\}$ logical parameters and g the extended update function (2.11). From Def. 3.5 and Def. 3.6, we have

$$g = g^{f^g} \text{ and thus } ESG(g) = ESG(g^{f^g}).$$

Using Prop. 3.5, we can associate an update function with a unique extended update function, and vice versa. In the following, we analyse differences and similarities between the STG and ESG given this association of the underlying update functions.

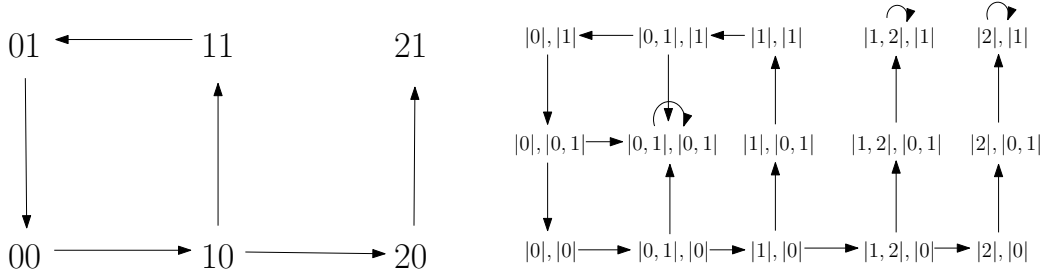


Figure 3.5: The transition graphs of the running example with the STG on the left and the corresponding ESG on the right.

Correspondence of Edges

Throughout the remainder of this section, we consider an update function $f : Q \rightarrow Q$ with unitary update function $\tilde{f} := f^{STG(f)}$ and corresponding extended update function g^f according to Def. 3.6. In the following, we want to compare the transition graphs $STG(f) = (Q, E)$ and $ESG(g^f) = (\Sigma, T)$.

Because it is not possible to recover f from $STG(f)$ or g^f from $ESG(g^f)$ (except in the case that $p_i = 1$ for all $i \in \{1, \dots, n\}$), it is not clear whether the information in the STG is sufficient to construct an ESG and vice versa. We are able to deduce the unitary update function \tilde{f} from $ESG(g^f)$ and also construct $ESG(g^f)$ from \tilde{f} . More specifically, for a singular state $s \in \Sigma$ and $i \in \{1, \dots, n\}$, it holds by definition of \tilde{f} that

$$\min_{q \in \delta(s)} f_i(q) \leq \min_{q \in \delta(s)} \tilde{f}_i(q) \text{ and } \max_{q \in \delta(s)} \tilde{f}_i(q) \leq \max_{q \in \delta(s)} f_i(q).$$

Therefore, by definition of the qualitative relations, $s_i \# g_i^f(s)$ if and only if $s_i \# \tilde{f}_i(s)$, where $\# \in \{<, >, \subset\}$, which immediately implies that $ESG(g^f) = ESG(\tilde{f})$. In other words, the unitary update function suffices in constructing both $STG(f)$ and $ESG(g^f)$. Consequently, we can construct an STG given an ESG and vice versa.

In spite of this common underlying information, we see in the following that the dynamics implied by the STG and ESG do not always coincide. The next result describes the overall correspondence of edges between the STG and ESG.

Theorem 3.2 *Let $f : Q \rightarrow Q$ be an update function with corresponding transition graphs $STG(f) = (Q, E)$ and let g^f be an extended update function according to Def. 3.6 with corresponding extended state graph $ESG(g^f) = (\Sigma, T)$. The function $\text{ord} : \Sigma \rightarrow \{0, 1, \dots, n\}$ describes how many qualitative values are singular for state $s \in \Sigma$. Consider states $s, s' \in \Sigma$.*

1. If $\text{ord}(s) < \text{ord}(s')$, then $(s, s') \in T$, where $s_i \neq s'_i$, if and only if
 - for some $q \in \delta(s)$ there exists $q' \in \delta(s') \setminus \delta(s)$ such that $(q, q') \in E$, and
 - for all $q \in \delta(s)$ and $p \in Q$ with $(q, p) \in E$ it holds that either
 - $q_i \leq p_i$ if $s_i < s'_i$, or
 - $q_i \geq p_i$ if $s_i > s'_i$.
2. If $\text{ord}(s) > \text{ord}(s')$, then $(s, s') \in T$ if and only if $(q, q') \in E$ and $(q', q) \notin E$ for all $q \in \delta(s) \setminus \delta(s')$ and $q' \in \delta(s')$, where $|q - q'| = 1$.

PROOF By definition of the qualitative values and the relation of the two update functions (Def. 3.6), for all $s \in \Sigma$, $i \in \{1, \dots, n\}$ and $s_i = |a, b|$, it holds that

$$s_i < g_i^f(s) \iff b = \min_{q \in \delta(s)} f_i(q) < \max_{q \in \delta(s)} f_i(q) \text{ or } b < \min_{q \in \delta(s)} f_i(q), \quad (3.8)$$

$$s_i > g_i^f(s) \iff \min_{q \in \delta(s)} f_i(q) < \max_{q \in \delta(s)} f_i(q) = a \text{ or } \max_{q \in \delta(s)} f_i(q) < a, \quad (3.9)$$

$$s_i \subset g_i^f(s) \iff a = \min_{q \in \delta(s)} f_i(q) \text{ and } \max_{q \in \delta(s)} f_i(q) = b \text{ or} \\ \min_{q \in \delta(s)} f_i(q) < a \text{ and } b < \max_{q \in \delta(s)} f_i(q). \quad (3.10)$$

These equivalencies allow us to address the two cases in the theorem.

1. Let $\text{ord}(s) < \text{ord}(s')$, $(s, s') \in T$ and $i \in \{1, \dots, n\}$ such that $s_i = |a| < s'_i$, i.e., $a := \max_{q \in \delta(s)} q_i = \min_{q \in \delta(s)} q_i$. The case $s_i > s'_i$ is done analogously. We have $s_i < g_i^f(s)$, which by (3.8) is valid if and only if either

$$a = \min_{q \in \delta(s)} f_i(q) < \max_{q \in \delta(s)} f_i(q) \text{ or } a < \min_{q \in \delta(s)} f_i(q). \quad (3.11)$$

For both cases in (3.11), the inequality $a < \max_{q \in \delta(s)} f_i(q)$ holds, which occurs if and only if $(q, q') \in E$ for some $q \in \delta(s)$ and $q' \in Q$ with $q'_i - q_i = 1$, by definition of STG edges. Moreover, $q' \in \delta(s') \setminus \delta(s)$.

Combining the remaining equality and inequality of the two cases in (3.11) gives $a \leq \min_{q \in \delta(s)} f_i(q)$, which occurs if and only if $(q, p) \in E$ for all $q \in \delta(s)$ and $p \in Q$ with $q_i \leq p_i$. The reverse statement follows the same arguments.

2. Let $\text{ord}(s) > \text{ord}(s')$, $(s, s') \in T$ and $i \in \{1, \dots, n\}$ such that $s_i = |a, a + 1| < s'_i$. We have $s_i < g_i^f(s)$, which by (3.8) is valid if and only if

$$a+1 := \max_{q \in \delta(s)} q_i = \min_{q \in \delta(s)} f_i(q) < \max_{q \in \delta(s)} f_i(q) \text{ or } a+1 < \min_{q \in \delta(s)} f_i(q). \quad (3.12)$$

Simplifying these two inequalities gives the following two cases:

- $q_i \leq f_i(q)$ for all $q \in \delta(s)$ with $q_i = a + 1$, i.e., $q \in \delta(s')$, and
- $q_i < f_i(q)$ for all $q \in \delta(s)$ with $q_i = a$, i.e., $q \in \delta(s) \setminus \delta(s')$.

The first case then implies that $(q', q) \notin E$ for all $q' \in \delta(s')$ and $q \in \delta(s) \setminus \delta(s')$ such that $|q - q'| = 1$. The second case, however, implies that $(q, q') \in E$ for all $q \in \delta(s) \setminus \delta(s')$ and $q' \in \delta(s')$ such that $|q - q'| = 1$, which are the conditions in the theorem. Again, the reverse statement follows the same arguments. The argument for $s_i > s'_i$ follows analogously with the help of (3.9). \square

Example 3.6 We illustrate the two conditions in Thm. 3.2 via our running example in Fig. 3.5. The condition 1 of Thm. 3.2 does not hold for the state $s'' := (|1|, |0, 1|)$ because s'' has no transition to $(|0, 1|, |0, 1|) = \Delta_1^-(s'')$ or $(|1, 2|, |0, 1|) = \Delta_1^+(s'')$. This lack of transition is reflected in the outgoing edges of the states $\delta(s'') = \{10, 11\}$ in the STG. In other words, the STG edges $(10, 20)$ and $(11, 01)$ make the singular value of s'' steady, that is $s''_1 \subset g_1^f(s'')$ and thus s'' has no outgoing edge in the direction of the first variable in the ESG.

The transition from $s := (|1, 2|, |0, 1|)$ to $s' := (|1, 2|, |1|)$ satisfies condition 2 of Thm. 3.2. The STG shows that there exists edges from states in $\delta(s) \setminus \delta(s') = \{10, 20\}$ to states in $\delta(s') = \{11, 21\}$ but not vice versa, and thus the transition $(s, s') \in T$ exists.

From Thm. 3.2, we state the basic correspondences that have already been observed by Richard et al [48].

Corollary 3.2 *Let $q, q' \in Q$ such that $|q - q'| = 1$, and $s, s', s'' \in \Sigma$ such that $\delta(s) = \{q\}$, $\delta(s') = \{q'\}$ and $\delta(s'') = \{q, q'\}$. Then*

- $(q, q') \in E$ and $(q', q) \in E$ if and only if $(s, s'') \in T$ and $(s', s'') \in T$.
- $(q, q') \in E$ and $(q', q) \notin E$ if and only if $(s, s'') \in T$ and $(s'', s') \in T$.
- $(q, q') \notin E$ and $(q', q) \notin E$ if and only if $(s, s'') \notin T$ and $(s'', s') \notin T$.

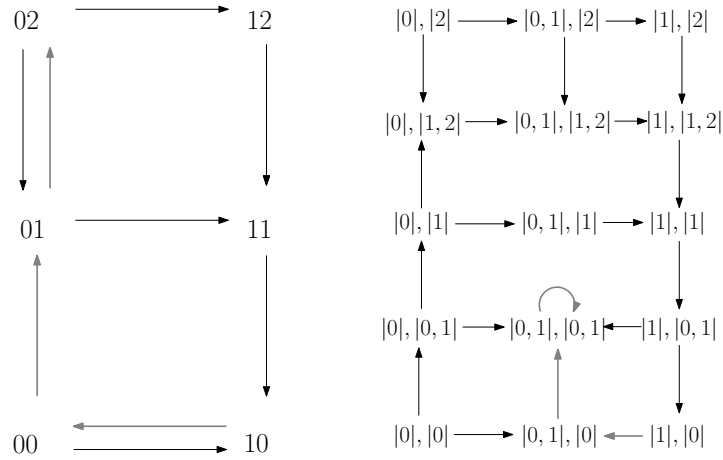


Figure 3.6: On the left the STG of the two-component network as in Fig. 3.2a) and on the right the corresponding ESG . Heavier grey edges illustrate reachability properties discussed in the text.

- $(q, q) \in E$ if and only if $(s, s) \in T$.

Despite the correspondences of edges in $STG(f)$ and $ESG(g^f)$, we are able to find differences in the paths and attractors of the two graphs. Thm. 3.2 can help in proving correspondences as well as providing ideas for counterexamples, where the paths and attractors are consistent resp. inconsistent between the two graphs. In the following, we look at these two applications of the theorem.

Comparing Paths and Attractors

First, we look at reachability properties between $STG(f)$ and $ESG(g^f)$. Repeating Cor. 3.2 gives the following correspondences of paths between the two graphs.

Lemma 3.2 *There exists a path (q^1, \dots, q^k) in the STG , such that $(q^j, q^{j-1}) \notin E$, for all $j = 2, \dots, k$, if and only if there exists a path (s^1, \dots, s^{2^k-1}) in the ESG such that $\delta(s^{2^j-1}) = \{q^j\}$, for all $j = 1, \dots, k$.*

Thus, Lemma 3.2 shows that some simple paths in the STG have corresponding paths in the ESG . Still, we are interested if reachability properties are generally conserved between the two graphs.

To test whether paths in the ESG that start or end at a singular state have a corresponding path in the STG , we would first need to define a state

or states in Q that correspond to a singular state $s \in \Sigma$. The association of a singular state with the adjacent regular states in the mapping δ gives such a correspondence, i.e., $q \in \delta(s)$. Hence, we exploit the mapping δ to show the following correspondence of any path in the ESG.

Lemma 3.3 *If we have a path (s^1, \dots, s^k) in the ESG, then for all $q^1 \in \delta(s^0)$ there exists $q^{k'} \in \delta(s^k)$ and a path $(q^1, \dots, q^{k'})$ in the STG.*

PROOF Let (s^1, \dots, s^k) be a path in the ESG. Because of the asynchronous update of the singular state formalism, the path can be decomposed into subpaths, where s^j and s^{j+1} differ by exactly one singular value. Consider a subpath (s^j, \dots, s^l) such that $\text{ord}(s^i) < \text{ord}(s^{i+1})$ for $i \in [j, l] \subset [1, k]$. Because $\text{ord}(s^j) < \text{ord}(s^{j+1})$, we have $\delta(s^j) \subset \delta(s^{j+1})$. Therefore, iterating over the subpath gives $\delta(s^j) \subset \delta(s^l)$.

Consider a subpath $(s^l, \dots, s^{j'})$ such that $\text{ord}(s^i) > \text{ord}(s^{i+1})$ for $i \in [l, j'] \subset [1, k]$. By Thm. 3.2, we know that for all $q \in \delta(s^l) \setminus \delta(s^{l+1})$ and $q' \in \delta(s^{l+1})$, where $|q - q'| = 1$, it holds that $(q, q') \in E$ and $(q', q) \notin E$. That is, every state in $\delta(s^l) \setminus \delta(s^{l+1})$ has an edge to a state in $\delta(s^{l+1})$. Applying this over the entire subpath $(s^l, \dots, s^{j'})$ yields: for all $\tilde{q} \in \delta(s^l)$ there exists $\tilde{q}' \in \delta(s^{j'})$ such that there is a path from \tilde{q} to \tilde{q}' . Because the path (s^1, \dots, s^k) can be decomposed into the above subpaths, by iteration for all $q^1 \in \delta(s^1)$, there exists $q^{k'} \in \delta(s^k)$ such that a path $(q^1, \dots, q^{k'})$ in the STG exists. \square

One consequence of Lemma 3.3 is that a path between two regular states in the ESG, where the path does not pass through any other regular states, has a corresponding path in the STG. However, the proof above shows that an ESG path between two regular states would immediately imply the existence of an ESG path of the simple form described in Lemma 3.2.

Despite these correspondences of paths, we are still able to find cases where reachability is not conserved between the ESG and STG.

Example 3.7 In Fig. 3.6, we see that the path $(10, 00, 01, 02)$ in the STG does not have a corresponding path in the ESG. In particular, the only path starting from $(|1\rangle, |0\rangle) = \delta^{-1}(10)$ ends up in the singular steady state $(|0, 1\rangle, |0, 1\rangle)$ in the ESG.

That is, not all paths in the STG have corresponding paths in the ESG. Therefore, the reachability properties between the Thomas and singular state formalisms are not conserved.

We now look at the attractors of the two graphs using the same terminology as in Sect. 3.1.1. We start by studying the correspondences of steady states, which are otherwise not accounted for in Thm. 3.2. The regular steady

states have already been addressed in Cor. 3.2, but the correspondences of the singular steady states still need to be determined.

Recall that the singular steady states are representative of equilibria in the related ODE model. Similar to Thm. 3.2, we are able to determine conditions on the STG that a singular steady state in the ESG exists. In other words, we are determining conditions on the STG that represent the existence of an equilibrium point in the related ODE model.

Lemma 3.4 *Let $s \in \Sigma$ be a singular state. Then $(s, s) \in T$ if and only if the following two conditions hold:*

1. *For all $i \in \{1, \dots, n\}$ where s_i is singular, one of the following conditions holds (where $e^i = (0, \dots, 1, \dots, 0)$ denotes the i -th unit vector in \mathbb{R}^n):*

(a) *there exist $q, q' \in \delta(s)$ with $q' = q + e^i$ such that $(q, q') \in E$ and $(q', q) \in E$.*

(b) *there exist $q, q' \in \delta(s)$ with $q' = q + e^i$ such that $(q, q') \notin E$ and $(q', q) \notin E$.*

(c) *there exist $q, q' \in \delta(s)$ and $\tilde{q}, \tilde{q}' \in \delta(s)$ with $q' = q + e^i, \tilde{q}' = \tilde{q} + e^i$ such that both $(q, q') \in E, (q', q) \notin E$, and $(\tilde{q}', \tilde{q}) \in E, (\tilde{q}, \tilde{q}') \notin E$.*

2. *For all $i \in \{1, \dots, n\}$ where s_i is regular, either*

(a) *there exists $q^1, q^2 \in \delta(s)$ and $p^1, p^2 \in Q$ such that $(q^1, p^1), (q^2, p^2) \in E$ and*

$$p_i^1 < q_i^1 = q_i^2 < p_i^2,$$

or,

(b) *for all $q \in \delta(s)$ and $p \in Q$ with $(q, p) \in E$ it holds that $p_i = q_i$.*

PROOF Let s be singular and $(s, s) \in T$. By (3.10), for all $i \in \{1, \dots, n\}$ where $s_i = |a, a + 1|$, we have that $s_i \subset g_i^f(s)$ if and only if

$$\min_{q \in \delta(s)} f_i(q) \leq a < a + 1 \leq \max_{q \in \delta(s)} f_i(q).$$

The inequality $\min_{q \in \delta(s)} f_i(q) \leq a$ implies that there exists either $q \in \delta(s)$ such that $f_i(q) \leq q_i = a$ or there exists $q' \in \delta(s)$ such that $f_i(q') < q'_i = a + 1$. By the STG definition, this implies that there exists $q, q' \in \delta(s)$ such that $q'_i - q_i = 1$ and either $(q, q') \notin E$ or $(q', q) \in E$. Similarly, we can show that the inequality $a + 1 \leq \max_{q \in \delta(s)} f_i(q)$, holds if and only if there exists $q, q' \in \delta(s)$ such that $q_i - q'_i = 1$, and either $(q, q') \notin E$ or $(q', q) \in E$. Logical

reformulation of these two conditions leads to the three cases (a), (b), (c) in condition 1 of the lemma.

Now, we look at the regular variables and how they correspond. If $s_i = |a|$, that is $q_i = a$ for all $q \in \delta(s)$, then $s_i \subset g_i^f(s)$ if and only if either

$$\min_{q \in \delta(s)} f_i(q) < a < \max_{q \in \delta(s)} f_i(q), \text{ or } \min_{q \in \delta(s)} f_i(q) = a = \max_{q \in \delta(s)} f_i(q),$$

by the definition of qualitative values. The former pair of inequalities imply 2.a) of the lemma while the latter pair of equalities imply 2.b) of the lemma by the STG definition. The reverse statements follow with the same arguments. \square

In other words, for a singular steady state s to exist, we need that for each variable i either there exists a transition from a state in $\delta(s)$ that increases in variable i and there exists a transition from a state in $\delta(s)$ that decreases in variable i (1. and 2a) of Lemma 3.4), or all transitions from states in $\delta(s)$ do not increase or decrease in variable i (1b) and 2b) of Lemma 3.4).

Using Lemma 3.4, we are able to relate some of the non-complex cyclic attractors in the STG with singular steady states in the ESG.

Corollary 3.3 *Let $q, q' \in Q$ such that (q, q', q) is a simple cycle in the STG. Then $s \in \Sigma$ is a singular steady state in the ESG where $\delta(s) = \{q, q'\}$. Let $(q^1, q^2, q^3, q^4, q^1)$ be a non-complex cyclic attractor in the STG. Then, $s' \in \Sigma$ is a singular steady state, where $\delta(s') = \{q^1, q^2, q^3, q^4\}$.*

Despite the constraints on the STG imposed by Lemma 3.4, the STG has no unique correspondence to a singular steady state in the ESG, which is reflected by the results in Cor. 2 and the singular steady state $(|1, 2|, |1|)$ in the ESG of Fig. 3.5. Also, in Fig. 3.5, we see the case of an oscillation in two variables that gives rise to the singular steady state $(|0, 1|, |0, 1|)$. Therefore, the trap set property of the STG attractor in the above corollary is not necessary for getting a singular steady state in the ESG. Moreover, we are able to show that the trap set property of the STG attractor does not suffice in obtaining a singular steady state in the ESG.

Example 3.8 Consider a cyclic attractor, $\mathcal{C} := \{q^1, \dots, q^6\}$, in the STG, where $n > 3$, and there exists $s \in \Sigma$ such that $q^1, \dots, q^6 \in \delta(s)$. Because \mathcal{C} oscillates in three variables, the first condition of Lemma 3.4 is satisfied. For the variables i where $s_i = |a, a + 1|$, suppose there exists $\tilde{q} \in \delta(s) \setminus \mathcal{C}$ and $\tilde{q}' \in Q \setminus \delta(s)$ such that $(\tilde{q}, \tilde{q}') \in E$, which would imply by Thm. 3.2 that $(s, s') \in T$ for $s' \in \Sigma$, where $ord(s') = 4$ and $\tilde{q}' \in \delta(s')$. Therefore, s is *not* a singular steady state even though \mathcal{C} is a trap set.

Ex. 3.8 results from the *general* form of the singular state formalism (cf. Rem. 3.1), where such an STG cannot be generated from an interaction graph and logical parameters. If we had not used the general singular state formalism, then by the findings of Richard et al [48], the state s in Ex. 3.8 would be characteristic of the cycle \mathcal{C} and consequently s would be a singular steady state. Therefore, every singular steady state in the general form of the singular state formalism does not necessarily characterise a feedback loop in the interaction graph.

In order to ensure that any cyclic attractor in the STG could correspond to an attractor in the ESG, i.e., the case in Ex. 3.8 does not occur, we require that the discrete hyperrectangle that encases the STG attractor is a trap set, which gives the following result.

Lemma 3.5 *Let $\mathcal{Y} := \mathcal{Y}_1 \times \dots \times \mathcal{Y}_n \subset Q$ be a discrete hyperrectangle, where $\mathcal{Y}_i = [a_i, b_i] \subset Q_i$. Then \mathcal{Y} is a trap set in $STG(f)$ if and only if $U' := \{s \in \Sigma \mid \delta(s) \subset \mathcal{Y}\}$ is a trap set in $ESG(g^f)$.*

PROOF Let \mathcal{Y} be a discrete hyperrectangle in $STG(f)$. Let $U' := \{s \in \Sigma \mid \delta(s) \subset \mathcal{Y}\}$ be a trap set. We assume for some $q \in \mathcal{Y}$ there exists $q' \notin \mathcal{Y}$ such that $(q, q') \in E$. Let $s \in U'$ such that $\delta(s) = \{q\}$. Thm. 3.2 implies that there exists $s' \in \Sigma$, where $\delta(s') = \{q, q'\}$, such that $(s, s') \in \mathcal{T}$, which due to the trap set property implies $s' \in U'$, which further implies $\delta(s') \subset \mathcal{Y}$ and we have a contradiction.

Let \mathcal{Y} be a trap set and $s, s' \in \Sigma$ such that $(s, s') \in T$. Let $s \in U'$ and assume $s' \notin U'$, i.e., U' is not a trap set. If $ord(s) < ord(s')$ then Thm. 3.2 implies there exists $q' \in \delta(s') \setminus \delta(s)$ and $q \in \delta(s) \subset \mathcal{Y}$ such that $(q, q') \in E$, i.e., $q' \in \mathcal{Y}$ because \mathcal{Y} is a trap set. However, because \mathcal{Y} is a discrete hyperrectangle and $\delta(s) \cup \{q'\} \subset \mathcal{Y}$, we have that $\delta(s') \in \mathcal{Y}$ and a contradiction. If $ord(s) > ord(s')$ then Thm. 3.2 implies there exists $q' \in \delta(s') \setminus \delta(s)$, for all $q \in \delta(s) \subset \mathcal{Y}$, such that $(q, q') \in E$, which directly implies that $\delta(s') \in \mathcal{Y}$ and we have a contradiction. \square

With the above trap set conditions, we are able to determine the association of attractors given that every trap set contains at least one attractor. Unfortunately, the number and form of the attractors is generally not deducible from the trap set alone. Nevertheless, the constraints imposed by the STG can be used to determine the structure of attractors in the ESG.

Example 3.9 Suppose that only one STG attractor is contained in the smallest hyperrectangular trap set \mathcal{Y} . Moreover, assume that $\max_{q \in \mathcal{Y}} q_i - \min_{q \in \mathcal{Y}} q_i \leq 1$ for all $i \in \{1, \dots, n\}$, which means there exists $s \in \Sigma$ such that $\delta(s) = \mathcal{Y}$. The strongly connected and trap set properties of the

STG attractor satisfy the conditions in Lemma 3.4, which imply that s is a singular steady state. Moreover, repeating condition 1 of Thm. 3.2 we have that, for any regular state $s' \in \mathcal{Y}$ such that $\delta(s')$ is in the STG attractor, we can find a path from s' to s in the ESG.

The example above suggests that cyclic attractors in the STG often correspond to singular steady states in the ESG. In other words, although the ESG is not a refinement of the STG, we can still use the STG to analyse the ESG. This reflects that the Thomas formalism contains fundamental dynamics of the system that we expect to see in all other formalisms.

3.3 Representation of ODE Equilibria in the Qualitative Formalisms

Because the singular state formalism and the qualitative PADE formalism each have a discrete representation of the thresholds in the ODE model, we expect that both formalisms are representing the same dynamics. In this section, we are particularly interested in how the singular state and qualitative PADE formalisms represent the equilibria in the ODE model with respect to each other. Therefore, we are comparing the $QTG^\Psi(\mathcal{A}) = (\mathcal{D}, \mathcal{T}^\Psi)$ and $ESG(g) = (\Sigma, T)$, where the extended update function g and PADE system \mathcal{A} , which satisfies a fixed set of ordering constraints, have a common standard update function, that is $f^g = f^{\mathcal{A}}$.

A direct consequence of the common underlying update function is that the node sets of the qualitative transition graph and the extended state graph are comparable. In mathematical terms, the functions H and δ map to the same subsets of Q , that is for any $D \in \mathcal{D}$, we can find a unique $s \in \Sigma$ such that $\delta(s) = H(D)$. Consequently, we can construct the mapping $\mu : \mathcal{D} \rightarrow \Sigma$, where

$$\mu(D) := s \in \Sigma \text{ such that } \delta(s) = H(D).$$

This mapping implies that $ord(\mu(D))$ is the order of domain D . Because the intention of the singular state formalism is a logical representation of the thresholds in the PADE model [48], it is not surprising that μ is bijective.

With the bijection of the node sets, we are also able to compare the overapproximated focal set of a singular domain D with the (extended) update of the corresponding singular state $\mu(D)$. Consider a singular domain D with a non-empty overapproximated focal set $\Psi(D)$. The hyperrectangularity of the focal set means that we can represent $\Psi(D)$ as $\Psi(D) = \Psi_1(D) \times \cdots \times \Psi_n(D)$,

where for the regular variable x_i in D

$$\Psi_i(D) := \left[\min_{D' \in \rho(D)} \phi_i(D'), \max_{D' \in \rho(D)} \phi_i(D') \right]. \quad (3.13)$$

Next, we want to see what $\Psi_i(D)$ represents in the Thomas formalism. Because every focal point lies in a regular domain, we can discretise the domains that contain the focal points of the above interval using the discrete mapping $d := d^A$ of Def. 3.2 and thus project $\Psi_i(D)$ onto Q_i to give the discrete interval

$$\left[\min_{D' \in \rho(D)} f_i(d(D')), \max_{D' \in \rho(D)} f_i(d(D')) \right].$$

With the fact that $\delta(\mu(D)) = \{d(D') \in Q \mid D' \in \rho(D)\}$, we recognise the bounds of the above discrete interval to be the same as the bounds of $g_i^f(\mu(D))$ in Def. 3.6. In other words, there is similarity between the dynamics being represented by the overapproximated focal set and the extended update function. Also, previous observations (Prop. 3.1 and Prop. 3.5) imply that every ESG is associated with a QTG^Ψ and vice versa. Consequently, we expect the singular domains in the QTG^Ψ to have common dynamics with the singular states in the ESG.

Some common dynamics of the two graphs is already reflected in our previous results, where one set of conditions on the STG edges of previous lemmas corresponds not only to a specific behaviour in the QTG^Ψ but also to a specific behaviour in the ESG. For example, Prop. 3.2 with Lemma 3.2 and Prop. 3.4 with Lemma 3.5 give the following results respectively

Lemma 3.6 *A path (D^1, \dots, D^{2k+1}) in the QTG^Ψ , where $D^{2j+1} \in \mathcal{D}_r$ for all $j \in \{0, \dots, k\}$, exists if and only if there is a path $(\mu(D^1), \mu(D^2), \dots, \mu(D^{2k+1}))$ in the ESG, where $\mu(D^{2j+1})$ is regular for all $j \in \{0, \dots, k\}$.*

Lemma 3.7 *Let $f : Q \rightarrow Q$ be an update function and $\mathcal{Y} := \mathcal{Y}_1 \times \dots \times \mathcal{Y}_n \subset Q$ be a discrete hyperrectangle, where $\mathcal{Y}_i = [a_i, b_i] \subset Q_i$. Then $U := \{D \in \mathcal{D} \mid H(D) \subset \mathcal{Y}\}$ is a trap set in $QTG^\Psi(\text{PADE}(f)) = (\mathcal{D}, \mathcal{T}^\Psi)$ if and only if $U' := \{s \in \Sigma \mid \delta(s) \subset \mathcal{Y}\}$ is a trap set in $ESG(g^f) = (\Sigma, T)$.*

In other words, paths that alternate between regular and singular domains in QTG^Ψ correspond to paths that alternate between regular and singular states in ESG. Also, hyperrectangular trap sets (as defined in the above lemma) of QTG^Ψ and ESG coincide.

We are able to determine the correspondence of specific edges between the QTG^Ψ and the ESG by combining the results in Thm. 3.1 and Thm. 3.2.

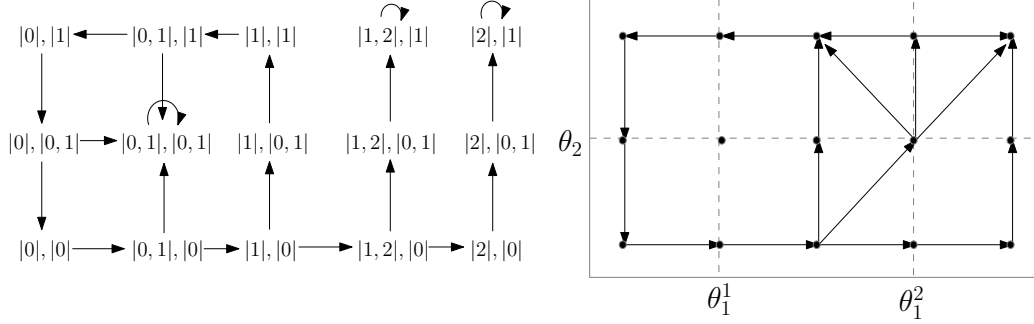


Figure 3.7: Transition graphs of the running example with the ESG on the left and QTG^Ψ on the right.

However, the transitions in QTG^Ψ are between domains that differ by multiple singular variables, whereas the transitions in the ESG are between qualitative values that differ by at most one singular value. In that sense, the 'update' of discrete transitions in the QTG^Ψ can be interpreted as synchronous, which is unlike the asynchronous update of the ESG. For this reason, we can immediately conclude that there is no *simple* correspondence of edges between the two graphs.

Example 3.10 The transition $(D, D') \in \mathcal{T}$ in the QTG^Ψ displayed on the right of Fig. 3.7, where $D := [\theta_1^2] \times (\theta_2, \max_2]$ and $D' := (\theta_1^1, \theta_1^2) \times (\theta_2, \max_2]$ has no corresponding transition in the ESG, that is $\mu(D) \rightarrow \mu(D') \notin T$. We also observe that $\mu(D)$ is a steady state in the ESG while D is not a steady state in the QTG^Ψ . In the same example, the transition from $(|0, 1|, |0|)$ to $(|0, 1|, |0, 1|)$ in the ESG does not correspond to a transition in the QTG^Ψ , that is $(D, D') \notin \mathcal{T}$, where $\mu(D) = (|0, 1|, |0|)$ and $\mu(D') = (|0, 1|, |0, 1|)$.

In other words, the singular state and qualitative PADE formalisms generally do not conserve reachability properties.

Nevertheless, this section wants to focus on the discrete representation of equilibria in the ODE model. We already know from Prop. 3.3 and Cor. 3.2 that a regular steady state in the ESG corresponds to a regular domain that is a steady state in QTG^Ψ . We now look at singular steady states in the ESG and their correspondences in the QTG^Ψ . By combining the results in Lemma 3.4 and Thm. 3.1, we get the following result.

Lemma 3.8 *Let $s \in \Sigma$ be singular and $D \in \mathcal{D}$ such that $\mu(D) = s$. We have $(s, s) \in T$ if and only if for all $i \in \{1, \dots, n\}$ where s_i is regular, either*

- *for all $\tilde{D} \subset \partial D$ with $\tilde{D}_i \subset \partial D_i$, it holds that $(\tilde{D}, D) \in \mathcal{T}$ and $(D, \tilde{D}) \notin \mathcal{T}$, or*

- for all $\tilde{D} \subset \partial D$ with $\tilde{D}_i \subset \partial D_i$, $\max_{x \in D} x_i \neq \max_i$ and $\min_{x \in D} x_i \neq 0$, it holds that $(\tilde{D}, D) \in \mathcal{T}$ and $(D, \tilde{D}) \in \mathcal{T}$.

PROOF Let s be singular and $i \in \{1, \dots, n\}$ such that $s_i = |a, a + 1|$. By Lemma 3.4, we have that $s_i \subset g_i^f(s)$ if and only if condition (1) of Thm. 3.1 is satisfied for the domain D , where $\mu(D) = s$. Therefore, if D is non-transparent, i.e., has transitions from higher order domains, then the singular variables of s are steady, which is implied by both conditions in the lemma. Consider the regular variables of D , that is $s_i = |a|$. Lemma 3.4 implies that if $s_i = |a|$, then either $f_i(q) = q_i$ for all $q \in \delta(s)$ or $\min_{q \in \delta(s)} f_i(q) < q_i < \max_{q \in \delta(s)} f_i(q)$, for all $q \in \delta(s)$.

- The former case occurs if and only if $\{0\} = V_i(D, \Psi(D))$ by Lemma 3.1, which by Thm. 3.1 is equivalent to $(\tilde{D}, D) \in \mathcal{T}$ and $(D, \tilde{D}) \notin \mathcal{T}$, for all $\tilde{D} \subset \partial D$ with $\tilde{D}_i \subset \partial D_i$.
- The latter case occurs if and only if $V_i(D, \Psi(D)) = \{-1, 0, 1\}$ by Lemma 3.1. Then it must hold that D_i is bounded by thresholds, that is $\max_{x \in D} x_i \neq \max_i$ and $\min_{x \in D} x_i \neq 0$. Furthermore, we have that $(\tilde{D}, D) \in \mathcal{T}$ as well as $(D, \tilde{D}) \in \mathcal{T}$, for all $\tilde{D} \subset \partial D$ such that $\tilde{D}_i \subset \partial D_i$.

□

Therefore, one sufficient condition of a singular steady state $\mu(D)$ to exist in the *ESG* is that there are no outgoing transitions from D to neighbouring domains in *QTG Ψ* . One natural implication of Lemma 3.8 is then the conservation of some steady states.

Corollary 3.4 *If $D \in \mathcal{D}$ is a steady state in the *QTG Ψ* , then $\mu(D)$ is a steady state in the *ESG*.*

The inverse statement, however, is not true, i.e., not every steady state in the *ESG* corresponds to a steady state in the *QTG Ψ* , as we have already seen in Ex. 3.10.

It is important to note that both Lemma 3.8 and the above Corollary only compare the nodes and transitions of *QTG Ψ* and *ESG*, but not the dynamics that is represented by these nodes and transitions. Next, we discuss how the singular steady states in the singular state formalism and singular equilibrium sets in the *PADEs* relate, both of which claim to represent equilibria in the *ODE* model.

For a singular equilibrium set to exist, we require $\emptyset \neq \Phi(D) \cap D \subset \Psi(D) \cap D$ for a singular domain D , which can only be determined with a

specific set of kinetic parameters that satisfy the ordering constraints. Still, with another set of kinetic parameters, it could be that $\Phi(D) \cap D = \emptyset$. In that sense, we can only determine *potential* singular equilibrium sets in QTG^Φ from qualitative parameter information, namely $\Psi(D) \cap D \neq \emptyset$ for a singular domain D .

The proof of Lemma 3.8 shows that a singular steady state, $\mu(D)$, always implies that $\mathbf{0} \in V(D, \Psi(D))$ for a singular domain D , where $\mathbf{0}$ is the zero vector. In other words, a singular steady state $\mu(D)$ implies that $\Psi(D) \cap D \neq \emptyset$. Therefore, if $\mu(D)$ is a singular steady state in ESG , then D has a potential singular equilibrium set in QTG^Φ . Unfortunately, the singular steady states in ESG do not account for all potential singular equilibrium sets in QTG^Ψ . For example, if we have a domain D with a non-singular variable i such that $V(D, \Psi(D)) = \{\mathbf{0}, e_i\}$, where $e^i = (0, \dots, 1, \dots, 0)$ denotes the i -th unit vector in \mathbb{R}^n , then $\mu(D)$ is not a steady state in ESG even though D has a potential singular equilibrium set. Except for the case above, the singular steady states in the singular state formalism have a close correspondence with potential singular equilibrium sets in the PADEs. The singular state formalism is otherwise mentioned in the final chapter when comparing the Thomas and ODE models.

Summary:

- The information in the Thomas, singular state and PADE-Q formalisms is equivalent in the sense that an extended update function or ordering constraints can be constructed from an update function and vice versa.
- Many simple behaviours are conserved but neither the singular state nor the PADE formalism is a refinement of the Thomas model.
- The Thomas formalism with its coarser representation can be used to impose constraints on the singular state and PADE-Q formalisms.

The PADE Formalisms

The Thomas and ODE formalisms each have different representation of dynamics, which have been generated from different parameter information. In the PADE setting, from both qualitative parameter information as well as precise kinetic parameters, we can represent the dynamics of the PADEs as transition graphs [15, 4, 7] and as solution trajectories [23]. More specifically, from kinetic parameters, we can represent the dynamics of the PADEs in terms of continuous solutions and the transition graph QTG^Φ . This transition graph conveniently has a common node set to the transition graph QTG^Ψ , which is constructed from qualitative parameter information, i.e., the ordering constraints. Increasing the qualitative parameter information of the ordering constraints to get the parameter inequality constraints (see Sect. 2.2.2 and 2.2.3), we could also include sign of derivative information into the transition system QTS . In other words, the different parameter information required for each analysis method of the PADEs yields subtle differences in the dynamics. In this chapter, we want to investigate these differences and moreover, determine how much of the precise dynamics generated from the kinetic parameters can be deduced from the ordering constraints.

4.1 Comparing the PADE-Q and PADE-R Formalisms

This section investigates the similarities and differences in the dynamics between the qualitative PADE (PADE-Q) [15] and the refined PADE (PADE-R) [4] formalisms. We first discuss the parameter information required for the two models.

A decrease in parameter information often implies a decrease in dynamical information. Suppose we have a PADE \mathcal{A} and a set of parameter inequality constraints (see Ex. 2.4), from which we can construct the $QTS(\mathcal{A})$

(Sect. 2.2.3). The parameter inequality constraints satisfy a set of ordering constraints and thus the QTS is associated with a unique $QTG^\Psi(\mathcal{A})$. The extra partitioning of the mode domains in the QTS , however, often leads to a larger node set than the QTG^Ψ . Consequently, the QTS and QTG^Ψ are very rarely isomorphic.

Conversely, supposing that the PADE \mathcal{A} has fixed ordering constraints but unknown parameter inequality constraints, i.e., the ordering of the focal point components with respect to each other is not known, there could be multiple QTS s related to $QTG^\Psi(\mathcal{A})$. We want to see if from a set of ordering constraints and corresponding QTG^Ψ , we are able to determine the possible number of QTS s that are associated with the single QTG^Ψ .

To discern between the different levels of parameter information, we introduce the following notation. We label a *parametrisation* as a set of parameter inequality constraints that also satisfy the ordering constraints of PADE \mathcal{A} . In other words, a parametrisation is the ordering of all focal point components $\phi_i(D), D \in \mathcal{D}_r$ within each *regular domain component* $\mathcal{P}_{ij}, i \in \{1, \dots, n\}, j \in \{0, \dots, p_i\}$, where $\mathcal{P}_{i0} = [0, \theta_i^1), \mathcal{P}_{ij} = (\theta_i^j, \theta_i^{j+1}), j \in \{1, \dots, p_i - 1\}$ and $\mathcal{P}_{ip_i} = (\theta_i^{p_i}, \max_i]$. We denote the number of focal point components within each regular domain component \mathcal{P}_{ij} by m_{ij} , where $m_{ij} := |\{\phi_i(D) \mid \phi_i(D) \in \mathcal{P}_{ij}, D \in \mathcal{D}_r\}|$.

Each parametrisation gives rise to a QTS and so, theoretically the maximum number of parameterisations should yield the number of QTS s associated to a single QTG^Ψ . Because the parameter inequality constraints are strict inequalities, there are $m_{ij}!$ different orderings of the focal point components within \mathcal{P}_{ij} . Therefore, the maximum number of parametrisations for a class of PADEs with fixed ordering constraints is

$$\prod_{i \in \{1, \dots, n\}, j \in \{0, \dots, p_i\}} m_{ij}!$$

Nevertheless, even in the case that the parameter inequality constraints are equal to the ordering constraints, we can associate multiple QTS s to a single QTG^Ψ .

Example 4.1 Suppose that $m_{ij} = 1$ for all $i \in \{1, \dots, n\}, j \in \{0, \dots, p_i\}$ and let there be a regular domain D with $D_i = [0, \theta_i^1)$ such that $v_i(D, \phi(D)) = 0$ and $v_j(D, \phi(D)) \neq 0$ for all $j \in \{1, \dots, n\} \setminus \{i\}$, which can be determined from the QTG^Ψ . It is clear that in the related QTS , the focal point $\phi(D)$ partitions D , that is $\phi_i(D) \in D_i$. However, if $\phi_i(D) = 0$, then D is partitioned into two flow domains, \tilde{M}^1 and \tilde{M}^2 say, where $\tilde{M}_i^1 = [0]$ and $\tilde{M}_i^2 = (0, \theta_i^1)$, whilst if $\phi_i(D) \in (0, \theta_i^1)$, then D is partitioned into three flow domains, M^1, M^2 and M^3 say, where $M_i^1 = [0, \phi_i(D)), M_i^2 = [\phi_i(D)]$ and $M_i^3 = (\phi_i(D), \theta_i^1)$.

Therefore, even with a single parametrisation, we are still unable to associate

the QTG^Ψ with a unique QTS . Let us look at a case where we know the partitioning of the regular domain component $[0, \theta_i^1)$.

Example 4.2 Consider Ex. 2.3, where the regular domain component $[0, \theta_2^1)$ is partitioned into $[0]$ and $(0, \theta_2^1)$ by the focal point component $\phi_2([0, \theta_1^1) \times [0, \theta_2^1)) = 0$, and the regular domain component $[0, \theta_1^1)$ is partitioned into $[0]$ and $(0, \theta_1^1)$ by the focal point component $\phi_1([0, \theta_1^1) \times (\theta_2^1, \max_2]) = 0$. Then, we have $m_{2j} = m_{1j} = 1$ for $j \in \{0, 1\}$ and $m_{12} = 3$, which implies 6 parametrisations of the ordering constraints (2.11). These parametrisations are presented as follows in terms of the ordering of the focal point components within the regular domain component $(\theta_1^2, \max_1]$:

$$\begin{array}{lll} 1. \kappa_1 < \kappa_2 < \kappa_1 + \kappa_2 & 2. \kappa_2 < \kappa_1 < \kappa_1 + \kappa_2 & 3. \kappa_2 < \kappa_1 + \kappa_2 < \kappa_1 \\ 4. \kappa_1 < \kappa_1 + \kappa_2 < \kappa_2 & 5. \kappa_1 + \kappa_2 < \kappa_1 < \kappa_2 & 6. \kappa_1 + \kappa_2 < \kappa_2 < \kappa_1 \end{array}$$

If we say that QTS^i represents the QTS of the parametrisation associated with the ordering $i \in \{1, \dots, 6\}$ above, then we have that

$$QTS^1 \cong QTS^2 \cong QTS^3 \not\cong QTS^4 \cong QTS^5 \cong QTS^6,$$

where \cong denotes isomorphism. In Fig. 4.1, we see QTS^1 on the left and QTS^4 on the right. We observe that the focal point component κ_1 does not influence the form of the QTS for either parametrisation.

Therefore, not all the extra parameter information that is provided by a parametrisation contributes in determining the refined dynamics in the QTS . For example, although there are 6 different parametrisations of Ex. 2.3 we only have two different partitions of the regular domain component $(\theta_1^2, \max_1]$ and thus only two different QTS s (see Fig. 4.1) are associated with the QTG^Ψ of Ex. 2.3. In other words, the increase in qualitative parameter information means that we cannot associate a QTS to a QTG^Ψ .

Next, we want to determine whether the refined PADE model is indeed a refinement of the qualitative PADE model. Let \mathcal{A} be a PADE with a fixed set of parameter inequality constraints. In the following, we compare the transition graphs $QTG^\Psi(\mathcal{A}) = (\mathcal{D}, \mathcal{T})$ and $QTS(\mathcal{A}) = (\mathcal{M}, \rightarrow)$.

Because they are modelling the same set of PADEs, we expect the transitions of the two graphs to be consistent, that is transitions in one graph to have corresponding transitions in the other graph. From the function $mode : \mathcal{M} \rightarrow \mathcal{D}$, we immediately have a mapping between the respective node sets. Also, we see by the transition definitions of the QTG^Ψ and QTS that there are many similarities. In particular, the conditions 1a) and 2 of Def. 2.13 are similar to conditions 1 and 2 of Def. 2.10 respectively, where

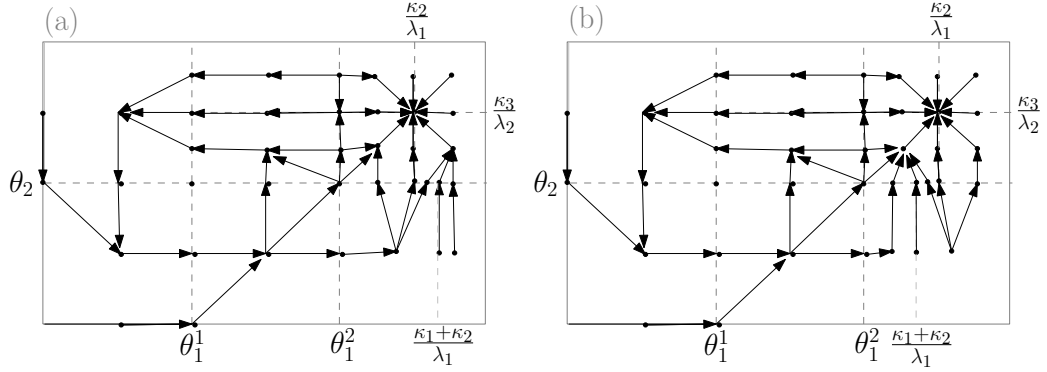


Figure 4.1: Two QTSs of the running example that are related to a common QTG^Ψ , where (a) illustrates the parameterisation $\kappa_2 < \kappa_1 + \kappa_2$ and (b) the parameterisation $\kappa_2 > \kappa_1 + \kappa_2$.

the former definition uses flow domains while the latter uses mode domains. We want to make sure that the similarity of these two definitions implies the same transitions in the two graphs, i.e., the dynamics is consistent between the refined and qualitative PADEs. Here, we again refer to domains in \mathcal{D} as mode domains and domains in \mathcal{M} as flow domains following their introduction in [4].

Proposition 4.1 *Let $D, D' \in \mathcal{D}$ such that $D' \subset \partial D$. Then:*

1. $(D, D') \in \mathcal{T}^\Psi$ if and only if for all $M^1 \subset D$ there exists a path $M^1 \rightarrow \dots \rightarrow M^k$, such that $M^2, \dots, M^{k-1} \subset D$ and $M^k \subset D'$.
2. $(D', D) \in \mathcal{T}^\Psi$ if and only if for all $M \subset D$ there exists a $M' \subset D'$ such that $M \rightarrow M'$.

PROOF Let I and I' be the singular variable sets of D and D' respectively and $D' \subset \partial D$. Now consider the two cases of the proposition.

1. Let $(D, D') \in \mathcal{T}^\Psi$. Reformulating 1) of Def. 2.10, there exists a $\psi \in \Psi(D)$ such that $(\psi - x_i)(x'_i - x_i) > 0$ for all $x \in D, x' \in D'$ and $i \in I' \setminus I$.

For any flow domain $M^1 \subset D$, there exists M^2 such that $(\tilde{x}'_i - \tilde{x}_i)(x'_i - x_i) > 0$ for $\tilde{x} \in M^1, \tilde{x}' \in M^2, x \in D, x' \in D'$ and either $M_i^2 \subset \partial M_i^1$ or $M_i^1 \subset \partial M_i^2$ for all $i \in I' \setminus I$, by the flow domain partition. With the point ψ , 1a) and 2) of Def. 2.13 is satisfied for the cases $M_i^2 \subset \partial M_i^1$ and $M_i^1 \subset \partial M_i^2$ respectively, which in both cases implies that $M^1 \rightarrow M^2$. Assume that $M^2 \subset D$ and repeat the above step, which implies there exists M^3 such that $M^2 \rightarrow M^3$. Repeating this process further, we then obtain a path from M^1 to a flow domain $M^{k-1} \subset D$ such that $\partial M^{k-1} \cap D' \neq \emptyset$.

By the definition of the flow domain partition, there exists a $M^k \subset D'$ such that $M_i^k \subset \partial M_i^{k-1}$ for all $i \in I \setminus I'$. Once again, with the point ψ , 1a) of Def. 2.13 is satisfied for M^{k-1} and M^k , which implies $M^{k-1} \rightarrow M^k$ and we are done. The reverse statement uses the same arguments.

2. Let $(D', D) \in \mathcal{T}^\Psi$. Reformulating 2) of Def. 2.10, there exists $\psi' \in \Psi(D)$ such that $(\psi' - x_i)(x_i - x'_i) > 0$ for all $x' \in D'$, $i \in I \setminus I'$, and for some $x \in D$. By the flow domain partition, for all $M' \subset D'$ there exists $M \subset D$ such that $M'_i \subset \partial M_i$ for all $i \in I \setminus I'$. So, with ψ' , the flow domains M and M' satisfy 2 of Def. 2.13 and thus $M' \rightarrow M$. The reverse statement uses the same arguments. \square

Therefore, although the transition definitions of the QTG^Ψ and QTS (Def. 2.10 and Def. 2.13) are not precisely the same, the transitions, and by extension paths and attractors, are conserved in both the QTG^Ψ and QTS . In particular, a transition in the QTG^Ψ has a corresponding path in the QTS and vice versa. In other words, the refined PADE model is indeed a refinement of the qualitative PADE model. Still, we continue our comparison by looking at the attractors.

Because of the extra sign of derivative information encoded in the flow domains, it could occur that the QTS describes the attractors of the QTG^Ψ differently. For example, if we have an attractor $A \subset \mathcal{D}$ in the QTG^Ψ , then by Prop. 4.1 the set $\bigcup_{D \in A} \mathcal{M}^D \subset \mathcal{M}$ is a trap set in the QTS . However, because a trap set can contain more than one attractor, it is not clear whether the number of attractors is conserved between a QTS and its associated QTG^Ψ . We look at some simple cases, where the number of attractors either do or do not coincide.

In the case that A is a steady state in the QTG^Ψ , we can find a unique corresponding attractor in the related QTS .

Lemma 4.1 *A steady state $D \in \mathcal{D}$ in the QTG^Ψ exists if and only if an attractor $A' \subset \mathcal{M}$ exists in the QTS where $\tilde{M} \subset D$ for all $\tilde{M} \in A'$.*

PROOF Let $A' \subset \mathcal{M}$ be an attractor in the QTS such that $\tilde{M} \subset D$ for all $\tilde{M} \in A'$. By Prop. 4.1 and the trap set condition of A' , there are no outgoing transitions from D , and thus D is a steady state in QTG^Ψ .

Let $D \in \mathcal{D}$ be a steady state in the QTG^Ψ , which by Prop. 4.1 implies that $\bigcup_{\tilde{M} \subset D} \tilde{M}$ is a trap set. By 1b) of Def. 2.13, there must exist $\psi \in \Psi(D)$ such that $\{\psi\} =: M \subset D$ is in the QTS attractor. Assume that there are two attractors in the trap set $\bigcup_{\tilde{M} \subset D} \tilde{M}$. Then in addition to M , there must also exist a $\psi' \in \Psi(D)$ such that $\{\psi'\} =: M' \subset D$ and no path exists between M and M' .

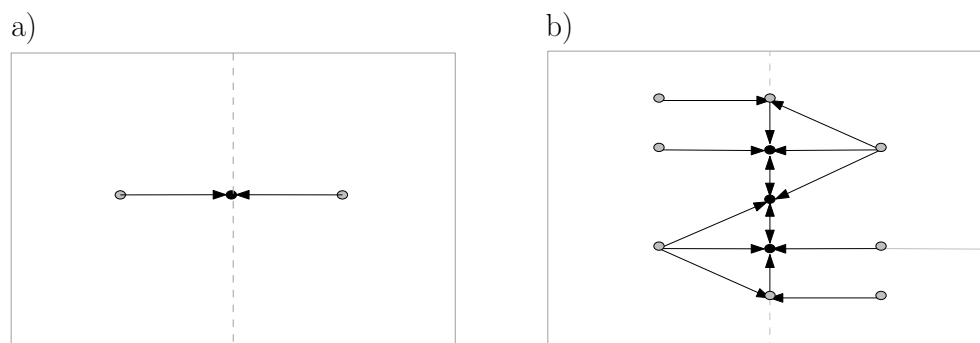


Figure 4.2: In (a), the QTG^Ψ and in (b), the QTS of a set of PADEs of a two component network. The two regular mode domains D, D' in QTG^Ψ , which are depicted by the grey boxes, are each partitioned into three flow domains in the QTS . The focal points $\phi(D) \in D'$ and $\phi(D') \in D$ satisfy the parameter inequality constraints $\phi_2(D) \neq \phi_2(D')$. The attractors in both graphs are depicted by the black nodes. The singular mode domain of order one contains a steady state in the QTG^Ψ but a cyclic attractor in the QTS .

There exists a sequence of flow domains M^1, \dots, M^k such that $M^1 = M$, $M^k = M'$ and either $M^j \subset \partial M^{j-1}$ or $M^{j-1} \subset \partial M^j$ for all $j \in \{2, \dots, k\}$. With ψ' , we have that $M^{j-1} \rightarrow M^j$ for all $j \in \{2, \dots, k\}$, by 1a) or 2) of Def. 2.13, and thus a path exists that connects M^1 to M^2 . The same argument allows us to trace a path from M' to M using ψ , which contradicts M and M' belonging to two disjoint attractors. That is, there is at most one attractor in the trap set $\bigcup_{M \subset D} M$. Fig. 4.2 displays an example of a QTS attractor that corresponds to a steady state in the QTG^Ψ . \square

Because it holds true for steady states in the QTG^Ψ , we ask whether a cyclic attractor in the QTG^Ψ corresponds to a unique attractor in the QTS . Unfortunately, we are able to find a counterexample, where the QTS has a greater number of attractors than the QTG^Ψ .

Example 4.3 Consider the PADE system of three variables with explicit kinetic parameters

$$\begin{aligned} \dot{x}_1 &= S^-(x_2, \frac{1}{2}) - x_1, \\ \dot{x}_2 &= S^+(x_1, \frac{1}{2}) - x_2, \\ \dot{x}_3 &= -x_3, \end{aligned}$$

where $\max_i = 1$ for $i = 1, 2, 3$. The kinetic parameters clearly satisfy a set of parameter inequality constraints, which are equal to the ordering constraints. The only focal point component of the third variable is equal to zero for all regular domains. As a result, for every mode domain D , we have that $D_3 = [0, 1]$ is partitioned into the flow domain components $[0]$ and $(0, 1]$. Fig. 4.3 displays the QTG^Ψ and QTS of the PADEs above. Focussing on the attractors, we see that the QTG^Ψ has a non-complex cyclic attractor of length 8 and steady state $[\frac{1}{2}] \times [\frac{1}{2}] \times [0, 1]$, whereas the QTS has two non-complex cyclic attractors of length 8 and steady state $[\frac{1}{2}] \times [\frac{1}{2}] \times [0]$.

Remark 4.1 If we consider the continuous behaviour of the PADE system in Ex. 4.3, we see that for every flow domain M , where $M_3 = (0, 1]$, it holds that $\dot{x}_3 < 0$ for all $x \in M$. That is, the PADE solutions in these flow domains are always decreasing and thus approaching $x_3 = 0$. In other words, although two non-complex cyclic attractors exist in the QTS , they could be representing a single non-complex cyclic attractor when considering the continuous dynamics of the PADE solutions. However, we also know from Snoussi's findings [56] that the non-complex cyclic attractor in the QTG^Ψ in Fig. 4.3 is a damped oscillation, when considering the PADE solutions. That is, all solution trajectories of Ex. 4.3 converge to the point $(\frac{1}{2}, \frac{1}{2}, 0)$ with increasing time, which is not accounted for in either the QTS or QTG^Ψ .

In other words, the number of attractors in the QTS is not always equal to the number of attractors in the QTG^Ψ . Still, the correspondence of edges as implied by Prop. 4.1 means that the location of attractors in the QTS is given by the attractors in QTG^Ψ . However, the additional sign of derivative information may not contribute more information about the attractors.

4.2 How do the PADE-Q and PADE-D Formalisms differ?

The logical parameters of the Thomas formalism and the kinetic parameters of the ODE formalism imply large differences between the resulting dynamics. In contrast, the PADE setting is more advantageous in distinguishing how the parameters generate specific dynamics. In particular, from the ordering constraints and kinetic parameters, we can generate two transition graphs that have the same node set, QTG^Ψ and QTG^Φ respectively, from which we can observe how sensitive the kinetic parameters are in generating specific dynamics. First, we look at how the ordering constraints and the kinetic parameters relate.

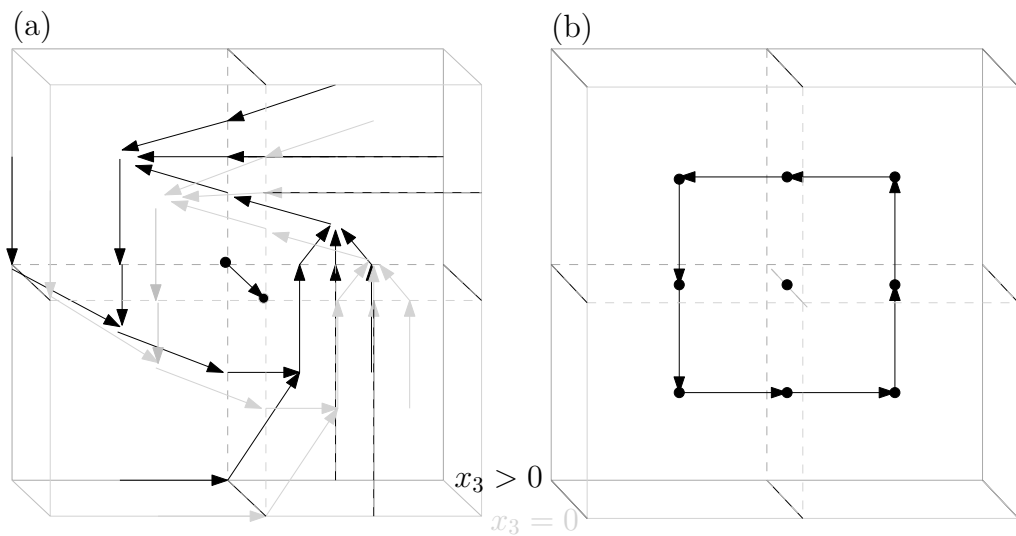


Figure 4.3: The PADE system in Ex. 4.3 generates the QTS in (a) and the QTG^Ψ in (b). In the QTS there are two copies of the same dynamics in black and grey that correspond to the partitions $x_3 \in (0, 1]$ and $x_3 = 0$ respectively. The only transition from the black layer to the grey layer in the QTS is between the flow domains of the singular mode domain of order two, which corresponds to the steady state in the QTG^Ψ .

Consider the PADE \mathcal{A} with a fixed set of kinetic parameters, from which we can generate the qualitative transition graph $QTG^\Phi(\mathcal{A}) = (\mathcal{D}, \mathcal{T}^\Phi)$. Since every set of kinetic parameters satisfies a set of ordering constraints, we can also generate $QTG^\Psi(\mathcal{A}) = (\mathcal{D}, \mathcal{T}^\Psi)$. In other words, for each QTG^Φ there exists a unique QTG^Ψ .

It is less trivial to generate a QTG^Φ from a QTG^Ψ . Although there are infinitely many kinetic parameters that satisfy a set of ordering constraints, only a finite number of QTG^Φ s can be associated with a given QTG^Ψ because there are finitely many subgraphs of QTG^Ψ (subgraph property shown in [15]). Nevertheless, calculating the convex hull of focal points is non-trivial. In turn, from a fixed set of ordering constraints, grouping the kinetic parameter sets that generate a single QTG^Φ is a difficult task. In other words, there is no simple way of deriving an explicit QTG^Φ from a QTG^Ψ in terms of conditions on the kinetic parameters.

Although the kinetic parameters cannot be specified by the ordering constraints, we still relate the two transition graphs for a given set of kinetic parameters. Consider the PADE system \mathcal{A} and a set of kinetic parameters that generate $QTG^\Phi(\mathcal{A}) = (\mathcal{D}, \mathcal{T}^\Phi)$, from which we have a set of ordering constraints that generate $QTG^\Psi(\mathcal{A}) = (\mathcal{D}, \mathcal{T}^\Psi)$. In the following, we want to determine the differences in dynamics between the two transition graphs.

By definition of the focal sets Φ and Ψ , it is clear that the overapproximation only affects the dynamics on singular domains, where the overapproximation is referring to the hyperrectangular definition of the differential inclusion instead of the convex hull definition as in (2.6). As a result, the majority of transitions are conserved between the two graphs QTG^Φ and QTG^Ψ because the regular domains exhibit the same dynamics by definition, and QTG^Φ is a subgraph of QTG^Ψ by Thm. 7.1 of [15].

Lemma 4.2 *For $D \in \mathcal{D}_r$ and $D' \subset \partial D$, we have that:*

- $(D, D') \in \mathcal{T}^\Phi$ iff $(D, D') \in \mathcal{T}^\Psi$
- $(D', D) \in \mathcal{T}^\Phi$ iff $(D', D) \in \mathcal{T}^\Psi$

For $D, D' \in \mathcal{D}_s$, we have that:

- if $(D, D') \in \mathcal{T}^\Phi$ then $(D, D') \in \mathcal{T}^\Psi$

In other words, the only difference between QTG^Φ and QTG^Ψ are some transitions between singular domains. For example, if $(D, D') \notin \mathcal{T}^\Phi$ for $D, D' \in \mathcal{D}_s$ then it could be that $(D, D') \in \mathcal{T}^\Psi$.

Example 4.4 Fig. 4.4 and Fig. 4.5 show that multiple behaviours implied by the ordering constraints are not all possible in a single PADE system with

kinetic parameters. Fig. 4.4 shows that different kinetic parameters for one PADE system yield only steady states in the QTG^Φ , while the QTG^Ψ implies an oscillation between these steady states. In Fig. 4.5, different sets of kinetic parameters yield either $(D, D') \in \mathcal{T}^\Phi$ or $(D', D) \in \mathcal{T}^\Phi$ between the two singular domains $D := [0, \theta_1] \times [\theta_2]$ and $D' := [\theta_1] \times [\theta_2]$ in QTG^Φ , whereas $(D, D') \in \mathcal{T}^\Psi$ and $(D', D) \in \mathcal{T}^\Psi$ are both present in the corresponding QTG^Ψ .

In the framework of the differential inclusion (2.6), an oscillation in QTG^Φ could occur between two singular domains D and D' , that is $(D, D'), (D', D) \in \mathcal{T}^\Phi$. In other words, even with an explicit set of kinetic parameters there exists PADE solutions that imply an oscillation between D and D' due to the non-unique dynamics of the differential inclusion (2.6). However, an oscillation between two singular domains in QTG^Ψ often corresponds to a single transition between the same singular domains in QTG^Φ , as shown by the above example.

For a singular domain D of order one, the convex hull of two focal points of $\rho(D)$ always traces a line, which can intersect $\text{supp}(D)$ at most once, that is $|\Phi(D)| \leq 1$. So, if D has transitions to and from an adjacent domain $D' \subset \partial D$ in QTG^Ψ , that is $(D, D'), (D', D) \in \mathcal{T}^\Psi$, then it is guaranteed that either $(D, D') \notin \mathcal{T}^\Phi$ or $(D', D) \notin \mathcal{T}^\Phi$, because either $\Phi(D) \subset D$ or $\Phi(D) \not\subset D$ respectively.

In summary, the qualitative parameter information encoded in the ordering constraints can imply transitions between adjacent singular domains in the QTG^Ψ that are not necessarily present in a QTG^Φ . Such transitions occur when the focal set of a non-transparent domain is empty, that is $\Phi(D) = \emptyset$ when $\Psi(D) \neq \emptyset$. In other words, the major difference between QTG^Ψ and QTG^Φ is whether the focal sets of singular domains are empty or non-empty.

From the QTG^Ψ , we may already know which singular domains have a non-empty focal set. More specifically, for a singular domain D to have a non-empty focal set, D must also be non-transparent, that is $\Phi(D) \neq \emptyset$ implies $\Psi(D) \neq \emptyset$. In the following, we investigate whether the non-emptiness of a focal set $\Phi(D)$ for a singular domain D can be determined by the information encoded in QTG^Ψ .

It is intuitively clear that if each regular domain in $\rho(D)$, for a singular domain D , has exactly one focal point, which can be determined from the QTG^Ψ , then the convex hull of these focal points would intersect the supporting hyperplane of D . That is, from the ordering constraints, we can determine the non-emptiness of a focal set.

Lemma 4.3 *Let D be a singular domain of order k with singular variable set I and $D_i = \{\theta_i^{r_i}\}$ for $i \in I$. We define an orthant $O \subset \Omega$ such that for*

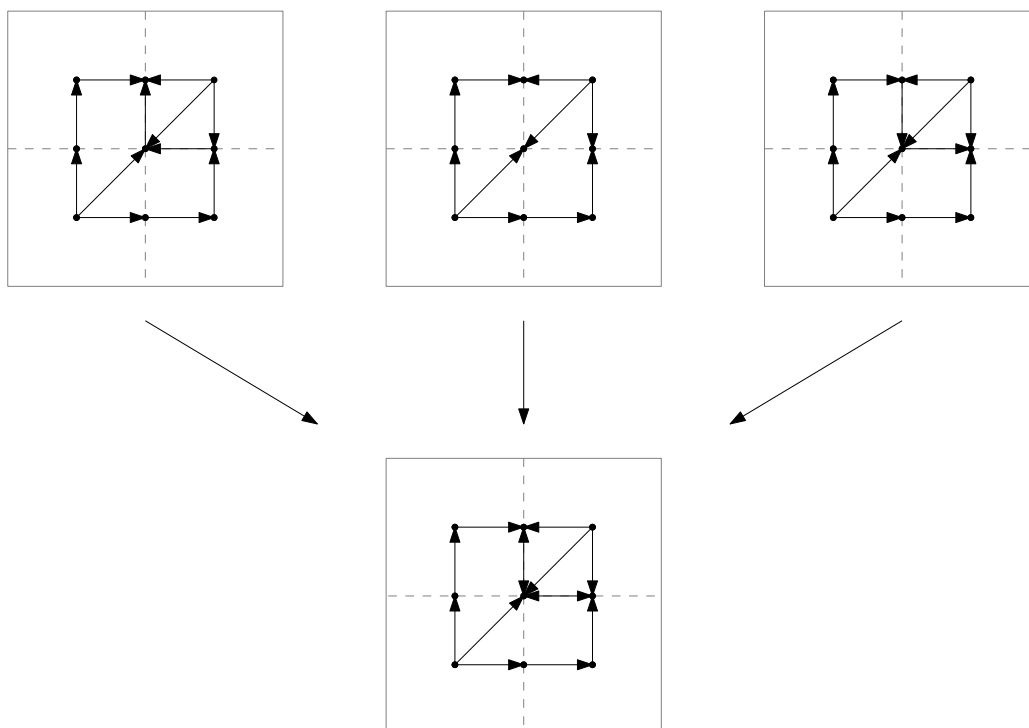


Figure 4.4: Each of the three QTG^Φ s of a two-component network on the top have kinetic parameters that satisfy a fixed set of ordering constraints, which generate the QTG^Ψ on the bottom. The upper right hand regular domain D of all four graphs has the origin as the focal point, i.e., $\phi(D) = (0, 0)$, and the remaining regular domains have a common focal point, $\psi \in D$. The three different QTG^Φ s correspond to three different choices of kinetic parameters and thus different positions of the focal point ψ within D .

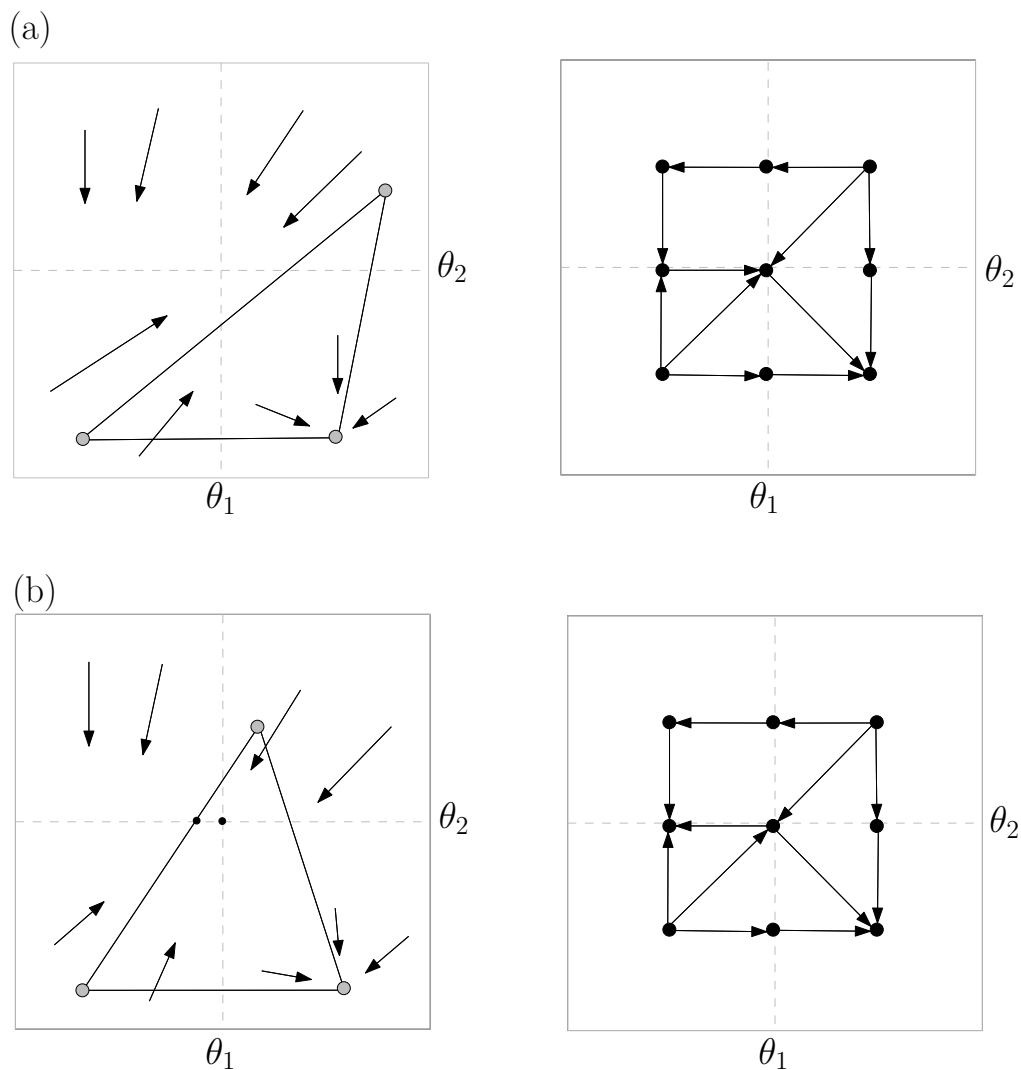


Figure 4.5: On the left of (a) is the phase space of a PADE system of a two-component network with explicit kinetic parameters. The grey dots depict the focal points, where we see that the convex hull of focal points does not intersect the domain $D := [\theta_1] \times [\theta_2]$ and thus $\Phi(D) = \emptyset$. The corresponding QTG^Φ is displayed on the right. On the left of (b) is the phase space of the same PADE system as in (a) but with another set of explicit kinetic parameters. We see in (b) that the convex hull of focal points does intersect with D , which gives rise to the singular equilibria depicted as black dots. Note that both kinetic parameters used in (a) and (b) satisfy the same ordering constraints to generate a common QTG^Ψ .

all $i \in I$ either $x_i < \theta_i^{r_i}$ for all $x \in O$ or $\theta_i^{r_i} > x_i$ for all $x \in O$. That is, there are 2^k orthants corresponding to domain D . If a focal point $\phi(D'), D' \in \rho(D)$ lies in each of the 2^k orthants, then $\Phi(D) \neq \emptyset$.

PROOF Let D be a singular domain of order k and each of the 2^k orthants corresponding to D have exactly one focal point $\phi(D'), D' \in \rho(D)$. We want to show that the convex hull of the focal points intersects with the supporting hyperplane of D . We prove by induction that the convex hull of $2^m, m < k$ focal points intersects with m threshold hyperplanes.

We initiate the induction for $i \in I$, i.e., $m = 1$. If $\phi_i(D^1) < \theta_i^{r_i} < \phi_i(D^2)$ for $D^1, D^2 \in \rho(D)$, and for all $j \in I \setminus \{i\}$ either $\phi_i(D^1), \phi_i(D^2) < \theta_i^{r_i}$ or $\theta_i^{r_i} > \phi_i(D^1), \phi_i(D^2)$, then there exists $x \in \overline{\text{co}}(\{\phi(D^1), \phi(D^2)\})$ such that $x_i = \theta_i^{r_i}$. That is, when the two focal points are on either side of a threshold hyperplane, then the convex hull of these two focal points intersects the hyperplane.

Next, we show the induction step for $I' \subset I$, where we let $D^1, \dots, D^l \in \rho(D), m := |I'|$ and $l := 2^m$. We assume that if for all $j \in I \setminus I'$ either $\phi_j(D^k) < \theta_j^{r_j}$ for all $k = 1, \dots, l$ or $\phi_j(D^k) > \theta_j^{r_j}$ for all $k = 1, \dots, l$ then there exists $x \in \overline{\text{co}}(\{\phi(D^k) \mid k = 1, \dots, l\})$ such that $x_j = \theta_j^{r_j}$ for all $j \in I \setminus I'$. That is, we assume the convex hull of 2^m focal points intersects with m threshold hyperplanes, from which we want to prove that the property also holds for $m + 1$. Consider $j^* \in I \setminus I'$ and $D^1, \dots, D^l, \tilde{D}^1, \dots, \tilde{D}^l \in \rho(D)$ such that $\phi_{j^*}(D^k) < \theta_{j^*}^{r_{j^*}} < \phi_{j^*}(\tilde{D}^k)$ for all $k = 1, \dots, l$, and for each $j \in I \setminus (I' \cup \{j^*\})$, either $\phi_j(D^k) < \theta_j^{r_j}$ and $\phi_j(\tilde{D}^k) > \theta_j^{r_j}$ for all $k = 1, \dots, l$ or $\phi_j(D^k) > \theta_j^{r_j}$ and $\phi_j(\tilde{D}^k) > \theta_j^{r_j}$ for all $k = 1, \dots, l$. By our assumption, there exists $x \in \overline{\text{co}}(\{\phi(D^k) \mid k = 1, \dots, l\})$ and $x' \in \overline{\text{co}}(\{\phi(\tilde{D}^k) \mid k = 1, \dots, l\})$ such that $x_j, x'_j = \theta_j^{r_j}$ for all $j \in I \setminus (I' \cup \{j^*\})$. However, we also have that $x_{j^*} < \theta_{j^*}^{r_{j^*}} < x'_{j^*}$, which implies that there exists $x'' \in \overline{\text{co}}(\{\phi(D^*) \mid D^* \in \{D^1, \dots, D^l, \tilde{D}^1, \dots, \tilde{D}^l\}\})$ such that $x''_{j^*} = \theta_{j^*}^{r_{j^*}}$. Therefore, by induction there exists $x^* \in \overline{\text{co}}(\{\phi(D') \mid D' \in \rho(D)\})$ such that $x_i^* = \theta_i^{r_i}$ for all $i \in I$, that is $x^* \in \Phi(D) \neq \emptyset$. \square

In other words, we do not always need the kinetic parameters to determine the non-emptiness of a focal set. Sometimes, we can determine whether a focal set is non-empty from the information encoded in QTG^Ψ . Now, we want to find a graph-theoretical condition on QTG^Ψ that would imply a non-empty focal set for one of the domains.

We see in both examples of Fig. 3.4 that the condition in Lemma 4.3 is satisfied for the singular domain of order two. This observation suggests that there may be some correlation between a steady state in the QTG^Ψ and the condition in Lemma 4.3. We exploit Thm. 3.1 by imposing restrictions

on the corresponding update function and STG in order to determine the conditions for a steady state in QTG^Ψ .

As we see in Fig. 3.4, if the singular domain of order two is a steady state in QTG^Ψ , then the restrictions imposed by Thm. 3.1 on the corresponding update function and STG are not unique. We also see, after experimentation, that Fig. 3.4 depicts the *only* two examples that lead to the singular domain of order two being a steady state in QTG^Ψ (the only exception being the reflection of the non-complex cyclic attractor in Fig. 3.4(b)). That is, the restrictions imposed by the STG to yield a singular domain, which is a steady state in QTG^Ψ , imply very particular STG edges. From the examples in Fig. 3.4, we observe that a singular domain of order two that has no transition to lower order domains in QTG^Ψ has a non-empty focal set. We generalise this observation in the following theorem to account for higher order singular domains.

Theorem 4.1 *Let \mathcal{A} be a PADE with $QTG^\Psi(\mathcal{A}) = (\mathcal{D}, \mathcal{T}^\Psi)$. Let D be a singular domain. If it holds that $(D, D') \notin \mathcal{T}^\Psi$ for all $D' \in \mathcal{D}$, where $D \subset \partial D'$, then $\Phi(D) \neq \emptyset$.*

We first introduce some notation and then two lemmas that break up the task of proving the theorem. In the following, we consider $D \in \mathcal{D}_s$ to be of order k as in the theorem with singular variable set I . We want to show that the conditions in the theorem, i.e., $(D, D') \notin \mathcal{T}^\Psi$ for all $D' \in \mathcal{D}$, where $D \subset \partial D'$, imply specific dynamics on the surrounding domains. This will then allow us to use Lemma 4.3 to show that the corresponding focal set is non-empty.

As a first step, we take advantage of the correspondence of STG to QTG^Ψ edges (Thm. 3.1) by converting the conditions in the theorem to conditions on $STG(f^A) = (Q, E)$. From Thm. 3.1, we know that in order to determine whether $(D, D') \notin \mathcal{T}$ for all D' such that $D \subset \partial D'$, we only need to consider the edges in $H(D)$, i.e., the discretisation of the regular domains $\rho(D)$. Consequently, we are able to transform the conditions of the theorem into STG conditions within $H(D)$, for which we identify each domain D' of lower order using the following notation.

Consider the $2k$ singular domains $D^{i\alpha}$ of order $(k-1)$, where $i \in I$ and $\alpha \in \{+, -\}$, such that $V(D, D^{i\alpha}) = \{w\}$, where $w_i = 1$ if $\alpha = +$ and $w_i = -1$ if $\alpha = -$, $w_j = 0$ for $j \in I \setminus \{i\}$ and $D \subset \partial D^{i\alpha}$. In other words, $D^{i+}(D^{i-})$ is the domain of order $k-1$ that has D in its boundary, has singular variable set $I \setminus \{i\}$, and $x_i < x'_i$ (resp. $x_i > x''_i$) for all $x \in D$ and $x' \in D^{i+}$ (resp. $x'' \in D^{i-}$).

This notation then implies that $H(D^{i\alpha})$ defines a $(k-1)$ -dimensional *face* of the hypercube $H(D)$. Using these faces, we are able to identify smaller

sub-hypercubes of $H(D)$. In particular, for every domain D' of order $k - m$, where $D \subset \partial D'$, there exists $\{i_1, \dots, i_m\} \subset I$ and $\alpha_1, \dots, \alpha_m \in \{+, -\}$ such that

$$H^{i_1\alpha_1\dots i_m\alpha_m} := \bigcap_{j=1,\dots,m} H(D^{i_j\alpha_j}) = H(D').$$

In other words, $\{i_1, \dots, i_m\}$ are the singular variables of D that are non-singular variables in D' and thus have fixed values in the sub-hypercube $H^{i_1\alpha_1\dots i_m\alpha_m}$. The sign α_j denotes whether the variable i_j is fixed at a lower or higher level. For example, for $m = k$, we have that $H^{i_1\alpha_1\dots i_k\alpha_k} = \{q\}$, where $q \in H(D)$ such that $q_{i_j} = \min_{q' \in H(D)} q'_{i_j}$ for $\alpha_{i_j} = -$ and $q_{i_j} = \max_{q' \in H(D)} q'_{i_j}$ for $\alpha_{i_j} = +, j \in \{1, \dots, k\}$. With the above notation, we can identify all domains that are neighbouring D and that are of order less than k .

In order to describe transitions between these sub-hypercubes, we introduce the following notation.

$$H^{i_1\alpha_1\dots i_{m-1}\alpha_{m-1}i_m\alpha_m} \rightarrow H^{i_1\alpha_1\dots i_{m-1}\alpha_{m-1}i_m-\alpha_m}$$

denotes $(q, q') \in E$ for all $q \in H^{i_1\alpha_1\dots i_{m-1}\alpha_{m-1}i_m\alpha_m}$ and $q' \in H^{i_1\alpha_1\dots i_{m-1}\alpha_{m-1}i_m-\alpha_m}$, where $|q - q'| = 1$, $-\alpha = -$ if $\alpha = +$ and $-\alpha = +$ if $\alpha = -$. In other words, there is an STG edge from every state in $H^{i_1\alpha_1\dots i_{m-1}\alpha_{m-1}i_m\alpha_m}$ to another state in $H^{i_1\alpha_1\dots i_{m-1}\alpha_{m-1}i_m-\alpha_m}$. Also,

$$H^{i_1\alpha_1\dots i_{m-1}\alpha_{m-1}i_m\alpha_m} \not\leftarrow H^{i_1\alpha_1\dots i_{m-1}\alpha_{m-1}i_m-\alpha_m}$$

denotes $(q', q) \notin E$ for all $q \in H^{i_1\alpha_1\dots i_{m-1}\alpha_{m-1}i_m\alpha_m}$ and $q' \in H^{i_1\alpha_1\dots i_{m-1}\alpha_{m-1}i_m-\alpha_m}$, where $|q - q'| = 1$. In other words, there is no STG edge from any state in $H^{i_1\alpha_1\dots i_{m-1}\alpha_{m-1}i_m\alpha_m}$ to any other state in $H^{i_1\alpha_1\dots i_{m-1}\alpha_{m-1}i_m-\alpha_m}$.

We now look at a domain D' , where $D \subset \partial D'$, and determine conditions in terms of edges on the STG that imply whether $(D, D') \notin \mathcal{T}^\Psi$. Let D' be of order $k - m$ with $\{i_1, \dots, i_m\} \subset I$ and $\alpha_1, \dots, \alpha_m \in \{+, -\}$ such that $H^{i_1\alpha_1\dots i_m\alpha_m} = H(D')$. In the case when D' is transparent, that is $\Psi(D') = \emptyset$, there are no transitions to or from D' , that is $(D, D') \notin \mathcal{T}^\Psi$. The STG edges that imply D' is transparent can be derived by negating (1) of Thm. 3.1. In the case when D' is non-transparent, that is $\Psi(D') \neq \emptyset$, we need that $(D, D') \notin \mathcal{T}^\Psi$, which can be deduced by negating the second part of condition (3) of Thm. 3.1. These two cases then imply the following conditions on $H(D)$ respectively.

(1*) D' is transparent iff there exists $i_{m+1} \in I \setminus \{i_1, \dots, i_m\}$ and $\alpha_{m+1} \in \{+, -\}$ such that

$$H^{i_1\alpha_1\dots i_m\alpha_m i_{m+1}-\alpha_{m+1}} \rightarrow H^{i_1\alpha_1\dots i_m\alpha_m i_{m+1}\alpha_{m+1}}$$

and

$$H^{i_1\alpha_1\dots i_m\alpha_m i_{m+1}-\alpha_{m+1}} \not\leftarrow H^{i_1\alpha_1\dots i_m\alpha_m i_{m+1}\alpha_{m+1}}.$$

(2*) For a non-transparent domain D' , there exists $j \in \{1, \dots, m\}$ such that $H^{i_1\alpha_1\dots i_j\alpha_j\dots i_m\alpha_m} \rightarrow H^{i_1\alpha_1\dots i_j-\alpha_j\dots i_m\alpha_m}$.

That is, (1*) implies that between any two states in $H^{i_1\alpha_1\dots i_j\alpha_j\dots i_m\alpha_m}$ that differ in variable i_{m+1} there is only an edge that is increasing (resp. decreasing) and not decreasing (resp. increasing). Condition (2*) implies that there is an edge that either increases in the variable i_j from every state in $H^{i_1\alpha_1\dots i_j\alpha_j\dots i_m\alpha_m}$ if $\alpha_j = -$ or decreases in the variable i_j from every state in $H^{i_1\alpha_1\dots i_j\alpha_j\dots i_m\alpha_m}$ if $\alpha_j = +$.

We require that either (1*) or (2*) is satisfied for every sub-hypercube $H^{i_1\alpha_1\dots i_m\alpha_m}$ in order for the conditions of the theorem to be satisfied. If neither (1*) nor (2*) is satisfied for $H^{i_1\alpha_1\dots i_m\alpha_m}$, we then have $(D, D') \in \mathcal{T}^\Psi$, which contradicts the theorem assumptions. Note that for every $i \in I$ and $\alpha \in \{+, -\}$, if the face $H^{i\alpha}$ satisfies (2*), then every sub-hypercube $H^{i_1\alpha_1\dots i_m\alpha_m} \subset H^{i\alpha}$ also satisfies (2*). We will show that if for every $H^{i\alpha}$ either (1*) or (2*) is satisfied, then every sub-hypercube also satisfies either (1*) or (2*). That is, our primary objective is to show how every face $H^{i\alpha}$ can satisfy either (1*) or (2*).

We break up this task into the following two lemmas.

Lemma 4.4 *If a face $H^{i_1-\alpha_1}$, $i_1 \in I$, $\alpha_1 \in \{+, -\}$ satisfies (2*), i.e., $H^{i_1-\alpha_1} \rightarrow H^{i_1\alpha_1}$, then under the conditions of the theorem, the opposite face $H^{i_1\alpha_1}$ also satisfies (2*).*

PROOF We prove by induction that $H^{i_1\alpha_1}$ satisfying (1*) would contradict the conditions of the theorem. Assume that $H^{i_1\alpha_1}$ satisfies (1*). Then there exists $i_2 \in I \setminus \{i_1\}$ and $\alpha_2 \in \{+, -\}$ such that $H^{i_1\alpha_1 i_2-\alpha_2} \rightarrow H^{i_1\alpha_1 i_2\alpha_2}$ and $H^{i_1\alpha_1 i_2-\alpha_2} \not\leftarrow H^{i_1\alpha_1 i_2\alpha_2}$. Repeating this procedure, we obtain the $k-1$ assumptions, namely $H^{i_1\alpha_1\dots i_j\alpha_j}$ satisfies (1*), where $i_j \in I \setminus \{i_1, \dots, i_{j-1}\}$ and $\alpha_j \in \{+, -\}$ for $j = 2, \dots, k$. Therefore, there exists $q \in H^{i_1\alpha_1}$ such that $(q, q') \notin E$ for all $q' \in H^{i_1\alpha_1} \setminus \{q\}$.

For $H^{i_1\alpha_1\dots i_k\alpha_k}$ to satisfy (2*), it must hold that $H^{i_1\alpha_1\dots i_k\alpha_k} \rightarrow H^{i_1-\alpha_1\dots i_k\alpha_k}$. However, $H^{i_2\alpha_2\dots i_k\alpha_k}$ cannot satisfy (1*) and thus must satisfy (2*), which would contradict the list of assumptions. Now comes the induction step where we assume m assumptions and then show why the m -th assumption contradicts the conditions of the theorem.

Consider the m assumptions that $H^{i_1\alpha_1\dots i_j\alpha_j}$ satisfies (1*), where $i_j \in I \setminus \{i_1, \dots, i_{j-1}\}$ and $\alpha_j \in \{+, -\}$ for $j = 2, \dots, m$ and $H^{i_1\alpha_1\dots i_m\alpha_m}$ does not satisfy (1*). Because $H^{i_1\alpha_1\dots i_m\alpha_m}$ must satisfy (2*), it must hold that

$H^{i_1\alpha_1\dots i_m\alpha_m} \rightarrow H^{i_1^{-\alpha_1}\dots i_m\alpha_m}$, which also means that $H^{i_2\alpha_2\dots i_m\alpha_m}$ cannot satisfy (1*). However, $H^{i_2\alpha_2\dots i_m\alpha_m}$ satisfying (2*) would contradict the m assumptions. Therefore, by induction, when a face $H^{i\alpha}$ does not satisfy (1*), then both $H^{i\alpha}$ and $H^{i^{-\alpha}}$ satisfy (2*), which implies that $(q, q')(q', q) \in E$ for all $q \in H^{i^+}$ and $q' \in H^{i^-}$ with $|q - q'| = 1$. \square

An example of Lemma 4.4 for a singular domain of order two is displayed in Fig. 3.4(a). For a singular domain of order one, the corresponding faces consist of single states and thus cannot satisfy (1*). After applying Lemma 4.4, the singular domain of order one has corresponding STG transitions as implied by Cor. 3.1. Now we introduce a lemma that considers the case where all faces in $H(D)$ satisfy (1*).

Lemma 4.5 *If each face satisfies (1*) then under the conditions of the theorem, all transitions in $H(D)$ are defined by the permutation $\sigma : I \rightarrow I$ and function $\beta : I \rightarrow \{+, -\}$ such that*

$$H^{i\pm\sigma(i)\beta(i)\mp} \rightarrow H^{i\pm\sigma(i)\beta(i)\pm} \text{ and } H^{i\pm\sigma(i)\beta(i)\mp} \not\leftarrow H^{i\pm\sigma(i)\beta(i)\pm}$$

for all $i \in I$, and $\sum_{j=1}^p \mathbb{1}_{\{\beta(\sigma^j(i))=-\}}$ is odd, where $\mathbb{1}$ is the indicator function and $p \in \mathbb{Z}$ is a minimal integer such that $\sigma^p(i) = i$.

PROOF Consider the case that (1*) is satisfied for all $H^{i\alpha}$. First we concentrate on the edges implied by condition (1*). Every element $i\alpha \in I \times \{+, -\}$ represents a face $H^{i\alpha}$. For $H^{i\alpha}$ to satisfy (1*), there must exist $j\alpha' \in I \setminus \{i\} \times \{+, -\}$, such that $(q, q') \in E$ and $(q', q) \notin E$ for all $q \in H^{i\alpha} \setminus H^{j\alpha'}$ and $q' \in H^{j\alpha'}$ such that $|q - q'| = 1$. We introduce the function $\eta : I \times \{+, -\} \rightarrow I \times \{+, -\}$ such that $\eta(i\alpha) = j\alpha'$. In other words, the function η describes all the STG edges that ensure (1*) is satisfied for all $H^{i\alpha}$. In particular, $\eta(i\alpha) = j\alpha'$ implies that $i \neq j$ and every transition between states that only differ in variable j is only increasing if $\alpha' = +$ and only decreasing if $\alpha' = -$. For example, in Fig. 3.4(b) we have that $\eta^4(1+) = \eta^3(2+) = \eta^2(1-) = \eta(2-) = 1+$. Note that for now, not all the edges of the STG are specifically defined by η . Fig. 4.6 depicts the above notation.

Now we look closely at the properties of the mapping η such that the conditions of the theorem are met, i.e., all sub-hypercubes of $H(D)$ satisfy either (1*) or (2*). Let $i \in I$ and $\alpha \in \{+, -\}$. Because η is an endomorphism of a finite set, there exists $p \leq 2k$ and $p' \in \{0, 1, \dots, p\}$ such that $\eta^{p'}(i\alpha) = \eta^p(i\alpha)$. Consider the sequence $i_j\alpha_j = \eta^j(i\alpha)$ for $j \in \{p', \dots, p\}$, that is a sequence that repeats itself after $p - p'$ iterations of η . We show in the following that this repeating sequence results in either the transitions in the lemma that are described by the functions σ and β or a contradiction.

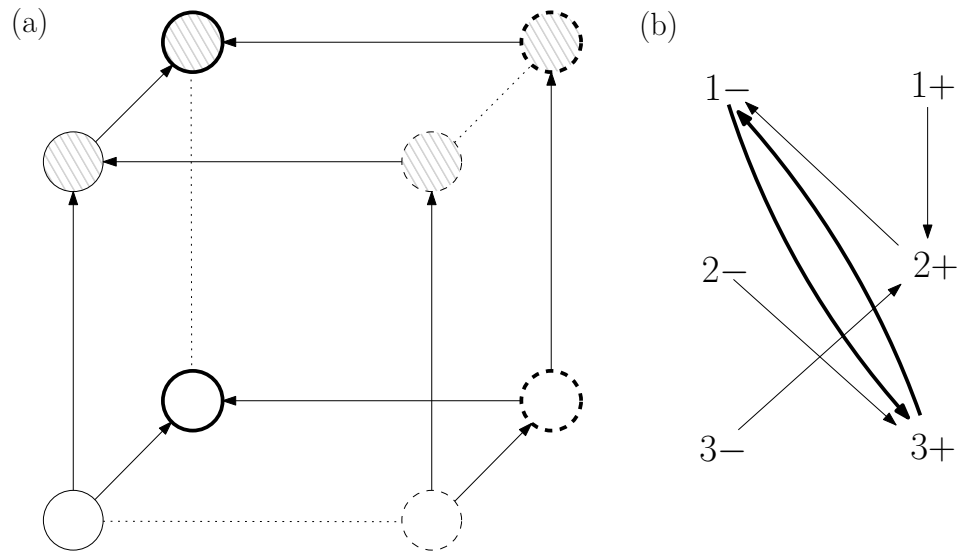


Figure 4.6: In (a), the hypercube $H(D)$ corresponding to a singular domain D of order 3 with singular variables $\{1, 2, 3\}$. The dashed circles represent H^{1+} and the unbroken circles represent H^{1-} . The striped circles represent H^{2+} while the white circles represent H^{2-} . The thickly drawn circles represent H^{3+} while the thinly drawn circles represent H^{3-} . The function η is displayed in (b) corresponding to the edges of the STG in (a). The thick arrows in (b) show the repeating sequence that is implied by this choice of η . Note that the edges in H^{1+2+} , H^{1-3+} and H^{2-3-} are not determined by η depicted by the dotted lines.

The first case considers when the sequence implies STG edges that increase and then decrease in a single variable i^* . Let $j, j' \in \{p', \dots, p\}$ such that $i_{j+1} = i_{j'+1} =: i^*$ and $\alpha_{j+1} = -\alpha_{j'+1}$, i.e., $\eta(i_j \alpha_j) = i^*+$ and $\eta(i_{j'} \alpha_{j'}) = i^*-$. If $j \neq j'$, then condition (1*) would imply $H^{i_j \alpha_j i^*-} \rightarrow H^{i_{j'} \alpha_{j'} i^*+}$ and $H^{i_{j'} \alpha_{j'} i^*+} \not\leftarrow H^{i_j \alpha_j i^*-}$, which implies a contradiction because $H^{i_j \alpha_j} \cap H^{i_{j'} \alpha_{j'}} \neq \emptyset$. Therefore, $j = j'$ by the argument above and $\alpha_j = -\alpha_{j'} \in \{+, -\}$ because one pre-image cannot map to two different images. Repeating this for the whole sequence, we have that $i_{j-m} = i_{j'-m}$ and $\alpha_{j-m} = -\alpha_{j'-m}$ for $m \in \{1, \dots, p' - p\}$, where $p + 1$ is identified with $p' + 1$. Therefore, it must hold that $i_{p'-1} \alpha_{p'-1} = i_{p-1} \alpha_{p-1}$, which implies that $p' = 0$, p is divisible by two and because i_j cannot be equal to i_{j-1} by definition of η , it holds that $p \geq 4$. In other words, the component $i_j = i_{j+p/2}$ has a unique pre-image variable $i_{j+1} = i_{j+p/2+1}$, which we can simplify with a function $\sigma : I \rightarrow I$, i.e. $\sigma(i_j) = i_{j+1}$. Also, either the sign remains the same, i.e. $\alpha_j = \alpha_{j+1}$ or the sign changes, i.e. $\alpha_j = -\alpha_{j+1}$, which can be defined by a function $\beta : I \rightarrow \{+, -\}$. To ensure that both i^*+ and i^*- are in this repeating sequence described by σ and β , we also need that $\sum_{j=1}^{p/2} \mathbb{1}_{\{\beta(\sigma^j(i))=-\}}$ is odd. If this sum of indicator functions is even then we have the second case below.

The second case considers when the sequence implies STG edges that only increase or only decrease in a single variable of the sequence. Consider the case where $j^* \in \{p', \dots, p\}$ such that $i_{j^*} \neq i_l$ for all $l \in \{p', \dots, p\} \setminus \{j^*\}$. If there was a variable i that has both $i+$ and $i-$ in the sequence then we would have the previous case. Therefore, all indices in the sequence only appear once, that is $i_j \neq i_{j'}$ for all $j, j' \in \{p', \dots, p\}$. By condition (1*) and definition of η , it holds that $(q, q') \notin E$ for all $q \in H^{i_{p'} \alpha_{p'} \dots i_p \alpha_p}$ and $q' \in H(D) \setminus H^{i_{p'} \alpha_{p'} \dots i_p \alpha_p}$. In other words, $H^{i_{p'} \alpha_{p'} \dots i_p \alpha_p}$ is a trap set within $H(D)$, which cannot satisfy (2*) and must satisfy (1*). So, by condition (1*), there exists $i^* \in I \setminus \{i_{p'}, \dots, i_p\}$ and $\alpha^* \in \{+, -\}$ such that $H^{i_{p'} \alpha_{p'} \dots i_p \alpha_p i^* - \alpha^*} \rightarrow H^{i_{p'} \alpha_{p'} \dots i_p \alpha_p i^* \alpha^*}$ and $H^{i_{p'} \alpha_{p'} \dots i_p \alpha_p i^* - \alpha^*} \not\leftarrow H^{i_{p'} \alpha_{p'} \dots i_p \alpha_p i^* \alpha^*}$. Once again, by the previous restrictions, $H^{i_{p'} \alpha_{p'} \dots i_p \alpha_p i^* \alpha^*}$ cannot satisfy (2*) and must satisfy (1*). We can then repeat this procedure until we obtain a fixed point in $H(D)$, which cannot satisfy (1*) or (2*). So, we would have a contradiction, which can be seen in Fig. 4.6 for the sub-hypercube H^{1-3+} . Therefore, we *cannot* have a sequence $i_j \alpha_j$, where there exists $j^* \in \{p', \dots, p\}$ such that $i_{j^*} \neq i_l$ for all $l \in \{p', \dots, p\} \setminus \{j^*\}$.

Therefore, when (1*) is satisfied for all $H^{i\alpha}$ then the function η has a specific form that can be reduced to the functions $\sigma : I \rightarrow I$ and $\beta : I \rightarrow \{+, -\}$, such that $\eta(i\alpha) = \sigma(i)\beta(i)\alpha$ and $\sum_{j=1}^m \mathbb{1}_{\{\beta(\sigma^j(i))=-\}}$ is odd. We now show surjectivity of σ . Because for all i it is true that $H^{i \pm \sigma(i)\beta(i)\mp} \rightarrow H^{i \pm \sigma(i)\beta(i)\pm}$

and $H^{i\pm\sigma(i)\beta(i)\mp} \not\leftarrow H^{i\pm\sigma(i)\beta(i)\pm}$, we have that 1c) of Thm. 3.1 is satisfied for all $j \in I \setminus \{i\}$. In particular, there exists $q, q', \tilde{q}, \tilde{q}' \in H^{j\pm}$ such that $(q, q')(\tilde{q}', \tilde{q}) \in E$ and $(q', q)(\tilde{q}, \tilde{q}') \notin E$ for $q_{\sigma(i)} - q'_{\sigma(i)} = 1 = \tilde{q}_{\sigma(i)} - \tilde{q}'_{\sigma(i)}$. Hence, $\sigma(j) \neq \sigma(i)$, i.e., σ is surjective and a permutation of I . \square

We are able to show that the permutation σ and function β from Lemma 4.5 imply that every sub-hypercube of $H(D)$ satisfies either (1*) or (2*). For all $i \in I$, we have that $H^{i+} \cup H^{i-} = H(D)$, which implies that the edges between every $q \in H^{\sigma(i)+}$ and $q' \in H^{\sigma(i)-}$, where $|q - q'| = 1$, are strictly defined by condition (1*). In other words, all edges of the STG are accounted for by this specific definition of the permutation σ and function β . If $H^{i_1\alpha_1}$ satisfies (1*), then all sub-hypercubes $H^{i_1\alpha_1 \dots i_m\alpha_m} \subset H^{i_1\alpha_1}$, where $i_j \neq \sigma(i_1)$ for all $j \in \{1, \dots, m\}$, also satisfy (1*). The sub-hypercubes $H^{i_1\alpha_1 \dots i_m\alpha_m} \subset H^{i_1\alpha_1}$, where $i_j = \sigma(i_1)$ for some $j \in \{1, \dots, m\}$, satisfy (2*) either because $H^{i_1\alpha_1}$ satisfies (1*) or because $H^{\sigma(i_1)\beta(i_1)\alpha_1}$ satisfies (1*). Therefore, we have confirmed that the conditions of the theorem are satisfied with the particular form of σ and β .

Finally, we prove Thm. 4.1 by combining the cases in Lemma 4.5 and Lemma 4.4.

PROOF (PROOF OF THM. 4.1) From the theorem conditions, each face $H^{i\alpha}$ must satisfy either (1*) or (2*). From Lemma 4.4, we know that if a face H^{i+} satisfies (2*) then H^{i-} must also satisfy (2*). So, let $I' \subset I$ such that $H^{i'\pm}$ satisfies (2*) for each $i' \in I'$, that is for all $i' \in I'$ it is implied that $(q, q'), (q', q) \in E$ for all $q, q' \in H(D)$ with $|q_{i'} - q'_{i'}| = 1$. Consequently, in order for $H^{i\pm}$, $i \in I \setminus I'$ to satisfy (1*), there must exist $j \in I \setminus (I' \cup \{i\})$ and $\alpha \in \{+, -\}$ such that $H^{i\pm j - \alpha} \rightarrow H^{i\pm j \alpha}$ and $H^{i\pm j - \alpha} \not\leftarrow H^{i\pm j \alpha}$. However, for this condition to be satisfied for all $i \in I \setminus I'$, we need to define a function of the same form as η except with variable set $I \setminus I'$ instead of I . In other words, when there is some $H^{i\alpha}$ that satisfies (2*), then the variable i is no longer in the co-domain of η and simultaneously is no longer in the image of η . Therefore, the theorem is just a combination of Lemma 4.5 and Lemma 4.4. Moreover, when $H^{i\pm}$ satisfies either (1*) or (2*) for each $i \in I$, every edge in the STG is still determined.

Conveniently, the above mixed case can be incorporated into the functions σ and β , where for all $i \in I'$ $\sigma(i) = i$ and $\beta(i) = -$. As a result, all edges in $H(D)$ are defined, namely for every $i \in I$

$$\begin{array}{ll} H^{i-} \rightarrow H^{i+} \text{ and } H^{i+} \rightarrow H^{i-} & \text{if } \sigma(i) = i \\ H^{i\pm\sigma(i)\beta(i)\mp} \rightarrow H^{i\pm\sigma(i)\beta(i)\pm} \text{ and } H^{i\pm\sigma(i)\beta(i)\mp} \not\leftarrow H^{i\pm\sigma(i)\beta(i)\pm} & \text{if } \sigma(i) \neq i \end{array}$$

From the specific edges of the STG implied by σ and β above, we can define

the unitary update function \tilde{f} , where for all $q \in H(D)$

$$\tilde{f}_{\sigma(i)}(q) = \begin{cases} \min_{q' \in H(D)} q'_i & \text{if } \beta(i) = - \text{ and } q_i = \max_{q' \in H(D)} q'_i, \\ & \text{or } \beta(i) = + \text{ and } q_i = \min_{q' \in H(D)} q'_i. \\ \max_{q' \in H(D)} q'_i & \text{if } \beta(i) = + \text{ and } q_i = \max_{q' \in H(D)} q'_i, \\ & \text{or } \beta(i) = - \text{ and } q_i = \min_{q' \in H(D)} q'_i. \end{cases}$$

Although \tilde{f} above is an incomplete unitary update function, it holds sufficient information to determine in which orthants the focal points are located. In particular, from this update function and Lemma 3.1, we know that for $D' \in \rho(D)$

$$v_{\sigma(i)}(D, \phi(D')) = \begin{cases} -1 & \text{if } \beta(i) = - \text{ and } V_i(D, D') = -1, \\ & \text{or } \beta(i) = + \text{ and } V_i(D, D') = +1. \\ +1 & \text{if } \beta(i) = + \text{ and } V_i(D, D') = -1, \\ & \text{or } \beta(i) = - \text{ and } V_i(D, D') = +1. \end{cases}$$

Because each orthant Q (and domain $D' \in \rho(D)$) can be identified by a k -tuple $(v_i(D, x))_{i \in I}$ for all $x \in O$ (resp. $x \in D'$), a focal point $\phi(D')$, $D' \in \rho(D)$, is in the orthant O when $V_i(D, O) = \{v_i(D, \phi(D'))\}$ for all $i \in I$. For a focal point to be in each of the 2^k orthants, it must hold that $(v_i(D, \phi(D')))_{i \in I} \neq (v_i(D, \phi(D'')))_{i \in I}$ for all $D' \neq D'' \in \rho(D)$. Therefore, because σ is a permutation, there is a focal point in each of the 2^k orthants of D , which by Lemma 4.3 gives the result. \square

This result is particularly surprising because the conditions of the theorem have assumed general dynamics (see Rem. 2), where the QTG^Ψ has not been constructed from a strictly defined interaction graph with parameters. Nonetheless, a singular domain, which is a steady state in QTG^Ψ , immediately implies that the local dynamics in the related STG exhibit oscillations in the singular variables. In the case where each continuous variable has at most one threshold, the result is less surprising as it is directly related to the findings of Thomas and Snoussi [57], who showed that the existence of a singular steady state would imply an oscillating attractor in the STG (see also Cor. 3.4).

The theorem above displays the strength of Thm. 3.1, where we are able to impose restrictions on the behaviour of the regular domains depending on the dynamics we want to observe on the singular domains.

Still, the theorem only says whether the focal set is non-empty, that is D could still have an outgoing edge to a singular domain of higher order. Nevertheless, the theorem would imply the following.

Corollary 4.1 *Every steady state in QTG^Ψ is also a steady state in QTG^Φ .*

Therefore, we have that the QTG^Ψ sheds some light on the singular equilibrium sets in QTG^Φ and not just the potential singular equilibrium sets that are dependent on the kinetic parameters. In other words, even though we require specific kinetic parameters to determine the specific dynamics in QTG^Φ , the singular domains that are steady states in QTG^Ψ are conserved in QTG^Φ irrespective of the choice of kinetic parameters.

We shortly discuss the significance of this result with respect to the findings of Casey et al. [7], who conjectured (recently proven in [67]) the stability of singular equilibrium sets in QTG^Φ . More specifically, they claim that if a singular domain D with non-empty focal set has no outgoing transitions in QTG^Φ and there is no cycle in $\{D' \in \mathcal{D} \mid D \subset \partial D'\}$ then $\Phi(D)$ is weakly asymptotically stable (see [7] for their stability definition). Thm. 4.1 implies that for such a steady state to exist in QTG^Ψ either there is at least one cycle in $\{D' \in \mathcal{D} \mid D \subset \partial D'\}$, or $(D', D) \in \mathcal{T}^\Phi$ for all $D \subset \partial D'$ (corresponding to the case in the proof of Thm. 4.1 when $\sigma(i) = i$ for all $i \in I$). In other words, Thm. 4.1 agrees with the findings of Casey et al., but only accounts for the steady states in QTG^Φ that are present in QTG^Ψ . In contrast, Casey et al. assume explicit kinetic parameters, which share information about all steady states in QTG^Φ unlike the result above. Nonetheless, further refinement of Thm. 3.1 could determine under what conditions the steady state in Casey et al.'s conjecture exists.

4.3 From Transition Graphs to PADE Solutions

The Thomas formalism represents dynamics by means of a discrete transition graph, whereas the ODE formalism represents dynamics through solution trajectories. In the PADE setting, we have the advantage that both a transition graph and solution trajectories can be extracted from a single PADE system with explicit kinetic parameters [13, 15]. In general, however, information is lost when discretising a differential equation system as shown in Fig. 4.7. Also, as stated in Rem. 4.1, the discrete representations of the PADEs do not always capture the dynamics implied by the PADE solutions. In this section, we assume explicit kinetic parameters for the PADE \mathcal{A} and explore how the dynamics implied by the PADE solutions $\xi(t)$ and the transition graph $QTG^\Phi(\mathcal{A}) = (\mathcal{D}, \mathcal{T}^\Phi)$ differ [13, 7].

Because the differential inclusion implies non-unique dynamics on the singular domains, we focus on the unique dynamics on regular domains. By Def. 2.5, the transitions in QTG^Φ represent the existence of a PADE solution

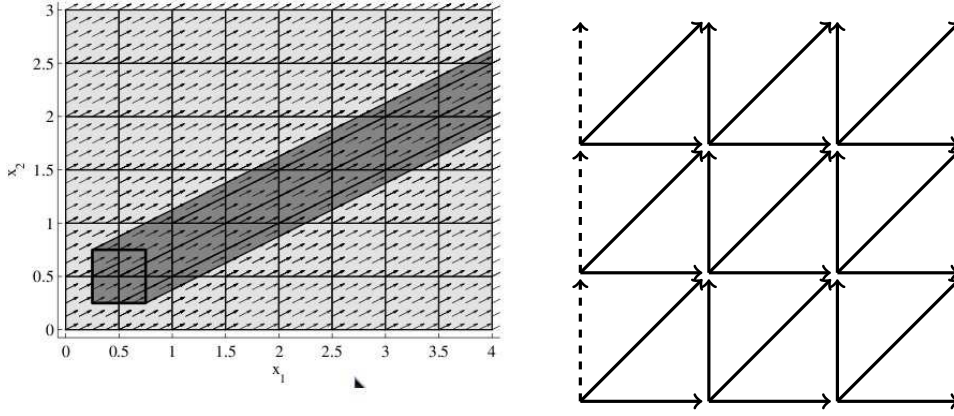


Figure 4.7: On the left is a phase space with constant vector field. The area in dark grey displays the reachability of starting values in the bottom left corner. On the right is a directed graph, where the nodes represent the boxes that partition the phase space and the transitions imply a solution that exists between the adjacent boxes. The dashed path, which is increasing in one variable but remains constant in the other, clearly has no corresponding solution in the phase space on the left.

between adjacent domains. In the following, we show the case of a path in QTG^Φ , which is composed of just two transitions, that does not have a corresponding PADE solution.

Lemma 4.6 *Let \tilde{f} be a unitary update function and $QTG^\Phi(PADE(\tilde{f})) = (\mathcal{D}, \mathcal{T}^\Phi)$, where $PADE(\tilde{f})$ is as in Def. 3.3. Let $D \in \mathcal{D}_r$. If $(D'', D), (D, D') \in \mathcal{T}^\Phi$ for some $D', D'' \subset \partial D$, where $V(D'', D) = V(D, D') \neq \{v(D, \phi(D))\}$, then no PADE solution $\xi(t)$ exists such that $\xi(0) \in D'', \xi(\tau) \in D'$ and $\xi(t) \in D$ for $0 < t < \tau$.*

PROOF We know that for each variable the solutions within $D \in \mathcal{D}_r$ are of the form (2.5). Because of the specific parameter values of $PADE(f)$, namely the degradation coefficients $G_l^D = 1, l = 1, \dots, n$, we have that

$$\frac{\xi_i(t, x^0) - \phi_i(D)}{x_i^0 - \phi_i(D)} = \frac{\xi_j(t, x^0) - \phi_j(D)}{x_j^0 - \phi_j(D)},$$

for all $i, j \in \{1, \dots, n\}$ and $t \in (0, \tau)$, where $\tau := \tau(x^0)$ is the time that the solution remains in domain D for the initial value $x^0 \in D$. That is, if $G_i(x) = \lambda \in \mathbb{R}_{>0}$ for all $i \in \{1, \dots, n\}$ and $x \in \Omega$, then the trajectories within a regular domain are straight lines.

We assume that variable i tends to increase (the cases that variable i tends to decrease follows analogously) and thus $\phi_i(D) = d_i(D) + 1$ by the definition of $PADE(\tilde{f})$. Suppose that $x^0 \in D''$ and $i \in \{1, \dots, n\}$ such that $(D'', D), (D, D') \in \mathcal{T}^\Phi$ for some $D', D'' \subset \partial D$, where $V(D'', D) = V(D, D') \neq \{v(D, \phi(D))\}$. We then have that $x_i^0 = \theta_i^k := k - \frac{1}{2}$, where $k = d_i(D)$. Therefore, the maximum amount of time it takes for a solution starting at x^0 to end up at a state x^* with $x_i^* = \theta_i^{k+1}$ is $-\ln\left(\frac{k+\frac{1}{2}-k-1}{k-\frac{1}{2}-k-1}\right) = -\ln(1/3)$ by (2.5).

If $j \in \{1, \dots, n\} \setminus \{i\}$ such that $\phi_j(D) = d_j(D) + 1$, then either $x_j^0 \in (k' - \frac{1}{2}, k' + \frac{1}{2})$ for some $k' \in \{1, \dots, p_j - 1\}$ or $x_j^0 \in [0, \frac{1}{2}]$. For the case $\phi_j(D) = d_j(D) - 1$, either $x_j^0 \in (k' - \frac{1}{2}, k' + \frac{1}{2})$ for some $k' \in \{1, \dots, p_j - 1\}$ or $x_j^0 \in (p_j - \frac{1}{2}, p_j + \frac{1}{2}]$. In both cases, the time it takes to leave domain D is less than $-\ln\left(\frac{k'+\frac{1}{2}-k'-1}{x_j^0-k'-1}\right)$, which is always less than $-\ln(1/3)$. Hence, no solution starting from D'' traverses D and exits into D' . \square

In other words, with explicit kinetic parameters a path in QTG^Φ going through a regular domain that is a non-deterministic node has no corresponding PADE solution that starts at the lower threshold bound and ends at the upper threshold bound of the regular domain. Here, a non-deterministic node is a node that has more than one outgoing transition in QTG^Φ .

The result of Lemma 4.6 implies that we can justify the exclusion of some discrete paths from QTG^Φ because not all paths correspond to solution trajectories or PADE solutions. For example, the dashed path in Fig. 4.8 can be excluded from the QTG^Φ because there is no solution trajectory that corresponds to the path. Consequently, the remaining paths in the QTG^Φ imply the existence of a cyclic attractor in addition to the two steady states. That is, by excluding the discrete paths in QTG^Φ that are of the form mentioned in Lemma 4.6, we attempt to make the discrete paths and continuous solutions more consistent. However, in order to exclude the paths that have no corresponding PADE solution, we require specific kinetic parameter values.

Because the above analysis focusses on the regular domain dynamics, the discrete paths in question are also present in the QTG^Ψ . That is, the paths in QTG^Φ that are of the form in Lemma 4.6 are also present in the corresponding QTG^Ψ . In that sense, we can impose restrictions on the kinetic parameters such that a PADE solution exists that corresponds to the QTG^Ψ path of the form in Lemma 4.6. In other words, unlike the previous sections, where we relate the parameters to compare the dynamics, here we compare the dynamics to estimate the kinetic parameters.

Consider the PADE \mathcal{A} with unknown kinetic parameters but known ordering constraints so that we can generate $QTG^\Psi(\mathcal{A}) = (\mathcal{D}, \mathcal{T}^\Psi)$. Let $D \in \mathcal{D}_r$

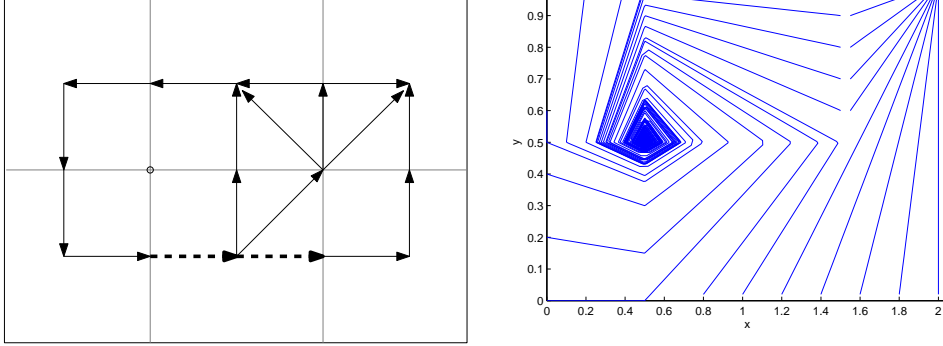


Figure 4.8: The QTG^Φ of Ex. 2.3 on the left where the dashed path satisfies the conditions in Lemma 4.6. On the right are the corresponding PADE solutions, where we see there is no solution starting at $\theta_1^1 = 0.5$ that ends up at $\theta_1^2 = 1.5$, i.e., there is no solution that corresponds to the dashed path.

and $(D'', D), (D, D') \in \mathcal{T}^\Psi$ for $D', D'' \subset \partial D$, where $V(D'', D) = V(D, D') \neq \{v(D, \phi(D))\}$. We want to find restrictions on the kinetic parameters that would imply the existence of a solution $\xi(t)$ such that $\xi(0) \in D'', \xi(\tau) \in D'$ and $\xi(t) \in D$ for $0 < t < \tau$, where $\xi(t)$ is as in (2.5).

Let $k \in J := \{i \in \{1, \dots, n\} \mid v_i(D, \phi(D)) \neq 0\}$ such that $D_k = \mathcal{P}_{kl} = (\theta_k^l, \theta_k^{l+1})$ for some $l \in \{1, \dots, p_i - 1\}$ and for all $i \in J \setminus \{k\}$ we have $D_i = \mathcal{P}_{il'}$ for some $l' \in \{0, \dots, p_i\}$. In other words, D_k is a regular domain component that is bounded by thresholds, whereas D_i can also be bounded by 0 or \max_i and J is the set of all variables that either are only increasing or only decreasing.

Suppose that $D'_k = [\theta_k^{l+1}]$, $D''_k = [\theta_k^l]$ and $D'_j = D''_j = D_j$ for all $j \in \{1, \dots, n\} \setminus \{k\}$. The inverse case, where $D'_k = [\theta_k^l]$, $D''_k = [\theta_k^{l+1}]$ follows analogously. Therefore, $v_k(D, \phi(D)) = 1$, that is the PADE solution $\xi_k(t)$ is increasing in D with time t . We define $\tau > 0$ such that

$$\xi_k(\tau) = \theta_k^{l+1} \text{ and } \xi_k(0) = \theta_k^l.$$

Solving (2.5) for τ gives

$$\tau = \frac{1}{G_k^D} \log \left(\frac{\phi_k(D) - \theta_k^l}{\phi_k(D) - \theta_k^{l+1}} \right).$$

Now, we want to make sure that $\xi(t) \in D$ for all $0 < t < \tau$, for which we need to consider the other variables.

For the variables $i' \in \{1, \dots, n\} \setminus J$ we have that $\phi_{i'}(D) \in D_{i'}$ and so $\xi_{i'}(t) \in D_{i'}$ for all $0 < t < \infty$. For the remaining variables, $i \in J \setminus \{k\}$, where

$D_i = \mathcal{P}_{i l'}$ for some $l' \in \{0, \dots, p_i\}$, we define a time τ_i , which is defined similar to τ

$$\tau_i = \begin{cases} \frac{1}{G_i^{D'}} \log \left(\frac{\phi_i(D) - \theta_i^{l'+1}}{\phi_i(D) - \theta_i^{l'}} \right) & \text{if } v_i(D, \phi(D)) = -1, \\ \frac{1}{G_i^{D'}} \log \left(\frac{\phi_i(D) - \theta_i^{l'}}{\phi_i(D) - \theta_i^{l'+1}} \right) & \text{if } v_i(D, \phi(D)) = 1. \end{cases},$$

where $\theta_i^0 = 0$ and $\theta_i^{p_i+1} = \max_i$. Therefore, there exists a PADE solution $\xi(t)$ such that $\xi(0) \in D''$, $\xi(\tau) \in D'$ and $\xi(t) \in D$ for all $0 < t < \tau$ only if

$$\tau < \min_{i \in J \setminus \{k\}} \tau_i.$$

This condition imposes restrictions on the kinetic parameters given that τ and τ_i are dependent on the focal points and thresholds.

Because the PADE solution on a singular domain \tilde{D} with empty focal set is of Lebesgue measure zero, there could be paths in QTG^Ψ that connect two regular domains via \tilde{D} . Repeating the above analysis to these longer paths in the QTG^Ψ , that is combining the PADE solutions of different regular domains, we can obtain further restrictions on the kinetic parameters. Therefore, from a fixed set of ordering constraints, we can estimate the kinetic parameters based on an observed behaviour of the biological system.

Summary:

- The PADE-R formalism is a refinement of the PADE-Q formalism.
- The dynamics on singular domains is the main difference between the PADE-Q and PADE-D formalisms. More specifically, the kinetic parameters are required to determine the emptiness or non-emptiness of the focal set for singular domains.
- The qualitative parameter information can suffice in describing some singular domain dynamics. For example, all steady states of the PADE-Q formalism are conserved in the PADE-D formalism.
- We can identify some discrete paths of the PADE-D formalism that may not have a corresponding PADE solution. With the aim of consistency, we can restrict kinetic parameters such that these discrete paths have corresponding PADE solutions.

Relating PADE, PMA and ODE models

To finalise our investigation, we would like to see whether the solution trajectories are consistent between the ODE, PMA and PADE formalisms. First, we assume the expression and degradation rate constants to be the same between the three formalisms. That is, the kinetic parameters are common between the differential equation modelling approaches because they represent the same reaction rates of the biological system. In the following, we show how the kinetic parameters and Hill coefficients are then restricted so that the three formalisms generate corresponding solution trajectories.

In order to compare the PADE, PMA and ODE models, we first show why approximating the ODE model with a PADE model can lead to qualitatively different dynamics.

By replacing all the Hill functions in the ODE model with step functions, we obtain a PADE model. This transformation means that except for the Hill coefficients, that is ϵ_{ij} for all $i \in \{1, \dots, n\}, j \in \{1, \dots, p_i\}$, all other parameter values are common in both models.

Conversely, to transform a PADE model to an ODE model, we need to choose appropriate Hill coefficients. When choosing the Hill coefficients, we want the dynamics in the PADE model to be also present in the ODE model. Polynikis et al. [42] and Widder et al. [68] show that for increasing values of the Hill coefficients the ODE trajectories converge to the PADE trajectories. In other words, for sufficiently large values of the Hill coefficients, the trajectories of the PADE model have corresponding trajectories in the ODE model.

For smaller values of the Hill coefficient, however, there could exist PADE solutions that have no corresponding trajectory in the ODE model.

Example 5.1 In Ex. 2.3, there is an asymptotically stable equilibrium $\phi(D)$ in the regular domain $D = (\theta_1^2, max_1] \times (\theta_2^1, max_2]$, which could also exist in

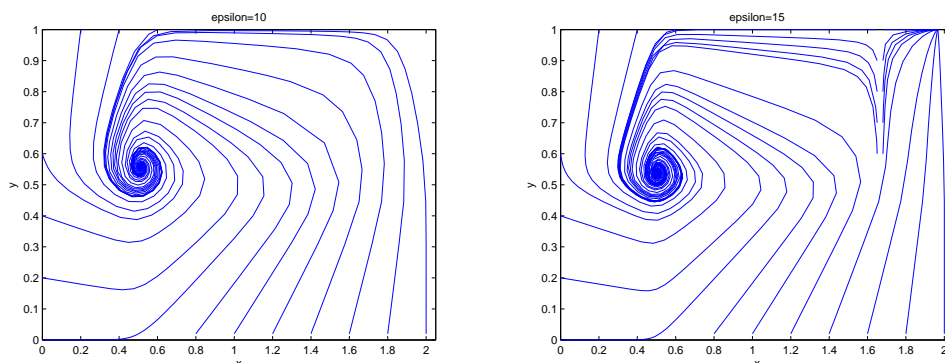


Figure 5.1: Trajectories of Ex. 2.1 with Hill coefficients $\epsilon_{11} = 10$ on the left and $\epsilon_{11} = 15$ on the right. Note for $\epsilon_{11} = 10$ the asymptotically stable equilibrium in the region $(\theta_1^2, \max_1] \times (\theta_2, \max_2]$ is absent and thus all trajectories converge to the focus close to the point (θ_1^1, θ_2) .

the related ODE model. That is, using fixed parameter values, we observe in Fig. 5.1 the equilibrium point in the upper right region of the phase space is present for larger values of the Hill coefficient ϵ_{11} , but is absent for smaller values of ϵ_{11} . In other words, a bifurcation with respect to ϵ_{11} can occur.

The reason for the bifurcation in Ex. 5.1 is the rough approximation of the Hill function by a step function. In Ex. 5.1, the equilibrium in the upper right hand region of the phase space would only exist if $H^+(x^*, \frac{3}{2}, \epsilon_{11}) - x^* = 0$ for some $x^* \in \Omega_1 \setminus \{0\}$. In Fig. 5.2, we see that x^* would not exist for smaller values of ϵ_{11} , whereas x^* exists for larger values of ϵ_{11} . Ex. 5.1, therefore, shows why the step function is a reasonable approximation of a Hill function *only* for larger values of the Hill coefficient.

The ramp function is, on the other hand, a less rough approximation of a Hill function with a smaller value of the Hill coefficient in that the sudden rise at the threshold value of the Hill function is replaced by a linear rise in the threshold interval of the ramp function. Furthermore, the ramp function is not only continuous but also piecewise linear. In that sense, the ramp function removes the discontinuities in the PADE model as well as the non-linearities in the ODE model. For that reason, we want to use the PMA model as an intermediate formalism when relating the PADE and ODE models. In the following, we first relate the PADE and PMA models, which imposes restrictions on the kinetic parameters, and then we relate the PMA and ODE models, which imposes restrictions on the Hill coefficient.

5.1 The Kinetic Parameters

In the following, we relate the PMA model \mathcal{B} (see (2.3) in Sect. 2.1.2) with the PADEs \mathcal{A} (see (2.4) in Sect. 2.2) and determine restrictions on the kinetic parameters such that there is consistent dynamics between both models. We assume that every threshold θ_i^j in \mathcal{A} corresponds to a threshold interval $[\theta_i^{j,0}, \theta_i^{j,1}] \ni \theta_i^j$ in \mathcal{B} and all other parameter values are common in both models. In other words, every step function in \mathcal{A} is replaced by a ramp function with the above threshold intervals to give \mathcal{B} .

We also assume that the threshold intervals in the PMA model are arbitrary but do not overlap. This assumption allows the rectangles of the PMA model to have a bijective correspondence with the domains of the PADE model.

Definition 5.1 Let \mathcal{D} be the domain set of \mathcal{A} and \mathcal{R} be the set of rectangles in \mathcal{B} . We define the mapping $\chi : \mathcal{R} \rightarrow \mathcal{D}$, where $\chi(R) = \chi_1(R) \times \cdots \times \chi_n(R)$ and

$$\chi_i(R) = \begin{cases} \{x_i \mid 0 \leq x_i < \theta_i^1\} & \text{if } R_i = \{x_i \mid 0 \leq x_i < \theta_i^{1,0}\} \\ \{x_i \mid \theta_i^k < x_i < \theta_i^{k+1}\} & \text{if } R_i = \{x_i \mid \theta_i^{k,1} < x_i < \theta_i^{(k+1),0}\} \\ & \text{for } k \in \{1, \dots, p_i - 1\}, \\ \{x_i \mid \theta_i^{p_i} < x_i \leq \max x_i\} & \text{if } R_i = \{x_i \mid \theta_i^{p_i,1} < x_i \leq \max x_i\}, \\ \{x_i \mid x_i = \theta_i^k\} & \text{if } R_i = \{x_i \mid \theta_i^{k,0} \leq x_i \leq \theta_i^{k,1}\} \\ & \text{for } k \in \{1, \dots, p_i\}. \end{cases}$$

Accordingly, we can label the rectangle R as either *singular* or *regular* depending on whether $\chi(R)$ is a singular or regular domain respectively. Note that a singular rectangle R is not *singular* in the sense that R has zero Lebesgue measure, rather it is only labelled singular because of its related singular domain $\chi(R)$.

With this labelling of rectangles, we observe the properties of every regular rectangle R to be common with its corresponding regular domain $\chi(D)$. More specifically, $\phi_i(\chi(R)) = F_i^L(x)/G_i^L(x)$ for all $x \in R$, which means that the regular rectangles have the same focal points as their corresponding regular domains and thus the same solution trajectories (2.5). For this reason, in what follows, we associate a regular rectangle R with the focal point $\phi(\chi(R))$.

In order for the regular domains and regular rectangles to display the same dynamics, we need that for all $D, D' \in \mathcal{D}_r$, where $\phi(D) \in D'$, it should hold that $\phi(D) \in R'$, where $D' = \chi(R')$. In other words, all focal points lie in regular rectangles. We refer to these constraints on the focal points as the *PMA parameter constraints*.

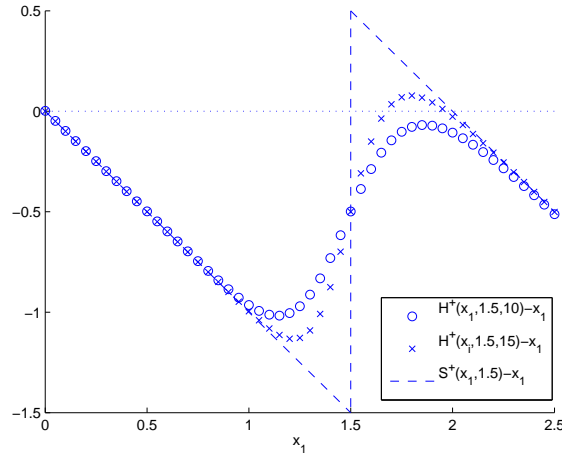


Figure 5.2: The right hand side of the first variable of the ODE model in Ex. 2.1 displayed as a function of x_1 with Hill coefficient $\epsilon_{11} = 10$ (circles) and $\epsilon_{11} = 15$ (crosses). When one of these curves intersects zero (the dotted line), there exists a nullcline for the first variable. The dashed line displays the right hand side of the first variable of the related PADE model.

By assuming the PMA parameter constraints, we are restricting the kinetic parameters of the PMA and PADE models. That is, we are studying a reduced class of general PMA models, where the focal points do not lie in the singular rectangles. Nonetheless, the PMA parameter constraints ensure that the dynamics of the regular rectangles in the PMA model correspond to the regular domain dynamics in the PADE model.

Proposition 5.1 *Let \mathcal{A} be a PADE model with $QTG^\Phi(\mathcal{A}) = (\mathcal{D}, \mathcal{T}^\Phi)$. Consider a PMA model with solutions $\bar{\xi}(t)$ and rectangle set \mathcal{R} such that for every threshold θ_i^j in \mathcal{A} there exists a threshold interval $[\theta_i^{j,0}, \theta_i^{j,1}] \ni \theta_i^j$, where the threshold intervals do not overlap and the PMA parameter constraints are satisfied. Let $D \in \mathcal{D}_r$ and $D' \in \partial D$ and $R, R' \in \mathcal{R}$ such that $\chi(R) = D$ and $\chi(R') = D'$.*

1. If $(D, D') \in \mathcal{T}^\Phi$, then there exists $\tau < \infty$ such that

$$\begin{aligned} \bar{\xi}(t) &\in R \text{ for } 0 \leq t < \tau, \text{ and} \\ \bar{\xi}(\tau) &\in R' \end{aligned}$$

2. If $(D', D) \in \mathcal{T}^\Phi$, then there exists $\tau < \infty$ such that

$$\bar{\xi}(0) \in R', \text{ and}$$

$$\bar{\xi}(t) \in R \text{ for } 0 < t \leq \tau$$

PROOF The non-overlapping threshold intervals allow us to map the rectangles to the domains using the mapping χ . The common focal point of the regular rectangle R and the regular domain $D := \chi(R)$ implies the same solution (2.5) for all $x^0 \in R$, where $x^0 \in R$ would also imply $x^0 \in D$. The PMA parameter constraints ensure that $\text{sgn}(\phi_i(\chi(R)) - x_i) = v_i(D, \phi(D))$ for all $x \in R, i \in \{1, \dots, n\}$. That is, the relative position of a focal point to its associated rectangle is the same as the relative position of the focal point with its related domain. So, by definition of the solution (2.5) every transition in \mathcal{T}^Φ between $D \in \mathcal{D}_r$ and $D' \subset \partial D$ corresponds to the existence of a trajectory between $R := \chi^{-1}(D) \in \mathcal{R}$ and $R' := \chi^{-1}(D') \in \mathcal{R}$. That is, if $(D, D') \in \mathcal{T}^\Phi$ then exists $x^0 \in R$ and finite time τ such that $\bar{\xi}(0) = x^0, \bar{\xi}(t) \in R$ for $0 \leq t < \tau$ and $\bar{\xi}(\tau) \in R'$. Similarly, if $(D', D) \in \mathcal{T}^\Phi$ then exists $x^0 \in R'$ and finite time τ such that $\bar{\xi}(0) = x^0, \bar{\xi}(t) \in R$ for $0 < t \leq \tau$. \square

Therefore, if the PMA parameter constraints are satisfied for \mathcal{B} , then the transitions between a regular domain D and $D' \subset \partial D$ in the QTG^Φ (resp. QTG^Ψ) also represent the existence of solution trajectories between R and R' , where $\chi(R) = D$ and $\chi(R') = D'$, in \mathcal{B} . In other words, the PMA parameter constraints ensure that there is consistent dynamics between the regular rectangles and regular domains of the PMA and PADE models respectively. Because a PMA model with focal points in singular rectangles does not guarantee the consistent dynamics described above, we do not consider them in what follows, even though they are still a valid and interesting class of PMA models.

Now, we look into how the dynamics of singular rectangles in the PMA model can be determined from the corresponding singular domains in the related PADE model.

Here, we focus on the existence of equilibria within the singular rectangles and whether they can be determined by the singular equilibrium sets. In the following, we assume that the PADE \mathcal{A} has $QTG^\Phi(\mathcal{A}) = (\mathcal{D}, \mathcal{T}^\Phi)$, the threshold intervals of \mathcal{B} do not overlap, and the PMA parameter constraints are satisfied for \mathcal{B} .

In order to find equilibrium points in a singular rectangle R , we would first need to deduce whether the nullclines intersect R . Conveniently, we can determine whether nullclines intersect the singular rectangle from the corresponding *qualitative* PADE model.

Lemma 5.1 *Let $QTG^\Psi(\mathcal{A}) = (\mathcal{D}, \mathcal{T}^\Psi)$ and $D \in \mathcal{D}_s$ with singular variable set I . If D has transitions to or from higher order domains, that is $\Psi(D) \neq$*

\emptyset , then for all $i \in I$ we have $Null_i \cap R \neq \emptyset$, where $R := \chi^{-1}(D)$ and $Null_i := \{x \in \Omega \mid F_i^L(x) - G_i^L(x)x_i = 0\}$.

PROOF Recall the result by [5], where $\dot{x}_i \in \overline{\text{co}}(\{F_i^L(v) - G_i^L(v)v_i \mid v \in \mathcal{V}(R)\})$ for any point $x \in R$ of any rectangle R . Because a corner $v \in \mathcal{V}(R)$ is in the boundary of a regular rectangle, that is $v \in \partial R'$ for an $R' := \chi^{-1}(D')$, $D' \in \rho(\chi(R))$ and by continuity of the ramp function, it holds that $\dot{v}_i = G_i^L(v)(\phi_i(\chi(R')) - v_i)$ for $i \in \{1, \dots, n\}$.

So, for the nullcline $Null_i$ to intersect R , we need that

$$0 \in \overline{\text{co}}(\{G_i^L(v)(\phi_i(D') - v_i) \mid D' \in \rho(\chi(R)), v \in \mathcal{V}(R)\}).$$

This condition is satisfied if there exists $D', D'' \in \rho(D)$ such that $\phi_i(D') - v_i < 0$ and $\phi_i(D'') - v_i > 0$ for all $v \in \mathcal{V}(R)$, which reformulated gives $\phi_i(D') < \min_{x \in R} x_i$ and $\phi_i(D'') > \max_{x \in R} x_i$. Let I be the singular variable set of $\chi(R)$. Due to the PMA parameter constraints, the first condition in Prop. 2.1 implies that there exists $D', D'' \in \rho(D)$ such that $\phi_i(D') < \min_{x \in R} x_i$ and $\phi_i(D'') > \max_{x \in R} x_i$ for all $i \in I$. Therefore, when $\chi(R)$ is non-transparent, that is has transitions to or from higher order domains, then $Null_i \cap R \neq \emptyset$ for all $i \in I$. \square

In other words, the nullclines of the singular variables of $\chi(R)$ intersect with the singular rectangle R if the singular domain $\chi(R)$ is non-transparent. However, nullclines intersecting with the singular rectangle does not mean that they intersect with each other within the rectangle to give an equilibrium point. Now, we give a necessary condition for the existence of an equilibrium point in the PMA model, which cannot be determined by the qualitative PADE formalism but perhaps the *discretised* PADE formalism.

Lemma 5.2 *Let $R \in \mathcal{R}$ be a singular rectangle, where \mathcal{R} is the set of rectangles of the PMA model \mathcal{B} . A necessary condition for an equilibrium point to exist in R is that*

$$\overline{\text{co}}(\{\phi(D') \mid D' \in \rho(\chi(R))\}) \cap R \neq \emptyset. \quad (5.1)$$

PROOF Reformulating the condition for the nullcline $Null_i$ to intersect with the rectangle R , we have that there exist $\lambda_v, v \in \mathcal{V}(R)$ such that

$$\sum_{v \in \mathcal{V}(R)} \lambda_v (\phi_i(D^v) - v_i) = 0 \text{ and } \sum_{v \in \mathcal{V}(R)} \lambda_v = 1. \text{ However, for an equilib-}$$

rium point to exist we require that there exists $\lambda_v, v \in \mathcal{V}(R)$ such that for all $i \in \{1, \dots, n\}$ it holds that $\sum_{v \in \mathcal{V}(R)} \lambda_v (\phi_i(D^v) - v_i) = 0$ and $\sum_{v \in \mathcal{V}(R)} \lambda_v = 1$. That is,

$$\sum_{v \in \mathcal{V}(R)} \lambda_v \phi_i(D^v) = \sum_{v \in \mathcal{V}(R)} \lambda_v v_i,$$

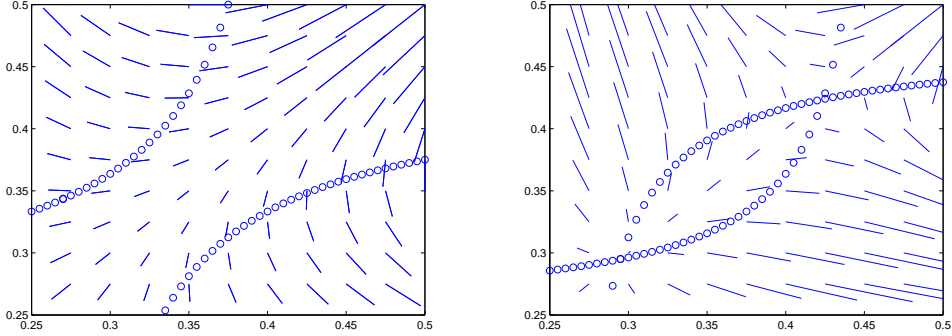


Figure 5.3: The vector field in the singular rectangle $[\frac{1}{2}, \frac{1}{4}] \times [\frac{1}{2}, \frac{1}{4}]$ of the two-component system in Ex. 5.2 with parameters $(k_1, k_2) = (1, 0), (\kappa_1, \kappa_2) = (0, 1)$ on the left and $(k_1, k_2) = (2, 0), (\kappa_1, \kappa_2) = (0, 2)$ on the right. The lines represent the vector field at each point within the rectangle and the circles trace the nullclines of the two variables. Equilibria are only present when the two nullclines intersect as on the right.

By definition of the convex hull the above condition is equivalent to (5.1) \square

In other words, for a singular rectangle R to have an equilibrium point, it is necessary that the convex hull of all focal points $\phi(D'), D' \in \rho(\chi(R))$ intersects with R . Still, the lemma above claims that (5.1) is only necessary for R to have an equilibrium point. Next, we look at an example that shows that (5.1) is not sufficient for an equilibrium point to exist.

Example 5.2 Consider the PMA model

$$\begin{aligned}\dot{x}_1 &= k_1 L^+(x_1, \frac{1}{4}, \frac{1}{2}) L^-(x_2, \frac{1}{4}, \frac{1}{2}) + \kappa_1 L^-(x_1, \frac{1}{4}, \frac{1}{2}) L^+(x_2, \frac{1}{4}, \frac{1}{2}) - x_1 \\ \dot{x}_2 &= k_2 L^+(x_1, \frac{1}{4}, \frac{1}{2}) L^-(x_2, \frac{1}{4}, \frac{1}{2}) + \kappa_2 L^-(x_1, \frac{1}{4}, \frac{1}{2}) L^+(x_2, \frac{1}{4}, \frac{1}{2}) - x_2.\end{aligned}$$

For the set of parameters $(k_1, k_2) = (1, 0), (\kappa_1, \kappa_2) = (0, 1)$, we would have that $R \subset \overline{\text{co}}(\{\phi(D') \mid D' \in \rho(\chi(R))\})$, that is condition (5.1) is satisfied, for the singular rectangle $R := [\frac{1}{4}, \frac{1}{2}] \times [\frac{1}{4}, \frac{1}{2}] = \chi^{-1}(D)$. Nonetheless, we see in Fig. 5.3(a) that the nullclines do not intersect in R , meaning that there is no equilibrium. However, with another set of parameters $(k_1, k_2) = (2, 0), (\kappa_1, \kappa_2) = (0, 2)$ displayed in Fig. 5.3(b), the nullclines intersect twice giving two equilibria. Therefore, condition (5.1) is not necessary for one equilibrium point to exist in $R := \chi^{-1}(D)$.

We recognise that (5.1) has a form similar to the existence of a singular equilibrium set in the discretised PADE model, that is $\overline{\text{co}}(\{\phi(D') \mid D' \in \rho(D)\}) \cap D \neq \emptyset$. In combination with the PMA parameter constraints, we have that the existence of a singular equilibrium set immediately implies that (5.1) holds. In other words, the singular domains in \mathcal{A} that contain singular equilibrium sets imply that the corresponding singular rectangle has potential equilibria. Again, potential means that the nullclines *could* intersect depending on the explicit kinetic parameters.

In the remainder of this section, we want to see if an equilibrium point in a singular rectangle of the PMA model can be deduced from the related discretised (resp. qualitative) PADE model.

Thm. 4.1 shows that a singular domain D , which has no transitions to domains of lower order in QTG^Ψ , has very particular dynamics in the surrounding regular domains $\rho(D)$. In particular, each singular variable i of D either is steady or oscillates with other singular variables (see Proof of Thm. 4.1). Both of these dynamics also happen independently, that is singular variables that oscillate do not influence the singular variables that are steady and vice versa. From this very particular dynamical behaviour, we can show that all nullclines of the singular variables of D are sure to intersect within $R := \chi^{-1}(D)$

Lemma 5.3 *Let D be a singular domain with singular variable set I . If D has no transitions to lower order domains in QTG^Ψ , that is satisfies the conditions of Thm. 4.1, then $R \cap \bigcap_{i \in I} \text{Null}_i \neq \emptyset$, where $\chi(R) = D$.*

PROOF Consider $D \in \mathcal{D}_s$ with singular variable set I and $r_i \in \{1, \dots, p_i\}$, $i \in I$ such that $D_i = [\theta_i^{r_i}]$. We want to use the results from previous chapters to prove the lemma, for which we need the associated Thomas formalism. Let $STG(f^A) = (Q, E)$ be the transition graph associated with the PADE \mathcal{A} , that is using $d := d^A$ from Def. 3.2. The conditions of the lemma are the same conditions as in Thm. 4.1, which implies that the dynamics in $H(D)$ can be defined by the permutation $\sigma : I \rightarrow I$ and function $\beta : I \rightarrow \{+, -\}$, which uniquely defines the restricted update function \hat{f} (see Lemma 4.3). In particular, for every $i \in I$

$$\hat{f}_{\sigma(i)}(q) \in \begin{cases} H^{\sigma(i)-} & \text{if } q_i \in H^{i+} \wedge \beta(i) = - \vee q_i \in H^{i-} \wedge \beta(i) = +, \\ H^{\sigma(i)+} & \text{otherwise,} \end{cases}$$

where $H^{i\alpha}$, $\alpha \in \{+, -\}$ is defined as in the proof of Thm. 4.1. By definition, if $H(D') \subset H^{i+}$ for $D' \in \rho(D)$ then $q \in H^{i+}$ for $d(D') = q$.

The restricted update function \hat{f} is associated with the focal points of the domains in $\rho(D)$. Therefore, summarising the information encoded in \hat{f} for

$D' \in \rho(D)$ and $i \in I$, it holds that $v_{\sigma(i)}(D, \phi(D')) < 0$ if $H(D') \subset H^{i\beta(i)}$, and $v_{\sigma(i)}(D, \phi(D')) > 0$ if $H(D') \subset H^{i-\beta(i)}$. In other words, all regular domains that are below the threshold hyperplane $\theta_i^{r_i}$ have focal point components that are either all below or all above $\theta_{\sigma(i)}^{r_{\sigma(i)}}$.

Translating the conditions $v_{\sigma(i)}(D, \phi(D')) < 0$ and $v_{\sigma(i)}(D, \phi(D')) > 0$ into the PMA model with corresponding PMA parameter constraints gives $\phi_{\sigma(i)}(D') < \min_{x \in R} x_{\sigma(i)}$ and $\phi_{\sigma(i)}(D') > \max_{x \in R} x_{\sigma(i)}$ respectively. That is, for all $v, v' \in \mathcal{V}(R)$, where $v_i \neq v'_i$ and $v_j = v'_j$ for all $j \in I \setminus \{i\}$, it holds that $\text{sgn}(\dot{v}_{\sigma(i)}) \neq \text{sgn}(\dot{v}'_{\sigma(i)})$. Note that the vector field of any point between two neighbouring corners of R is a convex combination of the vector field at these corners by definition of multi-affinity, i.e., for any $v, v' \in \mathcal{V}(R)$, where $v_i \neq v'_i$ and $v_j = v'_j$ for all $j \in I \setminus \{i\}$, it holds that $\dot{x} = \lambda \dot{v} + (1 - \lambda) \dot{v}'$ for $x = \lambda v + (1 - \lambda) v'$ and $\lambda \in (0, 1)$. Consequently, we have that $\text{sgn}(\dot{x}_{\sigma(i)}) \neq \text{sgn}(\dot{x}'_{\sigma(i)})$ for all $x, x' \in R$, where $x_i = \max_{x \in R} x_i$ and $x'_i = \min_{x \in R} x_i$. In other words, the two facets in R that are constant in variable i have opposite derivative sign for variable $\sigma(i)$.

By multi-affinity, it holds that for all $x_j \in R_j$, $j \in I \setminus \{i\}$ there exists a unique $x_i^* \in R_i$ such that $(x_1, \dots, x_i^*, \dots, x_n) \in \text{Null}_i$. Therefore, the vector $\bar{x} \in \bigcap_{i \in I} \text{Null}_{\sigma(i)}$, where $\bar{x}_i = x_i^*$ for $i \in I$ and $\bar{x}_j \in R_j$ for $j \in \{1, \dots, n\} \setminus I$. \square

So, within the singular rectangle R , the nullclines of all singular variables of $\chi(R)$ intersect each other given that there are no transitions to lower order domains from $\chi(R)$ in QTG^Ψ . We can extend this result so that the nullclines of the non-singular variables are also included.

Corollary 5.1 *If D is a steady state in QTG^Ψ of the PADE model, then there exists an equilibrium point $x^* \in R = \chi^{-1}(D)$ in the PMA model.*

PROOF Let i be a non-singular variable of D . The steady state D means that $V(D, \Psi(D)) = \{\mathbf{0}\}$. In particular, $V_i(D, \Psi(D)) = \{0\}$ which implies the two facets in R that are constant in variable i have opposite derivative sign for variable i , i.e., for all $v, v' \in \mathcal{V}(R)$, where $v_i \neq v'_i$ and $v_j = v'_j$ for all $j \in I \setminus \{i\}$, it holds that $\text{sgn}(\dot{v}_i) \neq \text{sgn}(\dot{v}'_i)$. Therefore, it holds that for all $x_j \in R_j$, $j \neq i$ there exists a unique $x_i^* \in R_i$ such that $(x_1, \dots, x_i^*, \dots, x_n) \in \text{Null}_i$. So only the point $x^* := (x_1^*, \dots, x_n^*) \in \bigcap_{i \in \{1, \dots, n\}} \text{Null}_i$ is an equilibrium point. \square

In other words, the singular equilibrium sets in the discretised PADE model shed light on potential equilibria in the PMA model. But, only steady states in QTG^Ψ guarantee a unique corresponding equilibrium point in the PMA model.

5.2 The Hill Coefficient

In general, when transforming a PMA model to an ODE model, we want the equilibria to be conserved based on suitable choices of Hill coefficients. The reason for this is to ensure that the Thomas and ODE formalisms are modelling the same system. One example of equilibria being conserved is in the ODEfy transformation in [69], which transforms a Boolean function to an ODE model. The Hill functions in the ODEfy transformation are normalised, i.e., kinetic parameters are altered, so that the fixed points of the Boolean function correspond to asymptotically stable equilibria in the corresponding ODE model. We want to ensure that the same consistent dynamics occurs when we compare the Thomas and ODE models, but we assume the PADE, PMA and ODE models to have the same kinetic parameters. Therefore, the only parameter values that can be altered to ensure consistent dynamics between the PMA and ODE models are the Hill coefficients. In other words, we want the asymptotically stable equilibria in the regular rectangles of the PMA model to also correspond to equilibria in the ODE model with appropriate choices of the Hill coefficients.

In the following, we assume that for every threshold θ_i^j in the ODE model there is a threshold interval $[\theta_i^{j,0}, \theta_i^{j,1}] \ni \theta_i^j$ in the PMA model. Because the PMA model is a continuous approximation of the ODE model, we expect both formalisms to have common dynamics. The fact that both formalisms are ODE systems means that we can utilise perturbation theory of dynamical systems [24] to ensure that the regular rectangle dynamics of the PMA model is also present in the ODE model. Here, we do not present perturbation theory in full detail but merely sketch how it can mathematically prove the conservation of equilibria between ODE systems.

Proposition 5.2 [*Perturbation theory*] Consider a system of differential equations

$$\dot{x} = \mathbf{f}(x, \tilde{\delta}), \quad x \in \mathbb{R}^n,$$

where $\mathbf{f} : \mathbb{R}^{n+1} \rightarrow \mathbb{R}^n$ and $\tilde{\delta} \in \mathbb{R}$. Equilibria are given by the equation $\mathbf{f}(x, \tilde{\delta}) = 0$. Assuming that $\mathbf{f}(x^0, 0) = 0$ and that the Jacobian $D_x \mathbf{f}(x^0, 0)$ has maximal rank, the Implicit Function Theorem guarantees existence of a function $x(\tilde{\delta})$ with $x(0) = x^0$ such that $\mathbf{f}(x(\tilde{\delta}), \tilde{\delta}) = 0$ for $\tilde{\delta} \ll 1$.

In other words, if we can show that one ODE system is a small perturbation of a second ODE system, then for every equilibrium point in the former, there exists a corresponding equilibrium point in the latter and vice versa. For our purposes, we want to show that the ODE model is a perturbation of the PMA model. More specifically, we want to show that the right hand

side of (2.2) within a regular rectangle is a perturbation of (2.3) in the same rectangle.

Proposition 5.3 *Consider an ODE model (2.2) and PMA model (2.3) such that for every threshold θ_i^j in the ODE model there is a threshold interval $[\theta_i^{j,0}, \theta_i^{j,1}] \ni \theta_i^j$ in the PMA model. We assume that the threshold intervals do not overlap and that all focal points lie in regular rectangles. Let every Hill function in the ODE model have the Hill coefficient ϵ_{ij}^* such that*

$$|b - H^+(\theta_i^{j,b}, \theta_i^j, \epsilon_{ij}^*)| < \tilde{\delta} \text{ for } b \in \{0, 1\},$$

where $\tilde{\delta} \ll 1$. Then, all equilibria in the regular rectangles of the PMA model correspond to equilibria in the ODE model.

PROOF The conditions in the lemma imply that there is a related PADE system with domain set \mathcal{D} such that we can map the rectangles of the PMA model to the domains via the mapping χ . Consider a regular rectangle R of the PMA model which contains an equilibrium point, namely $\phi(\chi(R)) \in R$.

By the definition of ϵ_{ij}^* , taking the limit $\tilde{\delta} \rightarrow 0$ implies that $H^+(x, \theta_i^j, \epsilon_{ij}^*) = 0$ for all $x \leq \theta_i^{j,0}$ and $H^+(x, \theta_i^j, \epsilon_{ij}^*) = 1$ for all $x \geq \theta_i^{j,1}$. Therefore, $\tilde{\delta} \rightarrow 0$ would imply that $F_i^L(x) - G_i^L(x)x_i = F_i^H(x) - G_i^H(x)x_i$ for all $x \in R$. Now, we want to show that the ODE model is a perturbation of the PMA model in R .

The functions $F_i^H(x)$ and $G_i^H(x)$ in the ODE model (2.2) are mainly composed of Hill functions. The derivative of the Hill function simplifies to

$$\frac{dH^+(x, \theta, \epsilon)}{dx} = \frac{\theta^\epsilon}{\theta^\epsilon + x^\epsilon} \frac{\epsilon x^{\epsilon-1}}{\theta^\epsilon + x^\epsilon}.$$

Also, $\frac{dH^-(x, \theta, \epsilon)}{dx} = 1 - \frac{dH^+(x, \theta, \epsilon)}{dx}$ by definition.

By the chain rule, the derivative of (2.2) with respect to x_j would be of the form

$$\frac{d\dot{x}_j}{dx_i} = \underbrace{\frac{(\theta_i^j)^{\epsilon_{ji}}}{(\theta_i^j)^{\epsilon_{ji}} + x_j^{\epsilon_{ji}}}}_{\leq \tilde{\delta}} \frac{\epsilon_{ji} x_i^{\epsilon_{ji}-1}}{(\theta_i^j)^{\epsilon_{ji}} + x_i^{\epsilon_{ji}}} \left(\frac{\partial F_j^H(x)}{\partial H_i} - \frac{\partial G_j^H(x)}{\partial H_i} x_i \right) - G_j(x) \mathbb{1}\{i = j\}.$$

where $\mathbb{1}$ is the indicator function, $\partial F_j^H(x)/\partial H_i := \partial F_j^H(x)/\partial H^+(x_i, \theta_i^j, \epsilon_{ji}) - \partial F_j^H(x)/\partial H^-(x_i, \theta_i^j, \epsilon_{ji})$ and $\partial G_j^H(x)/\partial H_i := \partial G_j^H(x)/\partial H^+(x_i, \theta_i^j, \epsilon_{ji}) - \partial G_j^H(x)/\partial H^-(x_i, \theta_i^j, \epsilon_{ji})$. We recognise the first term as being less than or equal to $\tilde{\delta}$ for any $x \in R$ by the definition of ϵ_{ij}^* . Therefore, for all $x^0 \in R$, the Jacobian $D_x \dot{x}(x^0, 0) = \text{diag}(G_1^H(x^0), \dots, G_n^H(x^0))$ has maximal rank. By Prop. 5.2, there exists a function $x(\delta)$ such that $x(\delta) \in R$ is an equilibrium point of the ODE model, where $x(0) := \phi(\chi(R))$. \square

In other words, the Hill coefficient ϵ_{ij}^* minimises the difference between the asymptotic values of the Hill function and the value at the bounds of the threshold interval. Note that the choice of $\tilde{\delta}$ decides whether the right hand side of the PMA model within a regular rectangle R is a small enough perturbation of the right hand side of the ODE model restricted to R . Therefore, with a small enough $\tilde{\delta}$, there are consistent dynamics between PMA and ODE models.

Applying the above procedure for singular domains, i.e., defining a Hill coefficient that minimises the difference between the right hand side of (2.2) and (2.3) within a singular rectangle, we could ensure that the equilibria in the singular rectangles of the PMA model are also present in the ODE model. In order to prove consistent dynamics within singular rectangles, however, we may need to choose a Hill coefficient that is different from ϵ_{ij}^* . For the dynamics in some regions of the phase space to be guaranteed, we consider only ϵ_{ij}^* when relating PMA and ODE models. This then implies that fixed points of the update function in the related Thomas formalism correspond to asymptotically stable equilibria in the ODE model.

Summary:

- Using the PMA model, we can relate the ODE and PADE models such that equilibria in the regular domains of the PADE model are conserved in the PMA and ODE models.
- The PMA parameter constraints imply that a lot of the dynamics between the PMA and PADE-D formalisms is conserved.
- Asymptotically stable equilibria are conserved when transforming a PMA model to an ODE model based on the choice of Hill coefficients in the ODE model.

Case Study: Cytokinin Signalling in *Arabidopsis thaliana*

In this chapter, we apply our previous analysis to the biological system of the cytokinin signal transduction network of the model plant *Arabidopsis thaliana*. We first construct a set of ODEs, where the components of the network follow basic mass action laws. Then, we approximate and discretise the ODE system to obtain a PADE and Thomas model respectively. Using the results of the previous chapters, we can then restrict the kinetic parameters of the ODE model. The main focus of this chapter is not a thorough investigation of the biological system, but rather to illustrate the results of the thesis.

6.1 Biological Background

Cytokinin plays an important role in many physiological and developmental processes in the plant, such as regulation of shoot and root growth, leaf senescence, chloroplast development, stress response and pathogen resistance. The literature [26] provides a biological model of the cytokinin signal transduction pathway, which we present in the following.

The signalling system in *Arabidopsis* uses a multi-step phosphorelay system, which comprises additional signalling steps. The naturally occurring cytokinins are molecules that have an aromatic side chain, which can bind to the receptor histidine kinase (AHK) causing it to autophosphorylate. The phosphoryl group is then transferred to a histidine phospho-transfer protein (AHP), which translocates to the nucleus, where it activates the B-type response regulators (ARRs) by further transference of the phosphoryl group.

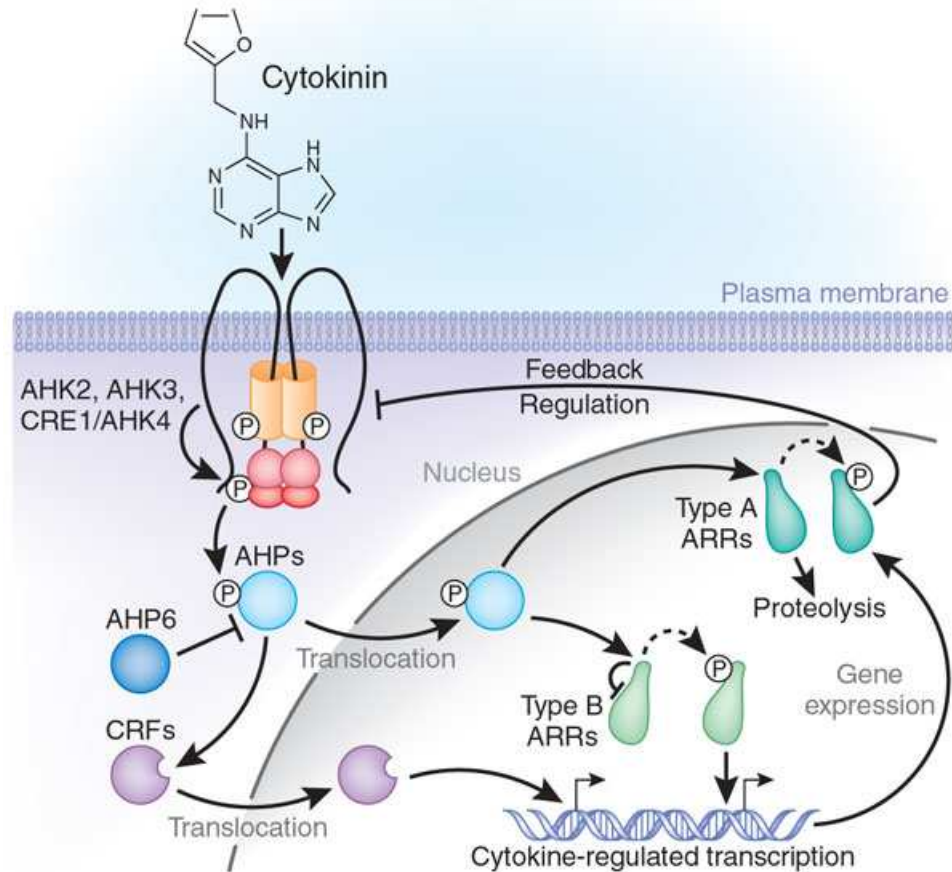


Figure 6.1: The cytokinin signal transduction network. Picture taken from [52].

The phosphorylated B-types activate the transcription of the cytokinin target genes, one group of which is the A-type ARRs. These regulate the activity of the signalling pathway and initiate other cellular signalling pathways [26]. An overview of the signalling network is depicted in Fig. 6.1.

Before we start modelling, we look at each of the protein classes AHKs, AHPs and ARRs in detail.

AHKs: In the class of AHKs there are three proteins, which dimerize and autophosphorylate upon binding with cytokinin. It was shown that all three AHKs can interact with all proteins in the AHP protein class [30, 27, 38]. The analysis of single, double and triple receptor mutants of *Arabidopsis*

demonstrated that the three AHK receptors have at least a partial overlap of their function. Simultaneous mutation of all three receptors, however, caused complete cytokinin resistance and strong plant growth inhibition. Single mutant experiments have shown that the receptors can mediate signal transfer of the gene to some extent, but full induction is only possible by the combined activities of the receptors.

AHPs: There are five proteins in the AHP protein class. The model of cytokinin transduction predicts that the phosphorylated AHPs transport the phosphoryl group from the cell membrane to the nucleus. Experiments that test this transportation can be found in [43, 28]. The central role of the AHPs as mediator of the cytokinin signal requires that they can interact with AHKs and the ARRs. In the presence of phosphorylated A-type ARRs, the AHPs (phosphorylated and non-phosphorylated) are said to accumulate in the nucleus [65], that is the AHP translocation from the nucleus to the cytoplasm is hindered.

ARRs: The ARR protein class has been identified in more than 25 different plant species. The ARR protein class contains 23 elements, which can be further subdivided into two major protein classes, the A-types consisting of 12 elements and the B-types consisting of 11 elements [26].

B-type ARRs: The B-types have a DNA binding domain and are therefore shown to function as transcriptional activators but are not induced by cytokinin. That is, all the B-types are found in the nucleus without the presence of cytokinin [27], which is consistent with their predicted role as transcription factors. Several of the target genes of the phosphorylated B-types have been identified, namely the A-types. Other genes that are activated by the B-types are also included in the list of cytokinin regulated genes and are labelled as Cytokinin Response Factors (CRFs) [44]. In accordance with the model for cytokinin signal transduction, interactions between AHPs and B-types have been detected [60].

A-type ARRs: A-types are induced by cytokinin and are thought to be involved in a negative feedback mechanism of the cytokinin signalling and in the modulation of the cellular response to cytokinin. The molecular function of the A-types, however, is not yet known. A-types are divided into five subclasses, which are closely related to each other. One would expect that closely related proteins have similar expression patterns, where experiments have been conducted that confirm [65] or reject [11] this statement. Several

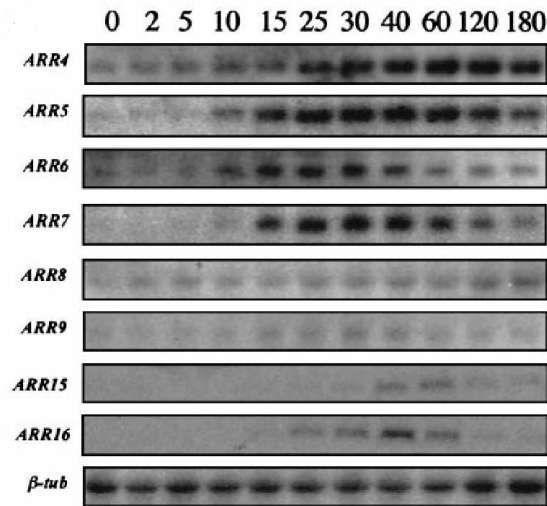


Figure 6.2: The northern blot analysis of the different A-types that are listed on the left side. Listed at the top are the times, in minutes, after which cytokinin is introduced.

A-types have been shown to be negative regulators of cytokinin signalling and the corresponding feedback regulation of the signalling pathways has been proposed [27, 66] but not confirmed. There are also examples of some A-types being positive regulators, that is they enhance the cytokinin response [39]. The wild-type expression patterns of the A-type ARRs were measured by D'Agostino et al. (2000) [11] as displayed in Fig. 6.2.

6.2 Model

Now that we have established the known components of the system, we wish to model the cytokinin signal mathematically. As most of the network is composed of kinetic reactions rather than gene regulation, we use mass action kinetics to derive an ODE system of the signalling pathway.

We begin by constructing the general ODE model from the essential reactions of the protein classes. For now, we assume functional overlap of proteins within each class, that is we do not distinguish between the individual proteins within a class but claim that all proteins within one class have the same function in our model. This assumption, however, implies that single mutant

experiments cannot be used to check the model.

To each of the phosphorylated and dephosphorylated protein classes, we assign a continuous variable, which represents the respective protein concentration over time.

Protein Class	Variable
Cytokinin	$Cyto$
AHK	K
Phosphorylated AHK	K_p
AHP	P
Phosphorylated AHP	P_p
B-type ARRs	B
Phosphorylated B-type ARR	B_p
A-type ARRs	A
Phosphorylated A-type ARRs	A_p

The variable $Cyto$ is an input variable, which we assume takes a constant value. Still, we leave it as a variable in the case that we want to include the change of cytokinin concentration over time into the model.

To accurately model the diffusion between the cytoplasm and the nucleus for the components P and P_p , we would need to use partial differential equations (PDEs). However, with the PDEs, we require spatial factors such as diffusion rates that are not available. Therefore, to avoid the use of PDEs, we define the variable P to represent the concentration of AHP in the cytoplasm and P_p to represent the concentration of phosphorylated AHP in the nucleus. Otherwise, we assume all proteins are well-stirred in their compartments, i.e., cytoplasm or nucleus.

Now that the variables are established, we state the reactions that they take part in:

1. $Cyto + K \rightarrow K_p$
2. $P + K_p \rightarrow P_p + K$
3. $P_p + B \rightarrow B_p + P$
4. $P_p + A \rightarrow A_p + P$
5. B_p activates A

Further to these reactions, we assume that each non-phosphorylated protein X has an expression rate γ_X and for each phosphorylated and non-phosphorylated protein Y , there is a degradation rate β_Y .

To model the activation of the A-types by the phosphorylated B-types, we assume that the expression of the A-types increases sigmoidally with

respect to the concentration of the phosphorylated B-types. In particular, the expression of the A-types is represented by the term $\gamma_A H^+(B_p, \theta_{B_p}, \epsilon)$, where $\theta_{B_p} \in \mathbb{R}_{>0}$ and $\epsilon \in \mathbb{N}$.

To mimic the direct inhibition caused by A_p , we assume that the AHPs accumulate in the nucleus in the presence of phosphorylated A-types [27, 66]. In order to replicate this behaviour, we first assume that the rate of inhibition with respect to the concentration of A_p follows a sigmoidal curve, that is $H^-(A_p, \theta_{A_p}, \epsilon')$, where $\theta_{A_p} \in \mathbb{R}_{>0}$ and $\epsilon' \in \mathbb{N}$. Also, the inhibition acts on reaction 2 or 3 because the translocation of the AHPs is occurring during these reactions. We apply the inhibition on reaction 3 because it is responsible for the increase of P , that is AHPs in the cytoplasm.

By mass action kinetics, the reaction rates of the signalling pathway take the following mathematical form.

$$\begin{aligned}
 v_1 &= \alpha_1 \text{Cyto}K & v_9 &= \beta_{P_p} P_p \\
 v_2 &= \alpha_2 K_p P & v_{10} &= \beta_B B \\
 v_3 &= \alpha_3 H^-(A_p, \theta_{A_p}, \epsilon') P_p B & v_{11} &= \beta_{B_p} B_p \\
 v_4 &= \alpha_4 P_p A & v_{12} &= \beta_A A \\
 v_5 &= \gamma_A H^+(B_p, \theta_{B_p}, \epsilon) & v_{13} &= \beta_{A_p} A_p \\
 v_6 &= \beta_K K & v_{14} &= \gamma_K \\
 v_7 &= \beta_{K_p} K_p & v_{15} &= \gamma_P \\
 v_8 &= \beta_P P & v_{16} &= \gamma_B,
 \end{aligned}$$

where α_x denotes the rate constant of reaction $x \in \{1, 2, 3, 4\}$. Hence, we obtain the ODE system

$$\begin{aligned}
 \dot{K} &= -v_1 + v_2 - v_6 + v_{14} \\
 \dot{K}_p &= v_1 - v_2 - v_7 \\
 \dot{P} &= -v_2 + v_3 + v_4 - v_8 + v_{15} \\
 \dot{P}_p &= v_2 - v_3 - v_4 - v_9 \\
 \dot{B} &= -v_3 + v_{16} - v_{10} \\
 \dot{B}_p &= v_3 - v_{11} \\
 \dot{A} &= -v_4 + v_5 - v_{12} \\
 \dot{A}_p &= v_4 - v_{13}
 \end{aligned} \tag{6.1}$$

This model, therefore, describes the signalling pathway of cytokinin.

Unfortunately, the only restrictions that we can force upon the parameters are concerning the decay terms as suggested in the literature, namely A_p has

a lower degradation rate compared to A [3, 32], i.e., $\beta_{A_p} < \beta_A$. Because no further restrictions can be made to the kinetic parameters from the literature, we model the system qualitatively. For this reason, we want to convert the ODEs (6.1) to a more qualitative model, e.g. a PADE-Q or Thomas model, so that we can capture the essential behaviours of the cytokinin network.

6.3 Reduction

As a first step of converting the ODEs to a Thomas formalism, we reduce the ODE system (6.1) into a more manageable five-dimensional model. The reduced dimension of the system would then allow us to illustrate the results of the thesis better.

The reduction method introduced by Heinrich et al. [25] is tailored for two-component phospho-relay, where we assume that the system is saturated, which means that the expression and degradation of each component is balanced out. For our model, this means that the sum of phosphorylated and non-phosphorylated proteins of each component have reached equilibrium. For example, we assume that

$$\dot{K} + \dot{K}_p = \gamma_K - \beta_K K - \beta_{K_p} K_p = 0.$$

Assuming that the degradation rates are equal, i.e., $\beta_K = \beta_{K_p}$, gives that $K + K_p = \gamma_K/\beta_K =: C_K \in \mathbb{R}_{\geq 0}$. In other words, the coupling of the two variables K and K_p means that we can describe one variable in terms of the other, hence reducing the dimension of the system. Similarly, we can relate the AHP and B-type variables to get $P + P_p = C_P := \gamma_P/\beta_P$ and $B + B_p = C_B := \gamma_B/\beta_B$ respectively. We do not apply the reduction for A and A_p because the expression rate changes with the system, i.e., γ_A has a coefficient that is dependent on the value of B_p . Also, the degradation rates of A and A_p are not equal.

Applying the reduction described above for K, P and B , we reduce the reaction rates of the eight-dimensional model to the following

$$\begin{aligned} v'_1 &= \alpha_1 \text{Cyto}(C_K - K_p) & v'_6 &= \beta_{K_p} K_p \\ v'_2 &= \alpha_2 K_p (C_P - P_p) & v'_7 &= \beta_{P_p} P_p \\ v'_3 &= \alpha_3 P_p (C_B - B_p) H^-(A_p, \theta_{A_p}, \epsilon') & v'_8 &= \beta_{B_p} B_p \\ v'_4 &= \alpha_4 P_p A & v'_9 &= \beta_A A \\ v'_5 &= \gamma_A H^+(B_p, \theta_{B_p}, \epsilon) & v'_{10} &= \beta_{A_p} A_p. \end{aligned}$$

Therefore, we have the ODE system

$$\begin{aligned}
\dot{K}_p &= v'_1 - v'_2 - v'_6 \\
\dot{P}_p &= v'_2 - v'_3 - v'_4 - v'_7 \\
\dot{B}_p &= v'_3 - v'_8 \\
\dot{A} &= -v'_4 + v'_5 - v'_9 \\
\dot{A}_p &= v'_4 - v'_{10}
\end{aligned} \tag{6.2}$$

Hence, we have a more manageable ODE system of five dimensions.

Now, we want to convert the five-dimensional ODE (6.2) to an ODE model of the form (2.2) so that we can apply the analysis in the thesis. We first group the terms on the right hand side of (6.2) into expression and degradation terms, where the former is composed of the positive terms and the latter the negative. Because the ODE model (2.2) is almost entirely constructed from Hill functions, we need to deal with the linear terms in (6.2).

Note that the following infinite sum of ramp functions equates with a linear term, i.e., for $x \in \mathbb{R}_{\geq 0}$ it holds that

$$x = \sum_{i=0}^{\infty} L^+(x, i, i+1).$$

Because we are dealing with finite variables, i.e., $\max_j < \infty$, we can approximate this sum by a finite number of ramp functions so that $x_j = \sum_{i=0}^{\max_j - 1} L^+(x_j, i, i+1)$. For simplicity, we let each linear term x_j in (6.2) be approximated by a single ramp function $L^+(x_j, 0, 1)$.

In order to approximate these ramp functions with Hill functions, we assign the threshold $\frac{1}{2}$ to the variables K_p, P_p, B_p and A and choose the Hill coefficient $\epsilon_{ij}^* = 7$ for each pair $i, j \in \{1, \dots, n\}$ corresponding to the perturbation $\tilde{\delta} = 0.01$ (see Prop. 5.3). Because C_X is referring to the maximum value of the variable $X \in \{K_p, P_p, B_p\}$, we let the terms $C_X - X$ be replaced by the Hill function $H^-(X, \frac{1}{2}, 7)$. Because each variable can be scaled, we set the threshold $\theta_{A_p} = \frac{1}{2}$. Finally, for convenience, we combine the two thresholds associated with the variable B_p , that is $\theta_{B_p} = \frac{1}{2}$. Transforming all linear terms into ramp functions and then all ramp functions to Hill functions

yields the ODE model,

$$\begin{aligned}
\dot{K}_p &= \alpha_1 H^+(Cyto, \frac{1}{2}, 7) H^-(K_p, \frac{1}{2}, 7) - (\beta_{K_p} + \alpha_2 H^-(P_p, \frac{1}{2}, 7)) K_p \\
\dot{P}_p &= \alpha_2 H^+(K_p, \frac{1}{2}, 7) H^-(P_p, \frac{1}{2}, 7) - \\
&\quad - \left(\beta_{P_p} + \alpha_3 H^-(B_p, \frac{1}{2}, 7) H^-(A_p, \frac{1}{2}, \epsilon_{A_p}) + \alpha_4 H^+(A, \frac{1}{2}, 7) \right) P_p \\
\dot{B}_p &= \alpha_3 H^+(P_p, \frac{1}{2}, 7) H^-(B_p, \frac{1}{2}, 7) H^-(A_p, \frac{1}{2}, \epsilon_{A_p}) - \beta_{B_p} B_p \\
\dot{A} &= \gamma_A H^+(B_p, \frac{1}{2}, \epsilon_{B_p}) - (\beta_A + \alpha_4 H^+(P_p, \frac{1}{2}, 7)) A \\
\dot{A}_p &= \alpha_4 H^+(A, \frac{1}{2}, 7) H^+(P_p, \frac{1}{2}, 7) - \beta_{A_p} A_p
\end{aligned} \tag{6.3}$$

Replacing the Hill functions in (6.3) with step functions gives the related PADE model.

$$\begin{aligned}
\dot{K}_p &= \alpha_1 S^+(Cyto, \frac{1}{2}) S^-(K_p, \frac{1}{2}) - (\beta_{K_p} + \alpha_2 S^-(P_p, \frac{1}{2})) K_p \\
\dot{P}_p &= \alpha_2 S^+(K_p, \frac{1}{2}) S^-(P_p, \frac{1}{2}) - (\beta_{P_p} + \alpha_3 S^-(B_p, \frac{1}{2}) S^-(A_p, \frac{1}{2}) + \alpha_4 S^+(A, \frac{1}{2})) P_p \\
\dot{B}_p &= \alpha_3 S^+(P_p, \frac{1}{2}) S^-(B_p, \frac{1}{2}) S^-(A_p, \frac{1}{2}) - \beta_{B_p} B_p \\
\dot{A} &= \gamma_A S^+(B_p, \frac{1}{2}) - (\beta_A + \alpha_4 S^+(P_p, \frac{1}{2})) A \\
\dot{A}_p &= \alpha_4 S^+(A, \frac{1}{2}) S^+(P_p, \frac{1}{2}) - \beta_{A_p} A_p
\end{aligned} \tag{6.4}$$

Now, we deduce the ordering constraints of the PADE model above so that (6.4) can be discretised using Def. 3.2 to yield a Thomas model. That is, for all $i \in \{K_p, P_p, B_p, A, A_p\}$ and $D \in \mathcal{D}_r$, where \mathcal{D}_r denotes the set of regular domains in (6.4), we discuss whether the focal point component $\phi_i(D)$ is above or below the threshold $\frac{1}{2}$, based on how we expect the system to evolve from states in D . We first consider the variables that have only two focal point component values.

The focal point components of variable B_p take only two values, namely either $\phi_{B_p}(D) = 0$ or $\phi_{B_p}(D) = \alpha_3/\beta_{B_p}$ for a regular domain $D \in \mathcal{D}_r$. If $\alpha_3/\beta_{B_p} < \frac{1}{2}$, then $S^+(B_p, \frac{1}{2}) = 0$ for all solutions that have an initial condition $B_p = 0$, which would imply that A converges to zero over time. Because we expect to see some increase in A , we choose the constraint

$$\alpha_3/\beta_{B_p} > \frac{1}{2}.$$

Similarly, the focal point components of variable A_p take two values, namely either $\phi_{A_p}(D) = 0$ or $\phi_{A_p}(D) = \alpha_4/\beta_{A_p}$ for regular domain $D \in \mathcal{D}_r$. If $\alpha_4/\beta_{A_p} < \frac{1}{2}$, then $S^-(A_p, \frac{1}{2}) = 1$ for all solutions that have an initial condition $A_p = 0$, which would imply that A_p has no inhibiting influence on the other variables. Because we assume direct inhibition of the signal by the A-types, we let

$$\alpha_4/\beta_{A_p} > \frac{1}{2}.$$

The focal point components of variable A take the three values $0, \gamma_A/\beta_A$ and $\gamma_A/(\beta_A + \alpha_4)$. By similar reasoning as for A_p and B_p , we let $\gamma_A/\beta_A > \frac{1}{2}$. However, we need to consider the value $\gamma_A/(\beta_A + \alpha_4)$, which is the focal point component of A when $B_p, P_p > \frac{1}{2}$. Because this case corresponds to the A-types being expressed and simultaneously phosphorylated, the condition $\gamma_A/(\beta_A + \alpha_4) < \frac{1}{2}$ would imply that A does not increase beyond $\frac{1}{2}$, representing the case that the A-types are being expressed and immediately phosphorylated. However, the phosphorylated A-types would not increase in such a case due to the switch-like behaviour of the PADE model. Therefore, for the event of expression and simultaneous phosphorylation to still imply an increase in the overall concentration of the A-types in our model, we choose the constraints

$$\gamma_A/\beta_A, \gamma_A/(\beta_A + \alpha_4) > \frac{1}{2}.$$

The variable K_p is similar to A in that its focal point components take three values, namely $0, \alpha_1/\beta_{K_p}$ and $\alpha_1/(\beta_{K_p} + \alpha_2)$. Following similar arguments, we choose the constraints

$$\alpha_1/\beta_{K_p}, \alpha_1/(\beta_{K_p} + \alpha_2) > \frac{1}{2}.$$

The focal point components of variable P_p take five different values, which following similar arguments as for A gives the ordering constraints

$$\alpha_2/\beta_{P_p}, \alpha_2/(\beta_{P_p} + \alpha_3), \alpha_2/(\beta_{P_p} + \alpha_4), \alpha_2/(\beta_{P_p} + \alpha_3 + \alpha_4) > \frac{1}{2}.$$

Because each variable is associated to a single threshold value, we expect the related Thomas model to be Boolean. Accordingly, we define the Boolean variables $cyto, k_p, p_p, b_p, a$ and a_p to correspond to the continuous variables $Cyto, K_p, P_p, B_p, A$ and A_p respectively. Note that $cyto$ is an input variable that takes a constant value, i.e., either 0 or 1. Because we are only interested in the transduction of the signal when cytokinin is present, we only consider the case $cyto = 1$ in the following. The state space of the related Thomas

model can be defined using these Boolean variables, namely $Q := \{0, 1\}^5$. Discretising the PADE system (6.4) using the method in Def. 3.2, we obtain a unique update function $f : Q \rightarrow Q$ from the ordering constraints above. Furthermore, we observe the individual Boolean variables to obey the following logical rules, which follows from the discretisation of (6.4) using the method in Def. 3.2.

$$\begin{aligned} k_p &= cyto \wedge \neg k_p \\ p_p &= k_p \wedge \neg p_p \\ b_p &= p_p \wedge \neg b_p \wedge \neg a_p \\ a &= b_p \\ a_p &= a \wedge p_p. \end{aligned}$$

From these logical equations, we have a single update function of the cytokinin network that satisfies the basic assumptions of the system. Fig. 6.3 displays part of the state transition graph, $STG(f)$, of the update function $f : \{0, 1\}^5 \rightarrow \{0, 1\}^5$.

As expected discretisation has reduced the system to its very basic components, where particular interactions of the signalling pathway are missing. In particular, if we were to construct a PADE model from the Thomas model above using Def. 3.3, we would have constant degradation terms, which are unlike the degradation terms in (6.4). This inconsistency between models emphasises the problem of discretisation and interpolation because multiple ODE models are related to a single Thomas model. That is, transforming a Thomas model to an ODE model is not a trivial task and can have very different implications on the resulting system behaviours.

6.4 Parameter Estimation

In this final section, we estimate the kinetic parameters of the ODE model (6.3) starting from the ordering constraints of the related PADE model (6.4),

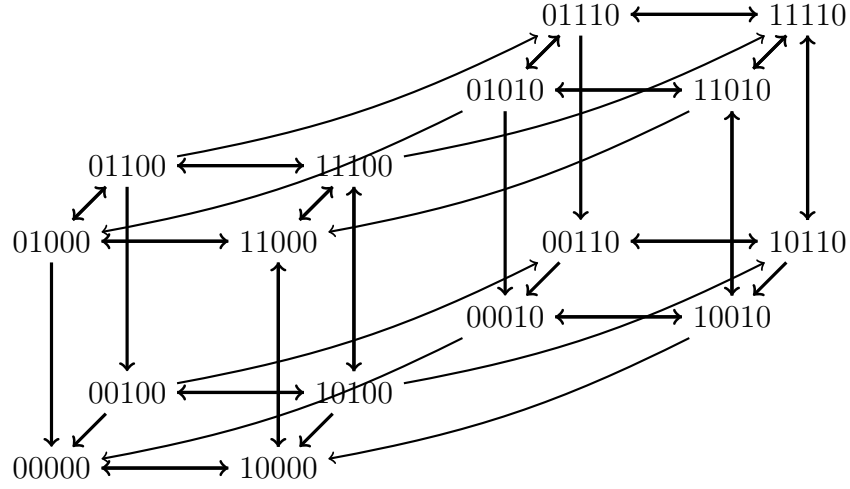


Figure 6.3: Subgraph of the STG of the reduced Thomas model of the signalling network. Each state is a 5-tuple representing the Boolean values of (k_p, p_p, b_p, a, a_p) .

which are

$$\begin{aligned}
 \frac{1}{2} < \phi_1 &:= \frac{\alpha_1}{\beta_{K_p} + \alpha_2} \\
 \frac{1}{2} < \phi_2 &:= \frac{\alpha_2}{\beta_{P_p} + \alpha_3} \\
 \frac{1}{2} < \phi_3 &:= \frac{\alpha_3}{\beta_{B_p}} \\
 \frac{1}{2} < \frac{\gamma_A}{\beta_A + \alpha_4}, \frac{\alpha_1}{\beta_{K_p}}, \frac{\alpha_2}{\beta_{P_p} + \alpha_3 + \alpha_4}, \frac{\alpha_4}{\beta_{A_p}}.
 \end{aligned} \tag{6.5}$$

Note that because reaction rates take positive values, some of the inequalities above imply the focal point component restrictions that have not been labelled above, e.g. $\frac{1}{2} < \frac{\alpha_2}{\beta_{P_p} + \alpha_3 + \alpha_4} < \frac{\alpha_2}{\beta_{P_p} + \alpha_4} < \frac{\alpha_2}{\beta_{P_p}}$. From the ordering constraints, we want to incrementally add constraints on the kinetic parameters so that the *observed behaviour*, that is the A-types are expressed given an initial value of zero for all components, is present in the different models.

At first glance, the lack of steady states in the STG implies that there are no asymptotically stable equilibria in the regular domains of the PADE model by Thm. 3.1. Nevertheless, we can find a path in the STG that reflects the observed behaviour, namely $(00000, 10000, 11000, 11100, 11110)$. We want this observed behaviour to be reflected in the QTG^Ψ .

Thus, we want that there exists a path from the regular domain corresponding to 00000, i.e. $D^0 := [0, \frac{1}{2}) \times [0, \frac{1}{2}) \times [0, \frac{1}{2}) \times [0, \frac{1}{2}) \times [0, \frac{1}{2})$, to a domain where the value of A is strictly positive. However, an STG path does not always correspond to a QTG path (Ex. 8) and thus we trace a QTG path from D^0 by considering a small set of transitions in the STG (Thm. 3.1).

The STG edge $(00000, 10000) \in E$ implies that $(D^0, D^1) \in \mathcal{T}^\Psi$, where $D^1 := [\frac{1}{2}] \times [0, \frac{1}{2}) \times [0, \frac{1}{2}) \times [0, \frac{1}{2}) \times [0, \frac{1}{2})$. The edge $(10000, 00000) \in E$ then implies that D^1 is non-transparent by 1a) of Thm. 3.1. The edges $(10000, 11000) \in E$ and $(01000, 00000) \notin E$ imply by (2) and (3) of Thm. 3.1 respectively that $(D^1, D^2), (D^2, D^1) \in \mathcal{T}^\Psi$, where $D^2 := [\frac{1}{2}] \times [\frac{1}{2}] \times [0, \frac{1}{2}) \times [0, \frac{1}{2}) \times [0, \frac{1}{2})$. From Fig. 6.3, we see that the edges to and from the state 11000 satisfy 1a) of Thm. 3.1 for the variables k_p, p_p and b_p . Hence, D^2 and $D^3 := [\frac{1}{2}] \times [\frac{1}{2}] \times [\frac{1}{2}] \times [0, \frac{1}{2}) \times [0, \frac{1}{2})$ are non-transparent. Furthermore, the edge $(01000, 01100) \in E$ implies by (2) of Thm. 3.1 that $(D^2, D^3) \in \mathcal{T}^\Psi$ and the edge $(00000, 00100) \notin E$ implies by (3) of Thm. 3.1 that $(D^3, D^2) \in \mathcal{T}^\Psi$. Finally, the edge $(01100, 01110) \in E$ implies by (2) of Thm. 3.1 that $(D^3, D^4) \in \mathcal{T}^\Psi$ and the edge $(01000, 01010) \notin E$ implies by (3) of Thm. 3.1 that $(D^4, D^3) \in \mathcal{T}^\Psi$, where $D^4 := [\frac{1}{2}] \times [\frac{1}{2}] \times [\frac{1}{2}] \times [\frac{1}{2}] \times [0, \frac{1}{2})$, i.e., A has a strictly positive value. Therefore, we have that the path $(D^0, D^1, D^2, D^3, D^4)$ in the QTG^Ψ reflects the observed behaviour. Because we are focussing on this particular path in the QTG^Ψ , rather than displaying the entire graph, we overlay the path of the QTG^Ψ on the $STG(f)$ in Fig. 6.4.

Next, we look at the individual transitions in the path and discuss whether they are present in QTG^Φ . By Lemma 4.2, we have that $(D^0, D^1) \in \mathcal{T}^\Phi$ for $QTG^\Phi(\mathcal{A}) = (\mathcal{D}, \mathcal{T}^\Phi)$. However, as we showed in Fig. 4.4 and Fig. 4.5, a transition between singular domains in QTG^Ψ may not be present in QTG^Φ depending on the kinetic parameters. Although the transition $(D^3, D^4) \in \mathcal{T}^\Psi$ yields a positive value for A , by nature of the PADE solutions the value A begins to increase as soon as $B_p = \frac{1}{2}$, i.e., A obtains a strictly positive value. Therefore, for the discretised PADE formalism to reflect the observed behaviour, we want the path (D^1, D^2, D^3) to be present in the $QTG^\Phi(\mathcal{A}) = (\mathcal{D}, \mathcal{T}^\Phi)$. That is, we want to restrict the kinetic parameters such that $(D^1, D^2), (D^2, D^3) \in \mathcal{T}^\Phi$ and $(D^2, D^1), (D^3, D^2) \notin \mathcal{T}^\Phi$.

For the transition (D^1, D^2) , we consider the focal points associated with D^1 , that is $(\phi_1, 0, 0, 0, 0)$ and $(0, \phi_2, 0, 0, 0)$. If the line connecting these two focal points intersects D^1 , then D^1 has a singular equilibrium set, which would not reflect the observed behaviour. To avoid this, we impose the condition

$$\frac{1}{\phi_1} + \frac{1}{\phi_2} < 2, \quad (6.6)$$

which ensures that the focal set of D^1 in the variable p_p is beyond the thresh-

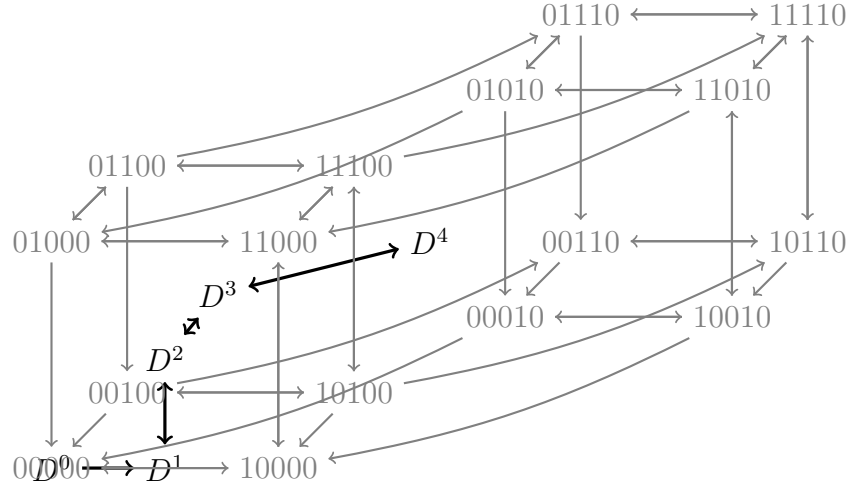


Figure 6.4: The same subgraph of the STG as in Fig. 6.3 is depicted in gray. Nodes and transitions of the QTG^Ψ are overlaid in black such that the location of the domains corresponds to their location with respect to the nodes of the STG.

old $\frac{1}{2}$. Moreover, the same condition ensures that D^2 has a non-empty focal set.

For the next transition (D^2, D^3) , we look at the focal points, $(\phi_1, 0, 0, 0, 0)$, $(0, \phi_2, 0, 0, 0)$, $(0, 0, \phi_3, 0, 0)$ and $(\alpha_1/\beta_{K_p}, 0, \phi_3, 0, 0)$. If the plane produced by the three focal points $(\phi_1, 0, 0, 0, 0)$, $(0, \phi_2, 0, 0, 0)$ and $(0, 0, \phi_3, 0, 0)$ intersects with D^2 , then there exists a singular equilibrium set in D^2 . Because we want all solutions to exit D^2 , we impose the constraint

$$\frac{1}{\phi_1} + \frac{1}{\phi_2} + \frac{1}{\phi_3} < 2. \quad (6.7)$$

Fig. 6.5 displays examples of conditions (6.6) and (6.7) not being satisfied for the ODE model (6.3), where the former has a steady state such that $P_p < \frac{1}{2}$ with zero concentration for B_p , A and A_p , and the latter has a steady state such that $B_p < \frac{1}{2}$ with zero concentration for A and A_p . Therefore, the constraints (6.6) and (6.7) ensure that the observed behaviour is present in QTG^Φ , that is $(D^1, D^2), (D^2, D^3) \in \mathcal{T}^\Phi$.

As discussed in Sect. 5.1, to ensure that the PADE solutions are conserved in the ODE model, we look at the PMA model. As mentioned above, the related PMA model replaces every step function with threshold $\frac{1}{2}$ in (6.4) with a ramp function with the threshold interval $[0, 1]$. The threshold intervals have the upper bound of 1, from which we can extend the ordering constraints

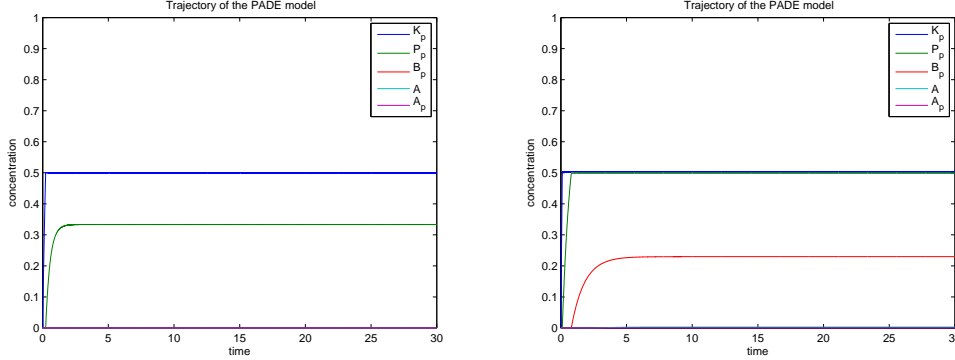


Figure 6.5: Trajectories of the PADE model (6.4), where (6.6) is not satisfied on the left with $\phi_1 = 1$ and $\phi_2 = 2/3$ and (6.7) is not satisfied on the right with $\phi_1 = 2$, $\phi_2 = 1$ and $\phi_3 = 3/5$. The trajectory on the left has zero values for variables B_p , A and A_p and the trajectory on the right has zero values for variables A and A_p .

to give the PMA parameter constraints, namely

$$1 < \phi_1, \phi_2, \phi_3$$

$$1 < \frac{\gamma_A}{\beta_A + \alpha_4}, \frac{\alpha_1}{\beta_{K_p}}, \frac{\alpha_2}{\beta_{P_p} + \alpha_3 + \alpha_4}, \frac{\alpha_4}{\beta_{A_p}}.$$

We extend the conditions (6.6) and (6.7) so that the path (D^1, D^2, D^3) in the QTG^Φ has corresponding trajectories between R^1 and R^2 as well as between R^2 and R^3 , where $R^j := \chi^{-1}(D^j)$, $j = 1, 2, 3$ in the PMA model. Although the conditions (6.6) and (6.7) may suffice for some trajectories to leave R^1 and R^2 in the direction of R^2 and R^3 respectively, we want to be sure that no solution stays in R^1 or R^2 . That is, we want to deduce conditions that there are no equilibria in R^j , $j = 1, 2, 3$ so that all solutions leave the rectangle. For this we need to check that the condition (5.1) is not satisfied.

Adapting the conditions (6.6) and (6.7) to incorporate the threshold intervals such that (5.1) is not satisfied for R^1 and R^2 yields

$$\frac{1}{\phi_1} + \frac{1}{\phi_2} < 1, \text{ and } \frac{1}{\phi_1} + \frac{1}{\phi_2} + \frac{1}{\phi_3} < 1. \quad (6.8)$$

From these restrictions, we see how the different reaction rates are coupled and thereby determine the sensitivities of the kinetic parameters with respect to each other. In particular, we see that decreasing the reaction rate α_2 we need to increase the reaction rate α_3 such that (6.6) holds in order for the observed behaviour to be replicated. In other words, with our parameter

restrictions, we establish some coupling and interdependencies of the different kinetic parameters.

With the above observations, we can simulate the ODE model (6.3) with kinetic parameters that satisfy the PMA parameter constraints as well as (6.8). Still, parameters that satisfy both conditions in (6.8) can be chosen in multiple ways. Fig. 6.6 displays two different parameter sets that satisfy the PMA parameter constraints as well as (6.8). We observe that both trajectories of the ODE model (6.3) reach a stable equilibrium point with increasing time. In other words, although we have restricted the parameters, there are still many kinetic parameters that satisfy these restrictions.

Note that in both trajectories of the ODE model in Fig. 6.6, the final values of each variable have the same ordering with respect to each other. In that sense, we claim that the qualitative behaviour of the two sets of kinetic parameters are *equivalent*. Similarly, the trajectories of the five dimensional and eight dimensional models also display an ordering of the equilibrium concentrations that also reflects the ordering of the ODE model. Before reaching an equilibrium, each trajectory in all the models and for all sets of kinetic parameters exhibits a damped oscillation. The longest oscillation is observed in the five-dimensional model, followed by the eight-dimensional model and then the ODE model, which exhibits a very slight damped oscillation after the initial increase in concentration. In other words, replacing the linear terms in (6.2) with Hill functions to create (6.3) conserves the qualitative dynamics, where qualitative dynamics refers to the ordering of the variables at the final concentration. Moreover, the reduction method of two-component phosphorelay systems in [25] also conserves the qualitative dynamics.

Our experience from modelling the cytokinin signal transduction pathway is that qualitative modelling can be done when analysing general ODE systems that consist of more than just Hill functions. More specifically, after converting the general ODE system into an ODE model of the form (2.2), we are able to transform the ODE model into the Thomas or PADE models, and thus can use the different available analysis techniques to study the ODE model. As we have shown in this section, we have been able to infer the kinetic parameters of the ODE model from the qualitative parameter information of the update function in the Thomas model resp. the ordering constraints in the PADEs. These kinetic parameters, which are more constrained than prior to the analysis, can then be applied to the ODE model to obtain dynamics that are consistent with the other modelling methods, thus reducing the artefacts of the formalisms. In summary, by comparing the dynamics that are generated from different modelling methods, we hope to gain a better understanding of how the biological system behaves as opposed to how the modelling method abstracts the system.

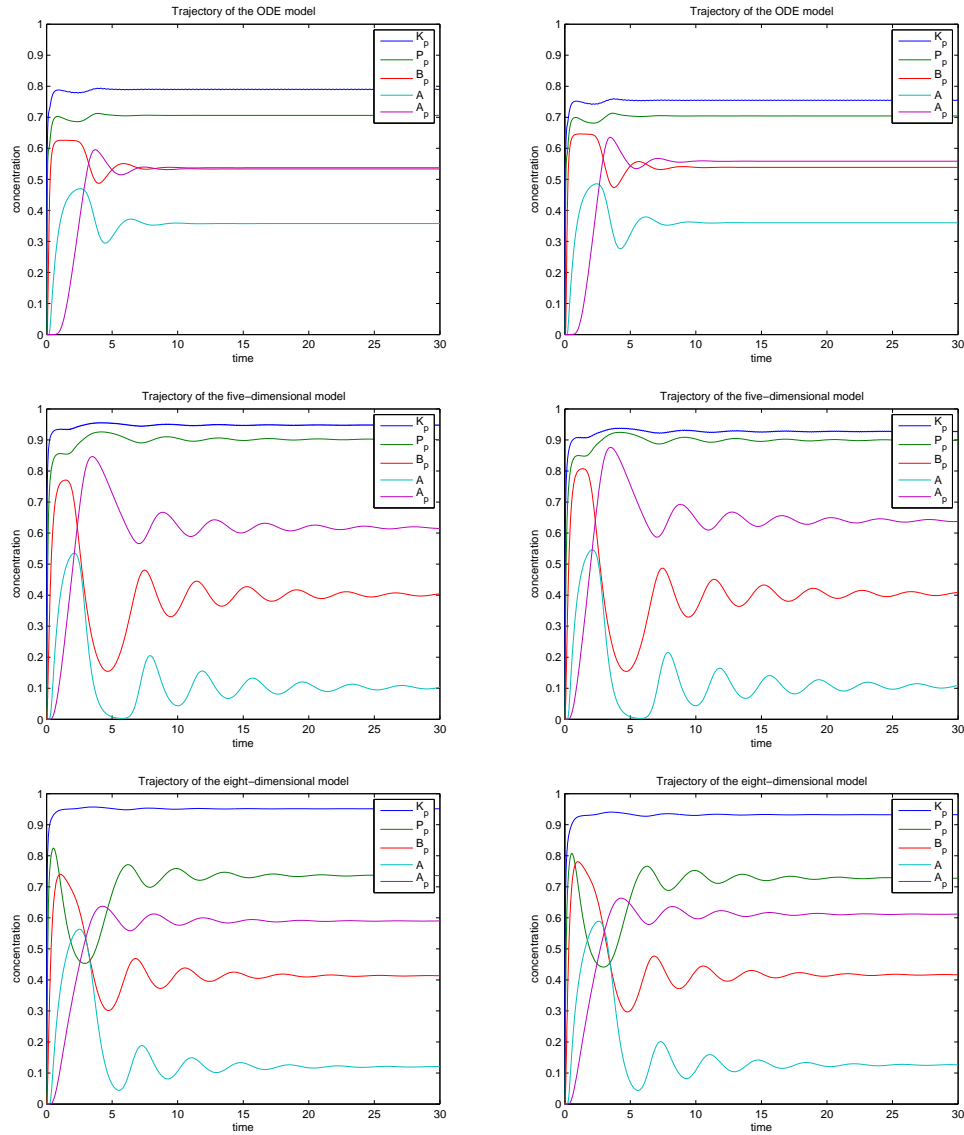


Figure 6.6: Trajectories of the different models that we have considered. The two top, two middle and two bottom diagrams display simulations of the ODE model (6.3), the five-dimensional model (6.2) and the eight-dimensional model (6.1) respectively. The left column displays the simulations resulting from the parameters $(\phi_1, \phi_2, \phi_3) = (3, 3, 4)$, whereas the right column uses the parameters $(\phi_1, \phi_2, \phi_3) = (2, 5, 5)$. Note that both parameter sets satisfy (6.8).

Summary:

- Qualitative modelling methods can help analyse general ODE systems.
- Kinetic parameters of the ODE model can be inferred from the qualitative parameter information of the update function in the Thomas model resp. the ordering constraints in the PADEs.
- Simulations of different parameter sets showed similar dynamics for the cytokinin signal transduction network.

Conclusion

Mathematical modelling helps in the understanding of biological processes. However, there are many modelling approaches that provide either coarse or fine representations of system behaviour. By relating different formalisms, the behaviours represented by each formalism can be compared to reveal consistencies or inconsistencies in the dynamics. In order to find conditions for such consistent or inconsistent dynamics, we need to conduct a thorough mathematical analysis.

In this thesis, we have established a relation between the discrete Thomas formalism and the continuous ODE formalism in order to discuss the consistent and inconsistent dynamics between them. Direct transformations between ODE and Thomas formalisms are very rough in the sense that a lot of explicit parameter information is lost resp. required in the transformation. To break up the large gap of information between the Thomas and ODE formalisms, we incorporated the hybrid modelling approach of PADEs as well as the discrete singular state formalism and the continuous PMA formalism. Fig. 7.1 displays the formalisms in our analysis and how they differ in terms of either their dynamics or their parameters. These modelling approaches provide a stepwise transformation, which is less rough than the direct transformation between Thomas and ODE models (see Fig. 7.2). We are then able to see at which step the inconsistent dynamics arises. In consequence, we are able to discuss the consistent and inconsistent dynamics between the Thomas and ODE models using the stepwise transformations.

When using stepwise transformations between ODE and Thomas models, we choose the parameters so that there is dynamics that is consistent between all formalisms. In particular, if the kinetic parameters of the ODE model satisfy the PMA parameter constraints (Sect. 5.1) and the Hill coefficient are chosen as in Sect 5.2, then a steady state in the Thomas formalism does not only correspond to an asymptotically stable equilibrium point in the related PADE model (cf. [56]), but also in the ODE model. Furthermore,

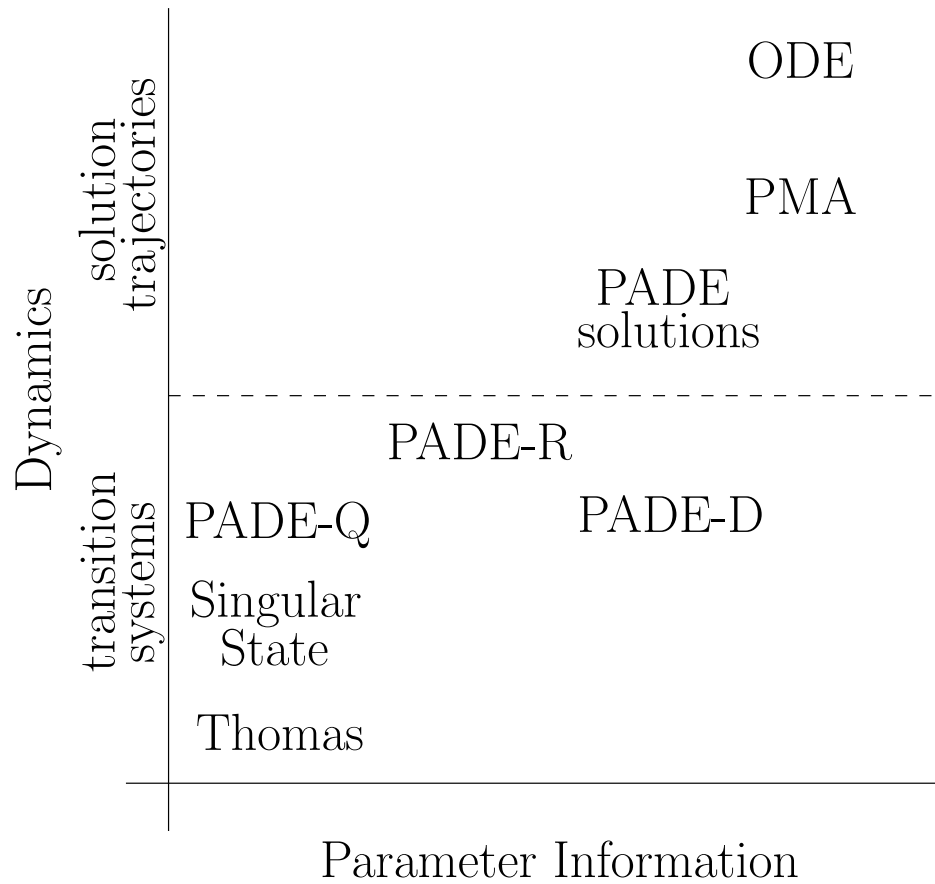


Figure 7.1: A plot of the different formalisms that have been addressed in the thesis in terms of how they relate with each other. The x -axis displays increasing parameter information going from left to right and based on the parameter relations established in the thesis. The y -axis is ranked by increasing detail of dynamical information, where the transition systems are ranked first by increasing node set size and then by update scheme and the solution trajectories are ranked by uniqueness and smoothness of solutions.

the result in [56, 17, 42, 21] (see Introduction) that a cyclic attractor in the Thomas model corresponds to an asymptotically stable equilibrium point or a limit cycle oscillation in the ODE model is confirmed by the results in Prop. 3.3, Prop. 3.2 and Prop. 5.1. In other words, by the results developed in the thesis, there are some behaviours that are conserved by the stepwise transformations.

Despite the coarse representation, the Thomas formalism also provides information about other equilibria that are not accounted for by the steady states in the state transition graph. Thm. 4.1 exploits the association of the Thomas and PADE-Q formalisms to show that every steady state in the PADE-Q formalism is also a steady state in the PADE-D formalism, which by Cor. 5.1 corresponds to exactly one equilibrium point in the PMA model. Assuming that the perturbation argument in Prop. 5.3 holds for singular rectangles of the PMA model, all equilibria are conserved between the PMA and ODE models. Therefore, the Thomas formalism can also determine equilibrium points in the ODE model that are not necessarily asymptotically stable.

By the proof of Thm. 4.1, a steady state in QTG^Ψ of the PADE-Q formalism, which is a singular domain, is characteristic of negative feedback loops in the interaction graph. By Cor. 4, we know that the singular state corresponding to this singular domain is also a steady state in the singular state formalism. This reflects the findings in [57, 48] that singular steady states are characteristic of feedback loops in the interaction graph. Moreover, the proof of Cor. 5.1 does not need the assumption that feedback loops be negative, which would imply that the singular steady states that are characteristic of *positive* feedback loops in the interaction graph would also lead to exactly one equilibrium point in the ODE model. In that respect, the original singular steady state formalism, whose dynamics is derived from a strictly defined interaction graph and logical parameters, is very successful in determining equilibria in the ODE model. This shows that, there is information encoded in the Thomas formalism that implies the existence of multiple equilibria in the ODE model.

We shortly address the role of the PADE-R formalism in the analysis of the Thomas and ODE formalisms. On the one hand, the PADE-R formalism is a refinement of the PADE-Q formalism (Sect. 4.1). On the other hand, the kinetic parameters of the PADE-D formalism convey more specific dynamics than the parameter inequality constraints of the PADE-R formalism (Sect. 4.2). Because of the close relation between the Thomas and PADE-Q formalisms (Sect. 4.1) as well as the relation between the PADE-D and ODE formalisms (Chap. 5), the PADE-R formalism does not improve our understanding of the consistent and inconsistent dynamics between Thomas and

ODE models and thus we disregard it in this final discussion.

When considering general attractors in the Thomas and ODE models, we can determine the location of attractors via hyperrectangular trap sets. More specifically, a hyperrectangular trap set in the Thomas formalism implies that a hyperrectangle U exists in the related PADE-Q formalism, which is also a trap set by Prop. 3.4. The subgraph property [15] would then imply that U is also a trap set in the PADE-D formalism. By Def. 2.5, the PADE solutions are restricted to the union of domains in U . The construction of the PMA model and the PMA parameter constraints then imply that the sign of the vector field on the boundary of a domain in the PADE model is reflected in the sign of the vector field at the corners of the corresponding rectangle in the PMA model (see [5, 33] and Prop. 5.1). Therefore, the union of rectangles, whose corresponding domains are in U , defines a positive invariant set in the PMA model. Here a positive invariant set means that a solution starting in the set will remain in the set with increasing time. Finally, we expect the trajectories in the PMA model to be conserved in the ODE model (Sect. 5.2). In other words, a hyperrectangular trap set in the Thomas model corresponds to a positive invariant hyperrectangular region of the ODE model. That is, the Thomas model can uncover the location, but not the number, of attractors in the ODE model.

Finally, we discuss the *potential dynamics* between formalisms, which refers to the dynamics that is potentially consistent between formalisms depending on explicit kinetic parameters. For example, the PADE-Q shares information about the potential singular equilibrium sets in PADE-D (end of Sect. 3.3), and singular equilibrium sets in PADE-D are potential equilibria in the PMA model (Sect. 5.1.1). Also, many discrete paths in PADE-D have potential PADE solutions (Sect. 4.3). In order for the potential dynamics to be consistent under a stepwise transformation, we impose restrictions on the kinetic parameters. Applying these restrictions over all the stepwise transformations allows mainly consistent dynamics to exist between the Thomas and ODE models. In other words, with the goal of maximising consistent dynamics between all formalisms, explicit kinetic parameters that are otherwise lacking can be inferred by the potential dynamics.

The interdependencies between different modelling approaches presented here are just the beginning. Other than expanding on the relations established above, one could also incorporate more complex formalisms such as stochastic models [53] and delay equations [19, 20] in order to shed some light on the random resp. delay features of the biological system. Also, including the relation between network structure and dynamics can help analyse some systems using their network topologies [54, 35]. These topics would help improve our understanding of how modelling methods represent a systems

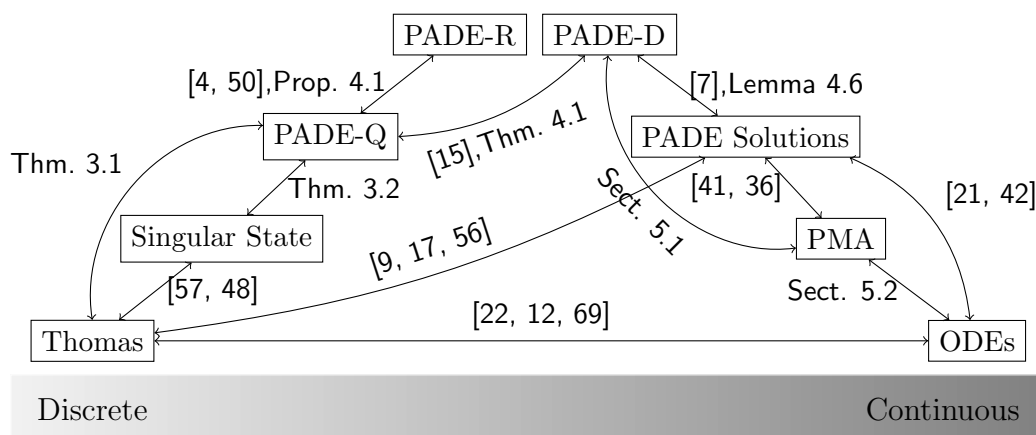


Figure 7.2: Our formalisms of interest from the introduction. The arrows depict transformations between the respective formalisms and are labelled with the references and results or sections of the thesis that deal with the transformation.

behaviour and are possibilities for future work.

In conclusion, the relations between the different formalisms allow us to use their respective analysis methods to analyse a single biological network. In particular, when explicit kinetic parameters are lacking, the qualitative parameter information allows us to identify some equilibria and limit cycle oscillations in the ODE model that are also present in the other formalisms. The stepwise transformations then allow us to see how the more precise dynamics firstly builds on the coarse representation, and secondly is sensitive to the kinetic parameters. When determining the more precise dynamics, e.g. existence of a trajectory implied by a time series, the kinetic parameters can be restricted so that there is consistent dynamics between the different modelling methods. This procedure does not only ensure that the dynamics are consistent regardless of the modelling method used, but also helps estimate the kinetic parameters that were lacking. In other words, the qualitative formalisms can be used as an analysis tool for the differential equation formalisms. In summary, by understanding the interdependencies between multiple formalisms, we are able to reduce the artefacts of the modelling methods and thereby model biological networks with greater precision.

Bibliography

- [1] J. Ahmad, G. Bernot, J.-P. Comet, D. Lime, and O. Roux. Hybrid Modelling and Dynamical Analysis of Gene Regulatory Networks with Delays. *ComPlexUs*, 3(4):231–251, 2006.
- [2] J. Ahmad, O. Roux, G. Bernot, and J.-P. Comet. Analysing formal models of genetic regulatory networks with delays. *International Journal of Bioinformatics Research and Applications*, 4(3):240–262, 2008.
- [3] Y. Asakura, T. Hagino, Y. Ohta, K. Aoki, K. Yonekura-Sakakibara, A. Deji, T. Yamaya, T. Sugiyama, and H. Sakakibara. Molecular characterization of His-Asp phosphorelay signaling factors in maize leaves: Implications of the signal divergence by cytokinin-inducible response regulators in the cytosol and the nuclei. *Plant molecular biology*, 52(2):331–341, 2003.
- [4] G. Batt, H. de Jong, M. Page, and J. Geiselmann. Symbolic reachability analysis of genetic regulatory networks using discrete abstractions. *Automatica*, 44(4):982–989, Apr. 2008.
- [5] C. Belta, L. Habets, and V. Kumar. Control of multi-affine systems on rectangles with applications to hybrid biomolecular networks. In *Decision and Control, 2002*, volume 1, pages 534–539. IEEE, 2002.
- [6] S. Berman, A. Halasz, and V. Kumar. MARCO: A Reachability Algorithm for Multi-Affine Systems with Applications to Biological Systems. In *International Conference on Hybrid Systems: Computation and Control (HSCC'07)*, pages 76–89. Springer, LNCS 4416, 2007.
- [7] R. Casey, H. de Jong, and J.-L. Gouzé. Piecewise-linear models of genetic regulatory networks: Equilibria and their stability. *Journal of Mathematical Biology*, 56:27–56, 2006.

-
- [8] M. Chaves, L. Tournier, and J.-L. Gouzé. Comparing Boolean and piecewise affine differential models for genetic networks. *Acta biotheoretica*, 58(2-3):217–32, Sept. 2010.
- [9] J.-P. Comet and G. Bernot. Introducing continuous time in discrete models of gene regulatory networks. *Proc. of the Nice Spring school on Modelling and Simulation of Biological Processes in the Context of Genomics*, 2010.
- [10] R. Coutinho, B. Fernandez, R. Lima, and A. Meyroneinc. Discrete time piecewise affine models of genetic regulatory networks. *Journal of Mathematical Biology*, 52:524–570, May 2006.
- [11] I. D’Agostino, J. Deruère, and J. Kieber. Characterization of the response of the Arabidopsis response regulator gene family to cytokinin. *Plant Physiology*, 124(December):1706–1717, 2000.
- [12] M. Davidich and S. Bornholdt. The transition from differential equations to Boolean networks: a case study in simplifying a regulatory network model. *Journal of Theoretical Biology*, 255(3):269–77, Dec. 2008.
- [13] H. de Jong. Modeling and simulation of genetic regulatory systems: a literature review. *Journal of Computational Biology*, 9(1):67–103, 2002.
- [14] H. de Jong, J.-L. Gouzé, C. Hernandez, M. Page, T. Sari, and J. Geiselmann. Dealing with discontinuities in the qualitative simulation of genetic regulatory networks. In *ECAI 2002: 15th European Conference on Artificial Intelligence, July 21-26, 2002, Lyon France: including Prestigious Applications of Intelligent Systems (PAIS 2002): proceedings*, pages 412–416. IOS Press, 2002.
- [15] H. de Jong, J.-L. Gouzé, C. Hernandez, M. Page, T. Sari, and J. Geiselmann. Qualitative simulation of genetic regulatory networks using piecewise-linear models. *Bulletin of Mathematical Biology*, 66(2):301–40, Mar. 2004.
- [16] H. de Jong, M. Page, C. Hernandez, and J. Geiselmann. Qualitative simulation of genetic regulatory networks: Method and application. In *International Joint Conference on Artificial intelligence*, volume 17, pages 67–73. Citeseer, 2001.
- [17] R. Edwards. Analysis of continuous-time switching networks. *Physica D: Nonlinear Phenomena*, 146(1-4):165–199, Nov. 2000.

-
- [18] A. F. Filippov. *Differential Equations with Discontinuous Righthand Sides*. Kluwer Academic Publishers, 1988.
- [19] M. Ghil and A. Mullhaupt. Boolean delay equations. II. Periodic and aperiodic solutions. *Journal of Statistical Physics*, 41, 1985.
- [20] M. Ghil, I. Zaliapin, and B. Coluzzi. Boolean delay equations: A simple way of looking at complex systems. *Physica D: Nonlinear Phenomena*, 237(23):2967–2986, Dec. 2008.
- [21] L. Glass and S. Kauffman. Co-operative components, spatial localization and oscillatory cellular dynamics. *Journal of Theoretical Biology*, pages 219–237, 1972.
- [22] L. Glass and S. A. Kauffman. The logical analysis of continuous, non-linear biochemical control networks. *Journal of Theoretical Biology*, pages 103–129, 1973.
- [23] J.-L. Gouzé and T. Sari. A class of piecewise linear differential equations arising in biological models. *Dynamical Systems*, 17(4):299–316, 2002.
- [24] H. Hanmann, H. Broer. Perturbation theory (dynamical systems). *Scholarpedia*, 3(7):2399, 2008.
- [25] R. Heinrich, B. G. Neel, and T. A. Rapoport. Mathematical Models of Protein Kinase Signal Transduction. *Molecular Cell*, 9:957–970, May 2002.
- [26] A. Heyl, T. Werner, and T. Schmölling. Cytokinin metabolism and signal transduction. *Plant hormone signaling*, pages 93–124, 2001.
- [27] I. Hwang and J. Sheen. Two-component circuitry in Arabidopsis cytokinin signal transduction. *Nature*, 413(6854):383–389, 2001.
- [28] A. Imamura, Y. Yoshino, and T. Mizuno. Cellular localization of the signaling components of Arabidopsis His-to-Asp phosphorelay. *Biosci. Biotechnol. Biochem.*, 65:2113–7, Sept. 2001.
- [29] S. Jamshidi, H. Siebert, and A. Bockmayr. Comparing discrete and piecewise affine differential equation models of gene regulatory networks. In *Information Processing in Cells and Tissues, IPCAT 2012, Cambridge, UK*, pages 17–24. Springer, LNCS 7223, 2012.
- [30] T. Kakimoto. Perception and signal transduction of cytokinins. *Annual Review of Plant Biology*, 54:605–27, Jan. 2003.

- [31] S. A. Kauffman. Metabolic stability and epigenesis in randomly constructed genetic nets. *Journal of Theoretical Biology*, 22(3):437–67, Mar. 1969.
- [32] J. Kim. Phosphorylation of A-type ARR to function as negative regulator of cytokinin signal transduction. *Nature Structural Biology*, 3(5):348–350, 2008.
- [33] M. Kloetzer and C. Belta. Reachability analysis of multi-affine systems. *Transactions of the Institute of Measurement and Control*, 32(5):445–467, Oct. 2009.
- [34] J. Krumsiek, S. Poelsterl, D. M. Wittmann, and F. J. Theis. Odefy - From discrete to continuous models. *BMC Bioinformatics*, 11(1):233, May 2010.
- [35] M. Mabrouki, M. Aiguier, J.-P. Comet, P. Le Gall, and A. Richard. Embedding of Biological Regulatory Networks and Property Preservation. *Mathematics in Computer Science*, 5(3):263–288, Nov. 2011.
- [36] T. Mestl, E. Plahte, and S. Omholt. A mathematical framework for describing and analysing gene regulatory networks. *Journal of Theoretical Biology*, 176(2):291–300, 1995.
- [37] A. Naldi, D. Thieffry, and C. Chaouiya. Decision diagrams for the representation and analysis of logical models of genetic networks. In *Proceedings of the 2007 international conference on Computational methods in systems biology*, pages 233–247. Springer-Verlag, 2007.
- [38] C. Nishimura, Y. Ohashi, S. Sato, T. Kato, and S. Genetic analysis of Arabidopsis histidine kinase genes encoding cytokinin receptors reveals their overlapping biological functions in the regulation of shoot and root. *The Plant Cell*, pages 1–13, 2004.
- [39] Y. Osakabe, S. Miyata, T. Urao, M. Seki, K. Shinozaki, and K. Yamaguchi-Shinozaki. Overexpression of Arabidopsis response regulators, ARR4/ATRR1/IBC7 and ARR8/ATRR3, alters cytokinin responses differentially in the shoot and in callus formation. *Biochemical and Biophysical Research Communications*, 293(2):806–815, 2002.
- [40] E. Plahte and S. Kjøglum. Analysis and generic properties of gene regulatory networks with graded response functions. *Physica D: Nonlinear Phenomena*, 201(1-2):150–176, Feb. 2005.

-
- [41] E. Plahte, T. Mestl, and S. Omholt. Global analysis of steady points for systems of differential equations with sigmoid interactions. *Dynamical Systems*, 9(4):275–291, 1994.
- [42] A. Polynikis, S. J. Hogan, and M. di Bernardo. Comparing different ODE modelling approaches for gene regulatory networks. *Journal of Theoretical Biology*, 261(4):511–30, Dec. 2009.
- [43] J. A. Punwani, C. E. Hutchison, G. E. Schaller, and J. J. Kieber. The subcellular distribution of the Arabidopsis histidine phosphotransfer proteins is independent of cytokinin signaling. *The Plant Journal : for Cell and Molecular Biology*, 62(3):473–82, May 2010.
- [44] A. M. Rashotte, M. G. Mason, C. E. Hutchison, and F. J. Ferreira. A subset of Arabidopsis AP2 transcription factors mediates cytokinin responses in concert with a two-component pathway. *Proceedings of the National Academy of Sciences*, 103(29):11081–11085, 2006.
- [45] E. Remy, P. Ruet, and D. Thieffry. Graphic requirements for multistability and attractive cycles in a Boolean dynamical framework. *Advances in Applied Mathematics*, 41(3):335–350, Sept. 2008.
- [46] A. Richard. Positive circuits and maximal number of fixed points in discrete dynamical systems. *Discrete Applied Mathematics*, 157(15):3281–3288, Aug. 2009.
- [47] A. Richard. Negative circuits and sustained oscillations in asynchronous automata networks. *Advances in Applied Mathematics*, 44(4):378–392, May 2010.
- [48] A. Richard, G. Bernot, and J.-P. Comet. R. Thomas; Modeling of Biological Regulatory Networks: Introduction of Singular States in the Qualitative Dynamics. *Fundamenta Informaticae*, 65:373–392, 2005.
- [49] A. Richard and J.-P. Comet. Necessary conditions for multistationarity in discrete dynamical systems. *Discrete Applied Mathematics*, 155(18):2403–2413, Nov. 2007.
- [50] D. Ropers, V. Baldazzi, and H. D. Jong. Model reduction using piecewise-linear approximations preserves dynamic properties of the carbon starvation response in Escherichia coli. *Computational Biology and Bioinformatics*, 8(1):166–181, 2011.

- [51] D. Ropers, H. de Jong, M. Page, D. Schneider, and J. Geiselmann. Qualitative simulation of the carbon starvation response in *Escherichia coli*. *Biosystems*, 84(2):124–52, May 2006.
- [52] A. Santner, L. I. a. Calderon-Villalobos, and M. Estelle. Plant hormones are versatile chemical regulators of plant growth. *Nature chemical biology*, 5(5):301–7, May 2009.
- [53] I. Shmulevich, E. R. Dougherty, S. Kim, and W. Zhang. Probabilistic Boolean networks: a rule-based uncertainty model for gene regulatory networks. *Bioinformatics*, 18(2):261, 2002.
- [54] H. Siebert. Dynamical and Structural Modularity of Discrete Regulatory Networks. *Electronic Proceedings in Theoretical Computer Science*, 6(CompMod):109–124, Oct. 2009.
- [55] H. Siebert and A. Bockmayr. Incorporating time delays into the logical analysis of gene regulatory networks. In *Computational Methods in Systems Biology*, pages 169–183. Springer, 2006.
- [56] E. H. Snoussi. Qualitative dynamics of piecewise-linear differential equations: a discrete mapping approach. *Dynamical Systems*, 4(3):565–583, 1989.
- [57] E. H. Snoussi and R. Thomas. Logical identification of all steady states: the concept of feedback loop characteristic states. *Bulletin of Mathematical Biology*, 55(5):973–991, 1993.
- [58] S. Soliman, C. Chaouiya, G. Batt, F. Fages, E. Remy, C. Calzone, and F. Pommereau. Modelling molecular networks: relationships between different formalisms and levels of details. *Analysis*, Feb. 2010.
- [59] C. Soulé. Graphic Requirements for Multistationarity. *ComplexUs*, 1:123–133, 2003.
- [60] T. Suzuki, A. Imamura, C. Ueguchi, and T. Mizuno. Histidine-containing phosphotransfer (HPT) signal transducers implicated in His-to-Asp phosphorelay in *Arabidopsis*. *Plant & Cell Physiology*, 39(12):1258–68, Dec. 1998.
- [61] D. Thieffry and R. Thomas. Dynamical behaviour of biological regulatory networks–II. Immunity control in bacteriophage lambda. *Bulletin of Mathematical Biology*, 57(2):277–97, Mar. 1995.

-
- [62] R. Thomas. Boolean formalization of genetic control circuits. *Journal of Theoretical Biology*, pages 563–585, 1973.
- [63] R. Thomas and R. D’Ari. *Biological Feedback*. CRC Press, 1990.
- [64] R. Thomas and M. Kaufman. Multistationarity, the basis of cell differentiation and memory. II. Logical analysis of regulatory networks in terms of feedback circuits. *Chaos (Woodbury, N.Y.)*, 11(1):180–195, Mar. 2001.
- [65] J. P. C. To, J. Deruère, B. B. Maxwell, V. F. Morris, C. E. Hutchison, F. J. Ferreira, G. E. Schaller, and J. J. Kieber. Cytokinin regulates type-A Arabidopsis Response Regulator activity and protein stability via two-component phosphorelay. *The Plant Cell*, 19(12):3901–14, Dec. 2007.
- [66] J. P. C. To, G. Haberer, F. J. Ferreira, and J. Deruère. Type-A Arabidopsis response regulators are partially redundant negative regulators of cytokinin signaling. *The Plant Cell*, 16(March):658–671, 2004.
- [67] J. Wang and L. Wang. State transition graph and stability of singular equilibria for piecewise linear biological models. *Physica D*, 246(1):39–49, 2013.
- [68] S. Widder, J. Schicho, and P. Schuster. Dynamic patterns of gene regulation I: simple two-gene systems. *Journal of Theoretical Biology*, pages 1–41, 2007.
- [69] D. M. Wittmann, J. Krumsiek, J. Saez-Rodriguez, D. A. Lauffenburger, S. Klamt, and F. J. Theis. Transforming Boolean models to continuous models: methodology and application to T-cell receptor signaling. *BMC Systems Biology*, 3:98, Jan. 2009.

APPENDIX A

Nomenclature

Ordinary Differential Equations (ODE) model

- Ω : phase space
- θ_i^j : j -th threshold of variable i
- $\bar{\xi}(t)$: solution trajectory over time $t > 0$
- ϵ_{ij} : Hill coefficient
- $H^\pm(x_i, \theta_i^j, \epsilon_{ij})$: Hill function of variable x_i at threshold θ_i^j with Hill coefficient ϵ_{ij}
- $Null_i$: Nullcline of variable i
- $\mathbf{0}$: zero vector

Piecewise Multi-Affine (PMA) model

- \mathcal{R} : rectangles
- $\mathcal{V}(R)$: corners of $R \in \mathcal{R}$
- $\theta_i^{j,0}, \theta_i^{j,1}$: j -th threshold interval of variable i
- $L^\pm(x_i, \theta_i^{j,0}, \theta_i^{j,1})$: ramp function of variable x_i with linear increase/decrease in the threshold interval $[\theta_i^{j,0}, \theta_i^{j,1}]$

Piecewise Affine Differential Equations (PADEs)

- $S^\pm(x_i, \theta_i^j)$: Step function of variable x_i at threshold θ_i^j
- \mathcal{D} : (mode) domains
- \mathcal{D}_r : regular domains
- \mathcal{D}_s : singular domains
- $\phi(D)$: focal point of domain $D \in \mathcal{D}_r$
- ∂D : boundary of domain D
- $supp(D)$: supporting hyperplane of domain D
- $\rho(D)$: regular domains that have $D \in \mathcal{D}_s$ in their boundary
- $\overline{co}(P)$: closed convex hull of all points in P
- $\Phi(D)$: focal set of domain D
- $\xi(t)$: PADE solution over time $t > 0$
- $QTG^\Phi(\mathcal{A})$: qualitative transition graph of PADEs \mathcal{A}
- $\overline{rect}(P)$: closed hyperrectangular set of all points in P

$\Psi(D)$: overapproximated focal set of domain D
$v(D, \phi(D))$: relative position of the domain $D \in \mathcal{D}_r$ with its focal point
$V(D, \Phi(D))$: relative position of the domain $D \in \mathcal{D}$ with its focal set
$QTG^\Psi(\mathcal{A})$: overapproximated qualitative transition graph of PADEs \mathcal{A}
\mathcal{M}	: flow domains
QTS	: qualitative transition system of the refined PADE formalism
$S_i(M)$: sign of derivative of variable i for flow domain $M \in \mathcal{M}$

Thomas formalism

Q	: state space
$AS(q)$: asynchronous successors of $q \in Q$
f	: update function
$STG(f)$: state transition graph of f
\tilde{f}	: unitary update function

Singular State Formalism

\bar{G}	: interaction graph
$\{K_{i,\omega}\}$: logical parameters
$Pred(i)$: predecessors of variable i in the interaction graph
$ a, b $: qualitative value
$ord(s)$: number of singular values of $s \in Sigma$
Σ	: extended state space
g	: extended update function
$Reg_i(s)$: regular resources of variable i for $s \in \Sigma$
$Sing_i(s)$: singular resources of variable i for $s \in \Sigma$
$ESG(g)$: extended state graph of g
$\Delta_i^\pm(s)$: evolution operators of the state $s \in \Sigma$ in variable i

Mappings between Formalism

d	: discretises the regular domains in the PADEs into states in the Thomas formalism
μ	: maps a domain in the PADEs to a state in the singular state formalism
H	: maps a domain in the PADEs to a group of states in the Thomas formalism
δ	: maps a state in the singular state formalism to a group of states in the Thomas formalism
χ	: maps a rectangle in the PMA model to a domain in the PADEs
$mode$: maps a flow domain to a mode domain in the PADEs

APPENDIX B

Curriculum Vitae

Education

- Since 02/2009 PhD at Freie Universität Berlin
Phase 2 of Berlin Mathematical School
Dahlem Research School Scholarship
- 10/2006 - 11/2008 Completion of Phase 1 at Berlin Mathematical School
Majors: Dynamical Systems, Stochastic Processes
Berlin Mathematical School Scholarship
- 02/2002 - 11/2005 BSc with first class Honours at University of Sydney, Australia
Majors: Applied Mathematics, Statistics
KE Bullen Memorial Prize for Applied Mathematics
- 02/1993 - 11/2001 Higher School Certificate (Score:97.25%)
Blue Mountains Grammar School, Sydney, Australia

Employment

- 09/2006 - 11 /2006 BP Hamburg
Bookkeeping
- 03/2006 - 07/2006 BODE, Hamburg
Statistical Analyst in the marketing department
- 01/2005 - 03/2005 GEMVIS, Montreal
Internship as a Statistical Analyst
- Data retrieval and analysis
- Schedule optimisation to increase efficiency
- 04/2004 - 05/2004 Sydney University (Geology Department)
Statistical analysis of pollution in Sydney Harbour

- 09/2003 - 12/2003 DSP Group, Sydney
Salesperson
- Customer Service
- Training of new employees
- 01/2003 - 06/2003 Yekta Pty Ltd, Sydney
Programmer and Bookkeeper

Teaching

- 01/2012 - 07/2012 English Tutor (private)
10/2011 - 02/2012 Linear Algebra I Tutor, FU Berlin
10/2010 - 02/2011 Analysis II Tutor, FU Berlin
09/2005 - 11/2005 Statistics Tutor (private)
11/2004 Tutor, Veronica James Science Workshop

Publications

- S. Jamshidi, H. Siebert, and A. Bockmayr. **Comparing discrete and piecewise affine differential equation models of gene regulatory networks.** *In Information Processing in Cells and Tissues, IPCAT 2012*, Cambridge, UK, pages 1724. Springer, LNCS 7223, 2012.

Knowledge and Skills

Soft Skills: Mathematical Writing
Graphics Workshop
Intercultural Training
Disputation Training
Stress and Time Management

Languages:

English native speaker
German fluent
Farsi good knowledge
Spanish good knowledge

Erklärung zur Dissertation

Sehr geehrte Damen und Herren,

Hiermit erkläre ich, dass ich die beigefügte Dissertation selbstständig verfasst und keine anderen als die angegebenen Hilfsmittel genutzt habe. Alle wörtlich oder inhaltlich übernommenen Stellen habe ich als solche gekennzeichnet.

Ich versichere ausserdem, dass ich die beigefügte Dissertation nur in diesem und keinem anderen Promotionsverfahren eingereicht habe und, dass diesem Promotionsverfahren keine endgültig gescheiterten Promotionsverfahren vorausgegangen sind.

Shahrad Jamshidi